Addis Ababa University
School of Graduate Studies

EFFECT OF INCOMPRESSIBILITY IN THE ANALYSIS OF METAL FORMING USING FINITE ELEMENT METHOD

By

Ahmed Nurye

Advisors

Dr. Alem Bazezew
&
Dr. Ing. Tamrat Tesfaye

November, 2005

Addis Ababa

EFFECT OF INCOMPRESSIBILITY IN THE ANALYSIS OF METAL FORMING USING FINITE ELEMENT METHOD

By

Ahmed Nurye

A thesis submitted to the school of Graduate Studies of Addis Ababa University in partial fulfillment of the requirements of the Degree of Masters of Science in Mechanical Engineering (Applied Mechanics Stream)

Advisors

Dr. Alem Bazezew

&

Dr. Ing. Tamrat Tesfaye

Department of Mechanical Engineering

Addis Ababa University

November, 2005

ADDIS ABABA UNIVERSITY
SCHOOL OF GRADUATE STUDIES
DEPARTMENT OF MECHANICAL ENGINEERING

EFFECT OF INCOMPRESSIBILITY IN THE ANALYSIS OF METAL FORMING USING FINITE ELEMENT METHOD

By

Ahmed Nurye

Approved by Board of Examiners:

Dr. Ing. Demiss Alemu _____

Chairman, Department Graduate Committee

Dr. Alem Bazezew _____

Dr. Ing. Tamrat Tesfaye _____

Advisors

Dr. Abiy Awoke _____

External Examiner

Dr.Ing. Daniel Kitaw _____

Internal Examiner

Acknowledgements

First of all, I would like to thank the almighty God for guiding and helping me through out my life.

There are many people who have helped me in one way or another to make this thesis possible. I am indebted to them all. I would like to express my sincere gratitude and appreciation to my advisors, Dr. Alem Bazezew and Dr. Ing. Tamrat Tesfaye, for their encouragement and advice to complete this work on time. Without their encouragement and patience, the completion of this work would not have been possible.

Special thanks go to Ato Yoseph Alemu who gave me resources materials to start the thesis work and forwarded valuable suggestions and encouragement through out this work. My sincere appreciation also goes to the other research group members and friends for their support.

Last but not least, I am grateful to my parents and relatives, who were supportive throughout my undergraduate and graduate studies.

TABLE OF CONTENTS

LIST OF FIGURES

LIST OF TABLES

NOMENCLATURE

Ω	A given body without its boundary
$\Gamma_{ui},\ i=1,2$	Dirichlet boundary
$\Gamma_{\sigma i},\ i=1,2$	Neumann boundary
$\Gamma=\Gamma_{ui}\cup\Gamma_{\sigma i}$	$\Omega' s$ Boundary
E	Young s modulus
ν	Poisson s ratio
K	Elastic bulk modulus
μ	Shear modulus
σ_{ij}	Stress tensor component
δ_{ij}	Kronecker's symbol
σ	Stress vector with components (in 2D): $\sigma=\{\sigma_{11},\sigma_{22},\sigma_{12}\}T$
ε	Total strain vector with components (in 2D): $\varepsilon=\{\varepsilon_{11},\varepsilon_{22},\varepsilon_{12}\}^T$
1	Kronecker's vector (in 2D): $\{1,0\}^T$
ε_{ij}	Total strain tensor component
ε_{ij}^p	Total plastic strain tensor component
$\boldsymbol{\varepsilon}^p$	Plastic strain vector with components ordered as above
f	Yield function
g	Plastic potential
$\dot{\gamma}$	Plastic multiplier
T	Cauchy stress
P	First Piolla-Kirchhoff stress
S	Second Piolla-Kirchhoff stress
λ	Lagrange multiplier trial functions $\lambda(\zeta^\alpha,t)$
$\zeta^\alpha,\alpha=1,...,(n_{sd}-1)$	Referential coordinates
$(n_{sd}-1)$	Number of spatial dimensions
t	Time

u_i	Displacement component
u	Displacement vector
G	Virtual work representation
d**G**	Linearized form of virtual work
p	Mean pressure
D_{ijkl}	Component of elastic constitutive tensor
$\overline{D}_{ijkl}$	Deviatoric projection of the elastic constitutive tensor
$\overline{D}^{uu}, \overline{D}^{up}, \overline{D}^{pu}, \overline{D}^{pp}$	Elastoplastic tangent constitutive sub-matrices
$\overline{K}^{uu}, \overline{K}^{up}, \overline{K}^{pu}, \overline{K}^{pp}$	Stiffness sub-matrices
F_u, F_p	Right-hand side (External force) sub-vectors
$\mathbf{T}'$	Deviatoric part of the Cauchy stress
$\tilde{\sigma}$	Equivalent stress
s	Internal Resistance Variable
F	Deformation gradient
D	Rate of deformation
W	Spin gradient
L	Velocity gradient
R	Rotation tensor
U	Deformation tensor
$\overset{\Delta}{\mathbf{T}}$	Jaumann rate of the Cauchy stress
τ	Stabilization factor matrix
ℓ^e	Elastic isotropic moduli
$\mathfrak{I}$	Unit fourth order tensor
I	Unit second order tensor
$\mathbf{K}^{geo}$	Geometric stiffness matrix (initial stress matrix)
$\mathbf{K}^{mat}$	Material tangent stiffness matrix
N_i	Displacement shape function
$\boldsymbol{N}$	Vector of displacement shape functions
$\tilde{N}_i$	Pressure shape function

$\tilde{\mathbf{N}}$	Vector of pressure shape functions
$(\cdot)^i$	Quantity $(\cdot)$ at iteration i
$(\cdot)_n$	Quantity $(\cdot)$ at step t_n
$\Delta(\cdot)$	Increment of quantity $(\cdot)$
$\Delta(\cdot)_{n+1}$	Increment of quantity $(\cdot)$ between time steps t_n and t_{n+1}
$(\cdot)_{,i}$	Indicates derivation of $(\cdot)$ with respect to x_i
$\vec{\nabla}(\cdot)$	Gradient of quantity $(\cdot)$
$\lvert(\cdot)\rvert$	Absolute value of $(\cdot)$
$(\cdot)^e$	Quantity $(\cdot)$ at an element node
$(\cdot)^h$	Quantity $(\cdot)$ approximated inside an element

ABSTRACT

Metal forming is one of the most common metal manufacturing processes used, which is noted for its minimum waste and dimensional precision, and usually improves the mechanical properties of the formed part. Metal forming process is a process that causes changes in the shape of solid metal particles via plastic (permanent) deformations. Hence, knowledge of metallurgy and mechanics combine to provide an insight to its behavior. Its applications are wide in the manufacturing of machinery, automotive, aerospace and other hardware components.

The material is modeled as a hyperelastic, viscoplastic solid. A constitutive model with a single scalar variable representing the isotropic resistance to the plastic flow is employed. Many finite elements exhibit the so-called 'volumetric locking' in the analysis of incompressible or quasi-incompressible problems in metal forming. Nearly incompressible plasticity in metal forming displays severe volume locking problems when low order standard nodal-based displacement methods are used. This means that after deformation each small portion of the medium has the volume as before the deformation.

In this thesis a finite element formulation for a frictionless large deformation contact problem in metal forming is presented. It is based on the formulation which introduces the contact constraints via Lagrange multipliers. The stabilized formulation which allows the use of low-order interpolation functions for both displacement and the pressure field is applied to eliminate volumetric locking effects and to circumvent numerical instabilities. Starting from the variational formulation of the constitutive and the kinematic problems, the linearization of the principle of virtual work relation, the contact potential energy, and finally the matrix formulation of the method is derived. To improve the convergence property of the method an augmentation step was included. Then the formulation is converted to a computer code written using Matlab. Finally the program is used to solve a benchmark example.

CHAPTER ONE

1. INTRODUCTION

The work that will be presented in this thesis consists two of interconnected parts: the first deals with the theoretical background related to the mathematical formulation of deformation and pressure fields in metal forming process considering incompressibility effects; and in the second part numerical computer analysis of the forming process using the finite element method is dealt with.

The outline of this thesis is the following. First, a brief introduction of the metal forming problem is given. Then literature survey is presented in the second chapter. In chapters three and four, problem formulation in nonlinear solid mechanics which serves as the background to the finite element formulation of metal forming is discussed. In chapter five, the metal forming problem is solved using the finite element method. In chapter six an example and an application of the method is presented. And finally, in chapter seven, conclusions and recommendations for subsequent research are discussed.

1.1 Background

Metal forming is one of the most common metal manufacturing processes used. It is a widely used manufacturing process noted for its minimum waste and dimensional precision, and it usually improves the mechanical properties of the formed part. Starting with the work piece, knowledge of metallurgy and mechanics combine to provide an insight to its behavior. Metal forming process is a process that causes changes in the shape of metal particles via plastic (permanent) deformations.

Its applications are wide in the manufacturing of machineries, automotive, aerospace and other hardware components. Some of the characteristics of metal forming processes are: (1) the work piece is metal or a part fabricated from metal; (2) the surfaces of the deforming material and of

the tools are in contact; (3) the deformation usually causes significant changes in shape, but not in total volume of the material; (4) in some cases, the magnitude of permanent plastic and recoverable elastic deformation is comparable, therefore elastic recovery or spring back may be significant(especially in sheet metal forming process).

The high cost of forming critical components can be significantly reduced with the development of mathematically and physically sound computational methods for process design and control. The complicated nature of polycrystalline materials and the induced changes in their microstructure during processing are among the main challenges that one must consider while developing means for the design and control of bulk forming processes that result in products of desired shape and material state. A very important concern in metal forming process is the design of the process in such a way that a final product with a desired material state and geometry is achieved. A precise determination of the occurring final shapes, residual stress distributions, minimum forming force, minimum porosity in the final product, and the resultant strain distribution are key results which lead to products with the desired quality.

The desired objectives for a metal forming operation, for example in a hot extrusion process, may include one or more of the following criteria: uniform deformation in the final product, minimum required work or extrusion pressure, desired microstructure in the final product, minimum or desired residual stress distribution, minimum deformation and wear of the die, desired shape of the final product, and minimum porosity in the final product. Any of these objectives can theoretically be achieved by appropriate design of the die surface, design of the preform, design of the material state (microstructure) in the initial billet, and appropriate selection of the process parameters (ram speed and pressure history, operating temperature, etc.). However, it is important to note that in a single step forming operation there is only a limited control of the material state in the final product that one can achieve using a single stage design and generally a multistage process design is required.

Most deformation process design, like metal forming, is currently focused on trial and error techniques based on previous experience and the results of the direct analysis. It is considered as the design of the initial work-piece and the subsequent shapes at each of the forming stages

known as the preforms as well as the design of the dies for each stage of production. It also requires extensive experience to estimate these design variables with in an acceptable tolerance, and often costly trials and modifications are necessary to determine the final stage.

Now-a-days, there is an increasing demand for high quality formed products with reduced material waste and low manufacturing costs. Finite element simulation plays a vital role in materials processing and accounts for coupled non-linear mechanisms like microstructure evolution, varying contact and incompressibility conditions, large deformation plasticity, thermal effects and dissipation. In contrast to direct analysis tools, most of the methods for industrial deformation process design are currently focused on traditional trial and error techniques which rely on handbooks and the experience of the design engineer. The high cost of manufacturing critical structural components can be greatly reduced with the development of mathematically and physically sound computational methodologies for process design and control. Metal forming design, hence, requires an accurate description of the thermo-mechanical deformation mechanisms in order to achieve the required design objectives [1].

1-2 Locking in incompressibility

Many problems of physical importance involve motions that essentially preserve volumes locally. This means that after some deformation each small portion of the medium has the same volume as before the deformation. Media that behave in this fashion are termed incompressible or nearly incompressible. Incompressibility in metal forming is characterized by a Poisson ratio (ν) approaching 0.5 and a bulk modulus tending to infinity [10]. Many finite elements exhibit the so-called 'volumetric locking' in the analysis of incompressible or quasi-incompressible problems in solid mechanics. Nearly incompressible elasticity in metal forming displays severe volume locking problems when low order standard nodal-based displacement methods are used. This means that after deformation each small portion of the medium has the volume as before the deformation. Situations of this type are usual in most bulk metal forming processes, structural analysis of rubber materials and some geomechanical problems. Volumetric locking is an undesirable effect leading to incorrect numerical results.

Let the displacement field in a bilinear element be described as

$$u_j = \sum_{i=1}^{4} N_i(\xi,\eta) u_{ij} \tag{1.1}$$

where u_j =displacement field with in the element field

j (coordinate variables) = x, y

u_{ij} =displacement values at node i i (node numbers) =1,..., 4

N_i is the shape function at node I and is given by

$$N_i(\xi,\eta) = \frac{1}{4}(1+\xi_i\xi)(1+\eta_i\eta) \tag{1.2}$$

As a simple example, let us refer to figure1.1. Given is an element which shall be clamped at nodes 1, 2, and 4. in addition, we assume that at node 3 a displacement has the same absolute value in the x- as well as in the y- directions in such a way that

$$\begin{aligned} u_x = \sum_{i=1}^{4} N_i(\xi,\eta) u_{ix} &= \frac{1}{4}(1-\xi-\eta+\xi\eta)u_{1x} + \frac{1}{4}(1+\xi-\eta-\xi\eta)u_{2x} + \\ &\frac{1}{4}(1+\xi+\eta+\xi\eta)u_{3x} + \frac{1}{4}(1-\xi+\eta-\xi\eta)u_{4x} \\ &= \frac{1}{4}(1+\xi+\eta+\xi\eta)u_{3x} \end{aligned} \tag{1.3}$$

$$\begin{aligned} u_y = \sum_{i=1}^{4} N_i(\xi,\eta) u_{iy} &= \frac{1}{4}(1-\xi-\eta+\xi\eta)u_{1y} + \frac{1}{4}(1+\xi-\eta-\xi\eta)u_{2y} + \\ &\frac{1}{4}(1+\xi+\eta+\xi\eta)u_{3y} + \frac{1}{4}(1-\xi+\eta-\xi\eta)u_{4y} \\ &= \frac{1}{4}(1+\xi+\eta+\xi\eta)u_{3y} \end{aligned} \tag{1.4}$$

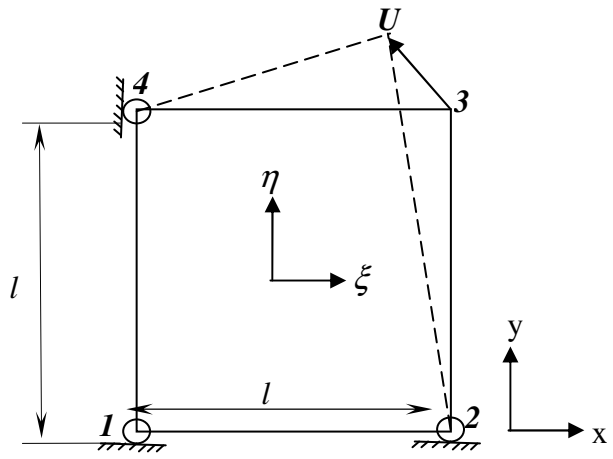

Figure1.1 Incompressible element with postulated displacement

The requirements of incompressibility (volume-constancy condition) lead to

$$\dot{\varepsilon}_x + \dot{\varepsilon}_y = 0 \tag{1.5}$$

where the strain rates are given by

$$\dot{\varepsilon}_x = \frac{\partial u_x}{\partial x} \qquad \text{and} \qquad \dot{\varepsilon}_y = \frac{\partial u_y}{\partial y} \tag{1.6}$$

with $x = \xi l$ and $y = \eta l$, equation (1.5) becomes

$$\begin{aligned} &\frac{1}{l}\frac{\partial u_x}{\partial \xi} + \frac{1}{l}\frac{\partial u_y}{\partial \eta} = 0 \\ &\frac{1}{l}\left[\frac{1}{4}(1+\eta)u_{3x} + \frac{1}{4}(1+\xi)u_{3y}\right] = 0 \end{aligned} \tag{1.7a}$$

since $u_{3x} = -u_{3y}$, we have

$$\frac{1}{4l}\left[(\eta - \xi)u_{3x}\right] = 0 \qquad \Rightarrow u_{3x} = 0 \tag{1.7b}$$

This shows that the displacement of node 3 is zero which, contradicts our assumption and this indicates that volumetric locking has occurred. Therefore the use of special element formulation is required to have an improved result.

To eliminate volumetric locking, two classes of techniques have evolved:

1. Multi-field elements in which the pressures or complete stress and strain fields are also considered as independent variables;
2. Reduced integration procedures in which certain terms of the weak form for the internal forces are under integrated.

In this thesis, the first technique is considered.

1.3 Research Objective

The main objective of this thesis is to investigate the effects of contact in the analysis of metal forming processes using finite element method. In the analysis of problems using finite element method, low order elements like triangles or quadrilaterals with linear displacement interpolations turn out to present unsatisfactory results due to the fact that metal forming process incorporates so many contact, geometric and material nonlinearities, as well as presence of severe conditions such as incompressibility. Thus attempt is made to know these problems and their solution methods, in a way to prepare a springboard and stimulate further research activities in the area. Finally a finite element code will be developed for solving a specific problem and investigates the efficiency of the method.

CHAPTER TWO

2. LITRETURE SURVEY

In the last two decades computer modeling of metal-forming processes has been undergoing a continuous development. The finite element method has been applied extensively to simulate metal forming processes ([1]-[7]). Due to large deformations in metal forming, plastic strains usually outweigh elastic strains, so many researchers and engineers idealize the material behavior as rigid-plastic or rigid-viscoplastic, which is known as the flow formulation. A detailed presentation of the *flow formulation* for the finite element method in metal forming can be found in [17]-[19]. Numerical results obtained with this method compare quite well with experimental results.

The rigid-plastic finite-element method [33] which is based on the variational principle for rigid-plastic deformation is particularly suited for solving metal flow problems involving large plastic strains. The basic concepts of the method are the use of the Lagrange multiplier and linearization. The accuracy and convergence of the method has been shown to be excellent and it is applicable to the analysis of both the steady-state and the non-steady-state problems.

Most deformation process designs are currently focused on trial and error techniques based on previous experience and the results of the direct analysis. A systematic review of such problems is given in reference [39]. The design approaches reported in this reference are not mathematically rigorous and/or realistic from a material representation point of view. However, a variety of important forming design problems were addressed. In the direct differentiation method, a set of field equations are developed by considering the variation of the continuum or discretized field equations of the direct problem with respect to small changes in design parameters [40-41]. The sensitivity field equations are linear and can be efficiently solved.

Researches have been conducted on the application of analytical techniques using the rigid-viscoplastic finite element method. For example, reduced integration [33] was proposed to avoid element locking, which may occur using the analysis, especially with the specified condition of incompressibility of plastic flow. In order to resolve both the element and the shear locking behavior using this approach, the selective reduced integration technique (SRI) [23] was also applied. Some researchers [24, 25] have also suggested methods to control the hourglass mode, which can be generated easily when applying the reduced integration technique in order to integrate the element stiffness. Any nodal displacement that is not a rigid body motion but results in no straining of the element is a spurious singular (hourglass) mode. Such nodal displacements will not generate any nodal forces i.e., they will not be resisted by the element, since in the absence of strain, the stresses will also vanish. A vertical pair of elements in the x-mode or a horizontal pair of elements in the y-mode looks like an hourglass, an ancient device for measuring time by the flow of sand from the top element to the bottom. For this reason, this spurious singular mode is often called hourglassing or the hourglass mode. Hourglass modes are zero-energy modes, since they do not result in any strain at the points in the element which are sampled. Therefore they do no work. The directional reduced integration technique (DRI) was also proposed, to avoid both the shear locking and the zero energy modes during the solution of different metal flow problems when applying the rigid-plastic finite-element method.

The computational modeling and analysis of contact problems have been important subjects of interest over the past several decades. Traditionally, the non-penetration condition has been enforced exactly by the *Lagrange multiplier technique* [46-52] or approximated by a penalty method [52]. The traditional Lagrange multiplier technique is essentially a two-field formulation. The Lagrange multipliers act directly as forces between contacting bodies. Recently, several researchers have proposed methods which formulate the so-called intermediate contact surfaces, over which contact quantities can be defined and discretized. Examples of such ideas are to be found in reference [47].

Further extensions of these approaches can be found in reference [16] and in the mortar-like approaches in reference [47], which enforce pressure continuity on the contact surface. Specifically, in order to circumvent over constraining in the approaches of references [46-52], the

pressure continuity is enforced at selected surface nodes and for the remaining nodes kinematic gap continuity is enforced. Consequently, this leads in general to an unsymmetric formulation.

The solution of the contact problem using the finite element method, in general, can be studied using the following three general approaches: adaptations of usual formulations using incremental and iterative schemes in order to take into account the contact conditions; formulation of variational inequalities (Duvaut and Lions, 1972; Glowinski, Lions and Trémolières, 1976), which can represent the contact problem, and the relationship of these inequalities with a mathematical programming method (Panayiotopoulos, 1975; Panayiotopoulos and Lazaridis, 1987); and the direct application of the mechanics minimum principles, and the solution through a constrained minimization problem (Haug, Chand and Pan, 1977; Klarbring and Björkman, 1988).

Considerable efforts have been made in recent years to develop linear triangles and tetrahedral producing correct (stable) results under incompressible situations. Brezzi and Pitkäranta [23] proposed to extend the equation for the volumetric strain rate constraint for Stokes flows by adding a Laplacian of pressure term. A similar method was derived for quasi-incompressible solids by Zienkiewicz and Taylor [22]. Zienkiewicz et al. [24] have proposed a stabilization technique which eliminates volumetric locking in incompressible solids based on a mixed formulation and a characteristic based split (CBS) algorithm initially developed for fluids [26] where a split of the pressure is introduced when solving the transient dynamic equations in time. Extensions of the CBS algorithm to solve bulk metal forming problems have been recently reported by Rojek et al. [27]. Other methods that have been proposed to overcome volumetric locking are based on mixed displacement (or velocity)–pressure formulations using the Galerkin-least-square (GLS) method [28], average nodal pressure and average nodal deformation [29] techniques and sub-grid scale (SGS) methods [11–14].

Volumetric locking in solids is present in all low-order elements based on the standard displacement formulation. The use of a mixed formulation or a selective integration technique eliminates the volumetric locking in many elements. These methods, however, fail in some elements such as linear triangles and tetrahedral, due to lack of satisfaction of the Babuska–

Brezzi conditions [10; see also section 5.1 of this thesis] or alternatively the mixed patch test not being passed.

Zabaras et al [3-4] have developed a sensitivity analysis method for large deformations of hyperelastic viscoplastic solids that can be applied to various design problems in metal forming. Sensitivity analysis and optimization theory, provide a fresh look at these problems and can lead to realistic and accurate designs. Traditional forming design problems that can be analyzed as optimization problems are the optimum design of dies, preforms and process parameters. To mathematically address such problems, one needs to calculate the sensitivity of the material state and geometry at various stages of deformation with respect to infinitesimal changes in each of the design variables.

In this thesis, the analysis of Zabaras et al for the design of metal forming processes is followed for the design of dies in bulk forming processes. Here, the algorithms for the solution of the independent problems, i.e. the constitutive problem, the kinematic problem, and the contact problem, are formulated and solved. A *radial return* method is employed to solve the governing equations by Euler-backward integration method. The consistent material moduli are employed while solving the linearized principle of virtual work. The contact problem is solved using *Lagrange multiplier* method. Unlike what Zabaras et al have done, this thesis concentrates on the analysis of frictionless contact problem. To check the accuracy and stability of the algorithm, a numerical example is worked out.

CHAPTER THREE

3. PROBLEM FORMULATION IN NONLINEAR SOLID MECHANICS

The theories that are described in this chapter are aimed at serving as the background to the following chapters, especially chapter four. It is meant to be a mathematical formulation of some of the important topics which are necessary for the finite element analysis of metal forming process. Metal forming operations are not trivial to model since they involve complicated processes such as large deformations, non-linear material behavior and complex contact conditions.

The chapter starts with nonlinear behavior followed by the most comprehensive part, large material deformation. This topic is a link between the kinematics of a body and the specific material's constitutive behavior, that is to say, a linkage between well known and relevant physical principles and a mathematical model of the internal constitutive behavior of a material. Finally, a short review of metal plasticity, with emphasis on the constitutive model used in the numerical analysis is presented.

3.1 Nonlinear Behavior

In metal forming, which is characterized by high loading conditions, a number of nonlinearities are encountered. In such problems, principle of superposition no longer holds true. Thus, in metal forming problems:

- The strain is no longer small; hence finite (large) strain analysis is required to solve problems of metal forming.
- The strain-displacement relationship is no longer linear. The changes in the deformed shape can no longer be ignored. The physics of metal forming, among others, requires that either a quadratic relationship exits between the strain and displacement (Green-Strain) or a

logarithmic relationship exists, i.e., engineering stress is no longer appropriate because of geometric changes and the true stress or Cauchy stress should be used [5].

- The stress-strain law may become nonlinear. This can happen even within the useful stress range of the material. This behavior is typical of most metals, rubbers and elastomers, and certain composite materials whose properties are unequal in tension and compression.
- The original equilibrium equations (relating stress to loads) may need updating. This is due to the geometrical changes in the shape of the structure. These relations mean that, in nonlinear FEA, the load is no longer proportional to the displacement, that is,

$$\frac{F}{u} = K$$

The three major types of nonlinearities encountered in metal forming process are:

- Material Nonlinearity (plasticity)
- Geometric Nonlinearity (large deformations, large strains)
- Boundary Nonlinearity (opening/closing of gaps, contact)

3.1.1 Material Nonlinearity

Material nonlinearities cause deviations from the linear (proportional) stress-strain relationships. When stresses go beyond the linear elastic range, material behavior can be broadly divided into two classes: (i) Time-independent behavior (plasticity-applicable to most ductile metals; nonlinear elasticity-applicable to rubber, elastomers) and (ii) Time-dependent behavior (creep, viscoplasticity-applicable to high-temperature applications, concrete; viscoelasticity-applicable to elastomers, glass, plastics). This thesis concentrates on the time-dependent behavior of materials.

Material nonlinearity itself may be subdivided in to some fundamentally different categories. In nonlinear elasticity the stress-strain relation is nonlinear but the behavior follows that of linear elasticity, i.e., no distinction is made between loading and unloading except for the sign. In the case of plastic or elasto-plastic materials, irreversible strains occur. The difference in behavior between these two materials is given in figure (3.1). For low stress levels both materials follow a linear stress-strain relation. This is followed by a decrease in stiffness as the stress increases. If however, the stress is reduced the nonlinear elastic material will follow the same stress-strain

curve as in loading, whereas unloading of the elasto-plastic material leads to a new branch on the $\sigma - \varepsilon$ curve where the material is again elastic, often with a stiffness equal to the initial elastic stiffness. Furthermore, it is clear that when the material is completely unloaded, an irreversible plastic strain ε^p remains. The curved part above the elastic limit in figure3.1 suggests that the stress-strain relation may be of a rather complicated nature. An elastic-plastic material may be defined as a material, which, upon reaching a certain stress state, undergoes deformation, which is irreversible. This results in a behavior which is path-dependent. A basic assumption in elastic-plastic analysis is that deformation can be divided into an elastic part and an inelastic (plastic) part.

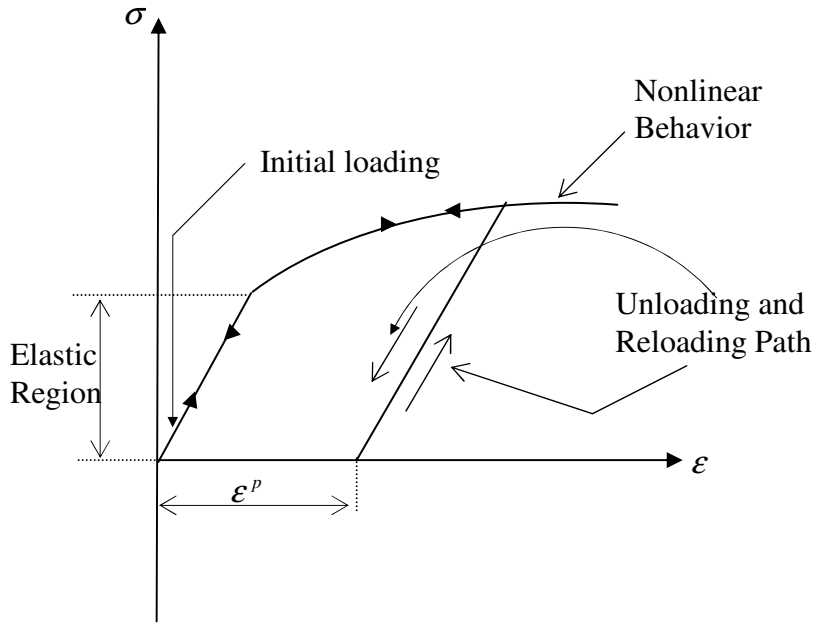

Figure 3.1 Material Nonlinearity

3.1.2 Geometric Nonlinearity

Geometric nonlinearities cause deformations of the structure that cannot be neglected and the calculation of stress and strain is based on the deformed configuration (Crisfield 1991, Fafitis 1996, Blandford 1997). Change in geometry as the structure deforms is taken into account in setting up the strain-displacement and equilibrium equations. From the strain-displacement equations:

$$\mathbf{e = Du} \tag{3.1}$$

where **e** is the strain and **u** is the displacement, the operator **D** is nonlinear when finite strains (as opposed to infinitesimal strains) are expressed in terms of displacements. And the internal equilibrium equations can be written as

$$\mathbf{b} = -\mathbf{D}^{*}\boldsymbol{\sigma} \tag{3.2}$$

where **b** is the body force and $\boldsymbol{\sigma}$ is the stress. From classical linear theory of elasticity, $\mathbf{D}^{*} = \mathbf{D}^{\mathbf{T}}$ is the formal adjoint of **D**, but that is not necessarily true if geometric nonlinearities are considered.

The term geometric nonlinearity models many of the physical problems: The strains themselves may be large, say over 5% [3]. These strains are frequently associated with material nonlinearities. However, they can also be associated with geometric nonlinearities, for the strains may produce finite displacements and/or rotation. For instance slender structures undergo finite displacements and rotation, although the deformational strains may be treated as infinitesimal. Examples can be found in various structures like cables, springs, bars, thin plates. Figure 3.2 shows graphical representation of sources of nonlinearities in solid continuum mechanics.

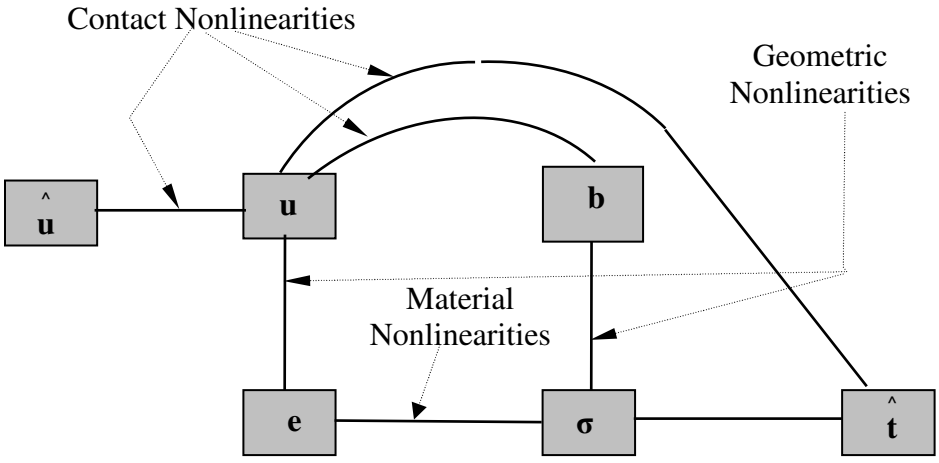

Figure 3.2 Graphical depiction of sources of nonlinearities in solid continuum mechanics.

$\hat{\mathbf{u}}$ =prescribed Displacements, $\mathbf{u}$ = Displacements,

$\mathbf{b}$ = Body forces, $\mathbf{e}$ = Strains,

$\boldsymbol{\sigma}$ = Stresses, and $\hat{\mathbf{t}}$ = Prescribed tractions or forces

Figure 3.2 is a general representation of nonlinearities in solid mechanics. The material nonlinearity arrow is used to indicate the deviations from the linear (proportional) stress-strain relationship discussed earlier. The geometric nonlinearity arrows represent equations 3.1a and 3.1b graphically. Similarly, the contact nonlinearity arrows are graphical representations of equations 3.1c-3.3.

3.1.3 Contact Nonlinearity

A final type of nonlinearity we wish to consider in this thesis is that created due to contact with another deformable or rigid entity. Contact, by nature, is a nonlinear boundary value problem. During contact, mechanical loads and perhaps heat are transmitted across the area of contact. If friction is present, shear forces are also transmitted. As a simple model problem for this case, consider the rigid obstacle problem shown in figure 3.3 where a prescribed motion of the left end of the moving body is $\bar{d}$ and the unknown displacement of the right end is d subjected to the constraint

$$g(d) = d - g_o \leq 0 \tag{3.1}$$

g_0 is the initial separation, or gap, between the right end of the moving body and the rigid obstacle.

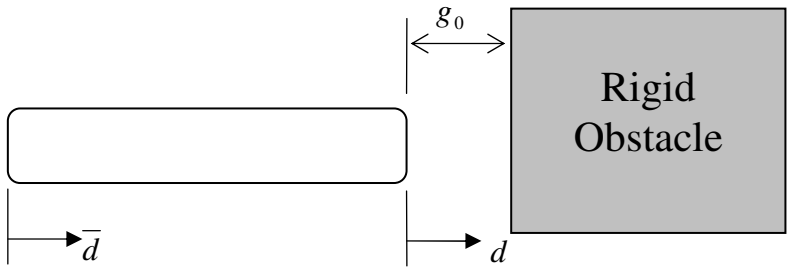

Figure 3.3 Schematic of the rigid obstacle problem.

The equations governing the response of the body are nonlinear. To see this, we can choose d as unknown and construct the following residual for the system

$$R(d) = M(*)(d - \bar{d}) + F_C = 0 \tag{3.2}$$

where M(*) is a function of the cross section and elastic modulus of the material, and F_C is the contact force between the obstacle and the moving body (assumed positive in compression), subject to the following constraints:

$$F_C \geq 0; \quad g(d) \leq 0 \quad \textit{and} \quad F_C g(d) = 0. \tag{3.3}$$

Equations (3.3) are called *Kuhn-Tucker conditions* in mathematical parlance and physically require that the contact force be compressive, that the right end of the moving body and the obstacle do not interpenetrate, and that the contact force is nonzero when g=0; i.e., when contact between the rod and obstacle occurs. It can be seen that the boundary condition operating the right end of the body is neither a Dirichlet (displacement) nor Neumann (stress) boundary condition; in fact, both the stress and the displacement at this point are unknown but are related to each other through constraints (equation 3.1).

3.2 Large deformation Problems

In this section, concepts from continuum mechanics that are necessary for rigorous specification of large deformation problems in metal forming are discussed. This is an extension of the linear elastic problem to accommodate two important features: potentially large motions and deformations, and nonlinear material response. This can be done by introducing a more general notational framework and then by examining in a fairly nonrigorous fashion how, provided certain concepts are kept in mind, the equations governing large deformation initial/boundary value problems are similar in form to their familiar counterparts from the small deformation theory. Rigorous prescription and understanding of large deformation problems can only be achieved through a careful examination of the concepts of nonlinear continuum mechanics.

3.2.1 Notational Framework

The basic system which is considered here is depicted schematically in Figure 3.4. We consider a body, initially in a location denoted by Ω, undergoing a time-dependent motion φ that describes its trajectory through the ambient space (assumed to be $\Re^3$). The set Ω is called the reference configuration and can be thought of as consisting of points **X** that serve as labels for the material points existing at their respective locations.

For this reason the coordinates **X** are often called *reference* or *material* coordinates. We assume that the surface $\partial\Omega$ of Ω can be decomposed into subsets Γ_σ (Neumann boundary condition) and Γ_u (Neumann boundary condition) obeying the following

$$\begin{aligned} \Gamma_u \cup \Gamma_\sigma &= \partial\Omega \\ \Gamma_u \cap \Gamma_\sigma &= \emptyset \end{aligned} \tag{3.4}$$

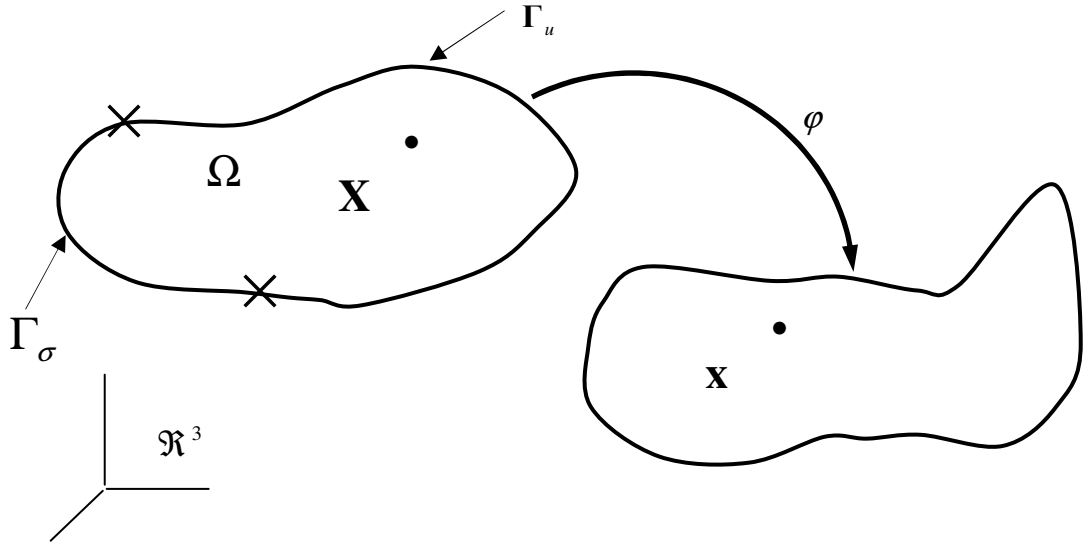

Figure 3.4 Notation for Large Deformation Initial/boundary value Problem

The general interpretation of these surfaces is: traction or Neumann boundary conditions will be imposed on Γ_σ, and displacement on Dirichlet boundary conditions will be imposed on Γ_u.

It has been mentioned that the motion is, in general, time dependent. In fact, we could write this fact in mathematical terms as the transformation $\varphi : \overline{\Omega} X\ (0,T) \to \Re^3$. If we fix the time argument of φ, we obtain a configuration mapping φ_t, summarized as $\varphi_t : \overline{\Omega} \to \Re^3$, which gives us the location of the body at time *t* given the reference configuration Ω. Coordinates in the current location $\varphi_t(\Omega)$ of the body will be denoted by **x**. The current location is often called the *spatial configuration* and the coordinates, **x**, *spatial coordinates*. Given a material point $\mathbf{X} \in \Omega$ and a configuration mapping φ_t, we may write

$$\mathbf{x} = \varphi_t(\mathbf{X}) \tag{3.5}$$

A key decision in writing the equations of motion for this system is whether to express the equations in terms of $\mathbf{X} \in \boldsymbol{\Omega}$ *or* $\mathbf{x} = \varphi_t(\boldsymbol{\Omega\zeta}$, material or spatial frame of reference, respectively.

The choice of whether to use reference coordinates **X** or spatial coordinates **x** in the problem description is generally highly dependent on the physical system to be studied.

In metal forming descriptions, the identity of specific material particles is of central interest in modeling a system. For example, the plastic response of metals is history dependent, meaning that the current relationship between stress and strain at a point in the medium depends on the deformation history associated with that material point. To use such models effectively requires knowledge of the history of individual particles, or material points, throughout a deformation process. Furthermore, many physical processes we wish to describe do not lend themselves to an invariant Eulerian frame. In a forging process, for example, the metal at the end of the procedure occupies a very different region in space than it did at the outset. For these and other reasons, the predominant approach to solid mechanics systems is to write all equations in terms of material coordinates or to use the Lagrangian frame of reference [1].

Therefore, in this thesis, the formulation is performed using the updated Lagrangian reference system where configurations will be updated after each incremental time step.

3.2.2. Measures of deformation

Referring to figure 3.4, restricting our attention to some time $t \in (0,T)$, and considering the corresponding configuration mapping φ_t, the deformation gradient **F** is given by the gradient of this transformation, i.e.:

$$\mathbf{F} = \frac{\partial \varphi_t}{\partial \mathbf{X}} = \frac{\partial \mathbf{x}}{\partial \mathbf{X}} \tag{3.6}$$

Or in indicial form:

$$F_{ij} = \frac{\partial \varphi_{ti}}{\partial X_j} = \frac{\partial x_i}{\partial X_j} \quad \text{, i, j =1, 2, 3} \tag{3.7}$$

When written in expanded form the above deformation gradient components will have the following form:

$$\mathbf{F} = \begin{bmatrix} \frac{\partial x_1}{\partial X_1} & \frac{\partial x_1}{\partial X_2} & \frac{\partial x_1}{\partial X_3} \\ \frac{\partial x_2}{\partial X_1} & \frac{\partial x_2}{\partial X_2} & \frac{\partial x_2}{\partial X_3} \\ \frac{\partial x_3}{\partial X_1} & \frac{\partial x_3}{\partial X_2} & \frac{\partial x_3}{\partial X_3} \end{bmatrix} \tag{3.8a}$$

Considering a cube of material in the reference configuration whose sides can be assumed to be aligned with the coordinate axes X_i, i =1, 2, 3, the initial differential volume of this cube is given by

$$d\mathbf{V} = dX_1 dX_2 dX_3 \tag{3.8b}$$

If we now consider the condition of this cube of material after the deformation φ_t is applied, we notice that its volume in the current configuration is $d\mathbf{v}$ spanned by the three vectors $\varphi_t(d\vec{X})_j$, here the notation $d\vec{X}_j$ is used to indicate a reference vector in coordinate direction j with magnitude dX_j. This volume can be written in terms of the vector triple product:

$$d\mathbf{v} = \varphi_t(d\vec{X}_1).\left(\varphi_t(d\vec{X}_2) \times \varphi_t(d\vec{X}_3)\right) \tag{3.8c}$$

Then we can write

$$\left(\varphi_t(d\vec{X}_j)\right)_i = .\begin{cases} F_{i1}dX_1, & j=1 \\ F_{i2}dX_2, & j=2 \\ F_{i3}dX_3, & j=3 \end{cases} \tag{3.8d}$$

We can write equation (3.8c) in indicial notation by first noting that the cross product of two vectors **a** and **b** is written as

$$(\mathbf{a}\times\mathbf{b})_i = e_{ijk}a_j b_k \tag{3.8e}$$

where e_{ijk} , the permutation symbol, has the following interpretation

$$e_{ijk} = \begin{cases} 1 & \text{if } (i,j,k) = (1,2,3) \text{ or } (2,3,1) \text{ or } (3,1,2) \\ -1 & \text{if } (i,j,k) = (3,2,1) \text{ or } (2,1,3) \text{ or } (1,3,2) \\ 0 & \text{otherwise} \end{cases} \tag{3.8f}$$

Equation (3.8c) is then reexpressed via

$$\begin{aligned} dv &= F_{i1}dX_1(e_{ijk}F_{j2}dX_2F_{k3}dX_3) \\ &= e_{ijk}F_{i1}F_{j2}F_{k3}dX_1dX_2dX_3 \\ &= \det(\mathbf{F})d\mathbf{V} \end{aligned} \tag{3.8g}$$

Introducing the notation **J**=det(**F**), called the Jacobean of the transformation, we can write

$$d\mathbf{v}=\mathbf{J}d\mathbf{V} \tag{3.8h}$$

Where $d\mathbf{V}$ = the initial differential volume of the body, and

$d\mathbf{v}$ = the current differential volume of the body

Equation (3.8h) tells us that the deformation converts reference differential volume d**v** to current volume d**V** according to the determinant of the deformation gradient.

Because the deformation **x** can be determined up to a rigid body motion, it can be written as

$$\mathbf{x} = \mathbf{X} + \mathbf{u} \tag{3.9}$$

where, **u** represents the displacement field. This leads us to another quantity called displacement gradient tensor which is defined by the following.

$$\mathbf{G} = \frac{\partial \mathbf{u}}{\partial \mathbf{X}} \tag{3.10}$$

Or in indicial form:

$$\mathrm{G}_{ij} = \frac{\partial u_i}{\partial X_j} \quad , i, j = 1, 2, 3 \tag{3.11}$$

The relationship between **F** and **G** is noticeable by writing

$$\partial \mathbf{u} = \mathbf{G}\partial \mathbf{X} = \partial \mathbf{x} - \partial \mathbf{X} \tag{3.12}$$

and

$$\partial \mathbf{x} = \mathbf{F}\partial \mathbf{X} = \mathbf{G}\partial \mathbf{X} + \partial \mathbf{X} \tag{3.13}$$

so

$$\mathbf{F} = \mathbf{G} + \mathbf{I} \qquad or \qquad \mathbf{G} = \mathbf{F} - \mathbf{I} \tag{3.14}$$

Where, **I** is the identity matrix. But **F** and **G** contain rigid-body rotations that do not contribute to the deformation of the continuum. And since only straining deforms the body and some other measures of deformation is required. One possibility is to define a stretch ratio between initial and current configuration for the material vector. It is the ratio of current length and initial length and can be written as

$$\lambda = \frac{dl}{dL} = \sqrt{\frac{dx_i dx_i}{dX_j dX_j}} \tag{3.15}$$

When the displacement gradients are finite, the symmetric and skew parts of the displacement gradient matrix no longer provide an additive decomposition of displacement gradient into the sum of pure strain and pure rotation, since the displacement gradient components are not small compared to unity the two matrices no longer represent pure strain and rotation, respectively.

The basic properties of the local behavior of deformation emerge from the possibility to decompose the deformation in to a rotation and stretch which is a change of the volume element. This decomposition is called the *polar decomposition of the deformation gradient* [2] (see figure 3.5). With the definition of **F** and **G** in hand, let's turn our attention to the quantification of local deformation in a body. For the matrix **F**, whose determinant is positive, the following decompositions can always be made:

$$\mathbf{F} = \mathbf{RU} = \mathbf{VR} \tag{3.15}$$

where **R** is the rotation tensor
U is the right stretch tensor and
V is the left stretch tensor

The significance of the polar decomposition is made clearer in Figure 3.5, where we consider the deformation of a neighborhood of material surrounding a point $\mathbf{X} \in \Omega$. By considering the polar decomposition, we see that this deformation of material neighborhoods can always be conceived as consisting of two parts. Considering the right polar decomposition as an example, **U** contains all information necessary to describe the distortion (stretch) of a neighborhood of material, while then **R** maps this distorted volume into the current configuration through pure (right-handed) rotation. In consideration of the left decomposition, the rotation **R** is considered first, followed by the distortion (stretch) by **V**. In developing measures of local deformation, we can then concentrate our attention on either **U** or **V**. The choice of which decomposition to use is typically based on the coordinates in which we wish to write strains: the right stretch **U** most naturally takes reference coordinates as arguments, while the left stretch **V** is ordinarily written in terms of spatial coordinates. We might indicate this explicitly via

$$\mathbf{F(X) = R(X)\ U(X) = V\ (\varphi_t\ (X))\ R(X).} \tag{3.16}$$

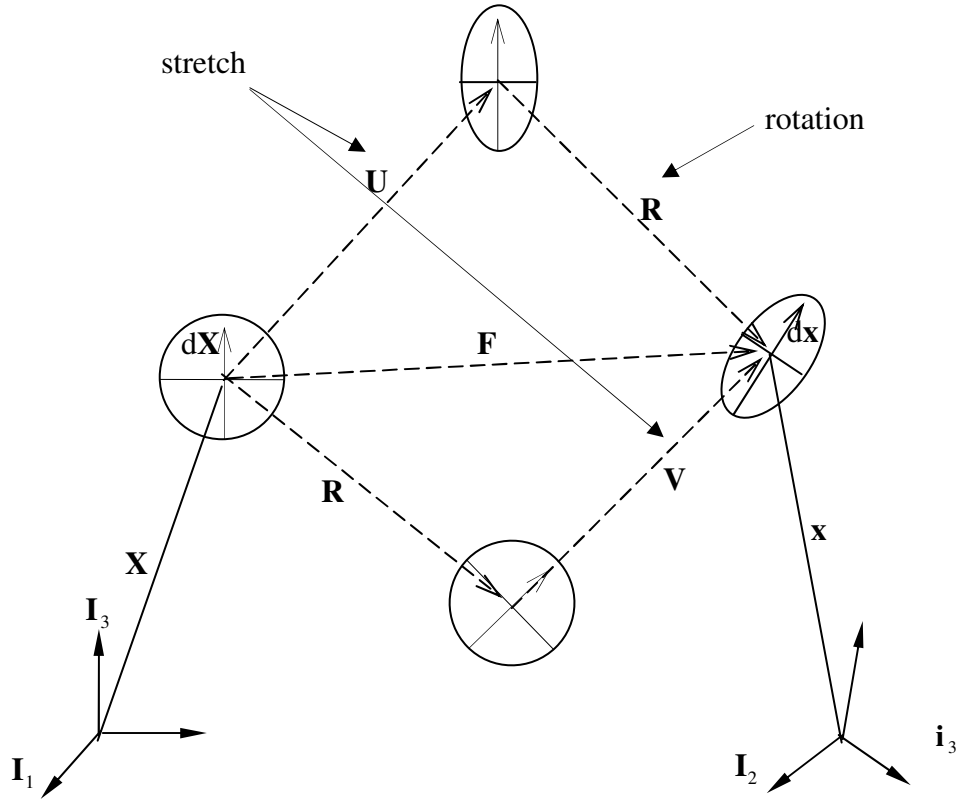

Figure 3.5 Polar Decomposition

The particular factors given above have the following properties:

1. The tensor **R** is orthogonal, $\mathbf{R}.\mathbf{R}^T = \mathbf{R}^T.\mathbf{R} = \mathbf{I}$, i.e., **R** is a rotational tensor.
2. The tensors **U** and **V** are symmetric and positive definite. [The necessary and sufficient condition for any tensor **T** to be positive definite is that all its eigenvalues be positive, i.e., the tensor **T** is positive definite if $\mathbf{v}\cdot\mathbf{T}\cdot\mathbf{v} > 0$ for all vectors $\mathbf{v} \neq 0$].
3. **U**, **V** and **R** are uniquely determined.
4. The eigenvalues of **U** and **V** are identical; if **e** is an eigenvector of **U**, then **R.e** is an eigenvector of **V**.

In characterizing large deformations, it is convenient also to define the right and left Cauchy-Green tensors, respectively, via

$$\mathbf{C} = \mathbf{F}^T\mathbf{F} \tag{3.17}$$

and

$$\mathbf{B} = \mathbf{F}\mathbf{F}^T \tag{3.18}$$

Since **F** is assumed to be non-singular (det $F \neq 0$) and $\mathbf{v}\cdot\mathbf{F} \neq 0$ if $\mathbf{v} \neq 0$, it follows that $(\mathbf{v}\cdot\mathbf{F})\cdot(\mathbf{v}\cdot\mathbf{F})$ is a sum of squares and hence greater than zero. Thus

$$0 < (\mathbf{v}\cdot\mathbf{F})\cdot(\mathbf{v}\cdot\mathbf{F}) = \mathbf{v}\cdot\mathbf{F}^{\mathbf{T}}\,\mathbf{F}\cdot\mathbf{v} = \mathbf{v}\cdot\mathbf{C}\cdot\mathbf{v}, \tag{3.19}$$

and **C** is positive definite. By the same argument, we may show that Finger's deformation tensor $\mathbf{B} = \mathbf{F}.\mathbf{F}^T$ is also positive definite. The right Cauchy-Green tensor is ordinarily considered to be a material object (i.e., **C(X)**), while the left Cauchy-Green tensor is a spatial object (**B** (φ_t (**X**))). Since **R** is orthogonal, one can write

$$\mathbf{R}^T\cdot\mathbf{R} = \mathbf{R}\cdot\mathbf{R}^T = \mathbf{I} \tag{3.20}$$

where **I** is the 3x3 identity tensor. Using this fact and manipulating Equations (3.16)-(3.20) also reveals that

$$\mathbf{U} = \sqrt{\mathbf{C}} \tag{3.21}$$

and

$$\mathbf{V} = \sqrt{\mathbf{B}} \tag{3.22}$$

3.2.3. Strain Measures

As a body deforms, various points in it will translate and rotate. Strain is a measure of the "stretching" of the material points within a body; it is a measure of the relative displacement without rigid-body motion and is an essential ingredient for the description of the constitutive behavior of materials. The easiest way to distinguish between deformation and the local rigid-body motion is to consider the change in distance between two neighboring material particles. We will use this to establish our strain measures.

If two material points before deformation have the coordinates (X_i) and ($X_i + dX_i$) and after deformation have the coordinates (x_i) and ($x_i + dx_i$), the initial distance between these neighboring points is given by

$$dS^2 = \sum_i dX_i dX_i = (dX_1)^2 + (dX_2)^2 + (dX_3)^2 \tag{3.23}$$

and the final distance between the points by

$$ds^2 = \sum_i dx_i dx_i = \sum_{i,j,m} \frac{\partial x_m}{\partial X_i} \frac{\partial x_m}{\partial X_j} dX_i dX_j \tag{3.24}$$

Only in the event of stretching or straining is ds^2 different from dS^2, that is,

$$ds^2 - dS^2 = ds^2 - \sum_i dX_i dX_i = \sum_{i,j,m} \left[\frac{\partial x_m}{\partial X_i} \frac{\partial x_m}{\partial X_j} - \delta_{ij} \right] dX_i dX_j \tag{3.25}$$

is a measure of the relative displacements. It is insensitive to rotation as can be easily demonstrated by considering a rigid-body motion. These equations can be written as

$$ds^2 - dS^2 = \sum_{i,j} 2E_{ij} dX_i dX_j, \qquad E_{i,j} = \frac{1}{2} \sum_m \left[\frac{\partial x_m}{\partial X_i} \frac{\partial x_m}{\partial X_j} - \delta_{ij} \right] \tag{3.26}$$

by introducing the strain measure E_{ij}. It is easy to observe that E_{ij} is a symmetric tensor of the second order. It is called the Lagrangian strain tensor. It is convenient to deal with displacements and displacement gradients instead of the deformation gradient. These are obtained by using the relations

$$x_m = X_m + u_m, \qquad \frac{\partial x_m}{\partial X_m} = \frac{\partial u_m}{\partial X_i} + \delta_{im} \tag{3.27}$$

Or from the small strain theory by considering the Green strain tensor **E**, defined with respect to the reference configuration:

$$\mathbf{E}=\frac{1}{2}(\mathbf{C}-\mathbf{I}) \tag{3.28}$$

Working in indicial notation, we can write **E**, the Lagrangian strain tensor, in terms of the displacement tensor u as follows:

$$\begin{aligned} E_{IJ} &= \frac{1}{2}\left(C_{IJ}-\delta_{IJ}\right)=\frac{1}{2}\left(F_{iI}F_{iJ}-\delta_{IJ}\right) \\ &= \frac{1}{2}\left(\frac{\partial}{\partial X_I}(u_i+X_i)\frac{\partial}{\partial X_J}(u_i+X_i)-\delta_{IJ}\right) \\ &= \frac{1}{2}\left(\left(\frac{\partial u_i}{\partial X_I}+\delta_{iI}\right)+\left(\frac{\partial u_i}{\partial X_J}+\delta_{iJ}\right)-\delta_{IJ}\right) \\ &= \frac{1}{2}\left(\delta_{iI}\frac{\partial u_i}{\partial X_J}+\delta_{iJ}\frac{\partial u_i}{\partial X_I}+\frac{\partial u_i}{\partial X_J}\frac{\partial u_i}{\partial X_I}\right) \end{aligned} \tag{3.29}$$

Where δ_{IJ}, the *Kronecker delta*, satisfies

$$\delta_{IJ}=\begin{cases}1 & if \;\; I=J \\ 0 & otherwise\end{cases} \tag{3.30}$$

Expressing E_{IJ} in unabridged notations

$$\begin{aligned}
E_{11} &= \frac{\partial u_1}{\partial X_1}+\frac{1}{2}\left[\left(\frac{\partial u_1}{\partial X_1}\right)^2+\left(\frac{\partial u_2}{\partial X_1}\right)^2+\left(\frac{\partial u_3}{\partial X_1}\right)^2\right] \\
E_{22} &= \frac{\partial u_2}{\partial X_2}+\frac{1}{2}\left[\left(\frac{\partial u_1}{\partial X_2}\right)^2+\left(\frac{\partial u_2}{\partial X_2}\right)^2+\left(\frac{\partial u_3}{\partial X_2}\right)^2\right] \\
E_{11} &= \frac{\partial u_3}{\partial X_3}+\frac{1}{2}\left[\left(\frac{\partial u_1}{\partial X_3}\right)^2+\left(\frac{\partial u_2}{\partial X_3}\right)^2+\left(\frac{\partial u_3}{\partial X_3}\right)^2\right] \\
E_{12} &= E_{21}=\frac{1}{2}\left(\frac{\partial u_1}{\partial X_3}+\frac{\partial u_2}{\partial X_3}\right)+\frac{1}{2}\left[\left(\frac{\partial u_1}{\partial X_2}\frac{\partial u_1}{\partial X_3}\right)+\left(\frac{\partial u_2}{\partial X_2}\frac{\partial u_2}{\partial X_3}\right)+\left(\frac{\partial u_3}{\partial X_2}\frac{\partial u_3}{\partial X_3}\right)\right] \\
E_{13} &= E_{31}=\frac{1}{2}\left(\frac{\partial u_3}{\partial X_3}+\frac{\partial u_1}{\partial X_3}\right)+\frac{1}{2}\left[\left(\frac{\partial u_1}{\partial X_1}\frac{\partial u_1}{\partial X_3}\right)+\left(\frac{\partial u_2}{\partial X_1}\frac{\partial u_2}{\partial X_3}\right)+\left(\frac{\partial u_3}{\partial X_1}\frac{\partial u_3}{\partial X_3}\right)\right] \\
E_{12} &= E_{21}=\frac{1}{2}\left(\frac{\partial u_1}{\partial X_3}+\frac{\partial u_2}{\partial X_3}\right)+\frac{1}{2}\left[\left(\frac{\partial u_1}{\partial X_1}\frac{\partial u_1}{\partial X_2}\right)+\left(\frac{\partial u_2}{\partial X_1}\frac{\partial u_2}{\partial X_2}\right)+\left(\frac{\partial u_3}{\partial X_1}\frac{\partial u_3}{\partial X_2}\right)\right]
\end{aligned} \tag{3.31}$$

3.2.4 Rates of deformation

Most of the industrial metal forming processes is characterized by a complex deformation history, which is composed of successive *strain paths* that may vary considerably in their orientation. Changes in strain path directions have a significant effect on the mechanical response of metals. Therefore, in order to cope up with path-dependence property of a material, a rate form definition of strain is necessary.

The material velocity **V'** can be obtained by fixing attention on a particular material particle (i.e., fixing the reference coordinate **X**), and then considering partial time derivatives of the motion. This can be written mathematically as

$$\mathbf{V'}(\mathbf{X},t) = \frac{\partial}{\partial t}\varphi(\mathbf{X},t) \tag{3.32}$$

The gradient grad(**v**) is taken with respect to spatial coordinates and is, therefore, called the spatial velocity gradient or rate of change of deformation gradient. It is denoted as **L**:

$$\mathbf{L} = \text{grad}\,(\mathbf{v}) \tag{3.33a}$$

Here the differential velocity between two neighboring particles in the current configuration becomes

$$d\mathbf{v'} = \frac{\partial \mathbf{v'}}{\partial \mathbf{x}} d\mathbf{x} = \frac{\partial \mathbf{v'}}{\partial \mathbf{X}} \frac{\partial \mathbf{X}}{\partial \mathbf{x}} d\mathbf{x} = \mathbf{L}d\mathbf{x} = \mathbf{L}\mathbf{F}d\mathbf{X}$$

$$or \qquad d\mathbf{v'} = d\dot{\mathbf{x}} = \frac{\partial}{\partial t}\left(\mathbf{F}d\mathbf{X}\right) = \dot{\mathbf{F}}d\mathbf{X} \tag{3.33b}$$

Comparing the above two equations reveals that the rate of change of deformation gradient, **L**, can be computed as

$$\mathbf{L} = \dot{\mathbf{F}}\mathbf{F}^{-1} \tag{3.33c}$$

From the rate of change of deformation gradient **L** defined in (3.33), we can define two tensors, considering the polar decomposition theorem, and known respectively as the *rate of deformation tensor*, **D**, (or the stretching tensor) and *the spin tensor,* **W**, (*or vorticity tensor*):

$$\mathbf{D} = \frac{1}{2}\left[\mathbf{L} + \mathbf{L}\right] \qquad and \qquad \mathbf{W} = \frac{1}{2}\left[\mathbf{L} - \mathbf{L}\right] \tag{3.34}$$

It is clear that **D** is merely the symmetric part of the velocity gradient, while **W** is the antisymmetric, or skew, portion. The quantities **D** and **W** are spatial measures of deformation. **D**

is effectively a measure of strain rate suitable for large deformations, while **W** provides a local measure of the rate of rotation of the material. It is of interest at this point to discuss whether appropriate material counterparts of these objects exist. Toward this end let us calculate the material time derivative of the deformation gradient **F**, noting in so doing that if **F** is an analytic function, then the order of partial differentiation can be reversed:

$$\dot{\mathbf{F}} = \frac{\partial}{\partial t}\left[\frac{\partial}{\partial \mathbf{X}}\varphi(\mathbf{X},t)\right] = \frac{\partial}{\partial \mathbf{X}}\left[\frac{\partial}{\partial t}\varphi(\mathbf{X},t)\right] = \frac{\partial \mathbf{V}}{\partial \mathbf{X}} \tag{3.35}$$

Recalling the definition for the right Cauchy-Green strain tensor **C** (equation 3.17), we compute its material time derivative via:

$$\begin{aligned}
\dot{\mathbf{C}} &= \frac{\partial}{\partial t}\left[\mathbf{F}^T\mathbf{F}\right] = \dot{\mathbf{F}}^T\mathbf{F} + \mathbf{F}^T\dot{\mathbf{F}} \\
&= \left(\frac{\partial}{\partial \mathbf{X}}\left(\frac{\partial \mathbf{x}}{\partial t}\right)\right)^T \mathbf{F} + \mathbf{F}^T\frac{\partial}{\partial \mathbf{X}}\left(\frac{\partial \mathbf{x}}{\partial t}\right) \\
&= \left(\frac{\partial v}{\partial \mathbf{X}}\right)^T \mathbf{F} + \mathbf{F}^T\frac{\partial v}{\partial \mathbf{X}} = \left(\frac{\partial v}{\partial \mathbf{x}}\frac{\partial \mathbf{x}}{\partial \mathbf{X}}\right)^T \mathbf{F} + \mathbf{F}^T\left(\frac{\partial v}{\partial \mathbf{x}}\frac{\partial \mathbf{x}}{\partial \mathbf{X}}\right) \\
&= (\mathbf{LF})^T\mathbf{F} + \mathbf{F}^T(\mathbf{LF}) = \mathbf{F}^T\mathbf{L}^T\mathbf{F} + \mathbf{F}^T\mathbf{LF} \\
&= \mathbf{F}^T\left(\mathbf{L} + \mathbf{L}^T\right)\mathbf{F}
\end{aligned} \tag{3.36}$$

From equation 3.36, we can conclude that

$$\dot{\mathbf{C}}(\mathbf{X},t) = 2\mathbf{F}^T(\mathbf{X},t)\mathbf{D}(\varphi(\mathbf{X}),t)\mathbf{F}(\mathbf{X},t) \tag{3.37}$$

Recalling the definition of Green's strain **E** given in Equation (3.28), we can easily see that

$$\dot{\mathbf{E}} = \frac{\mathbf{1}}{\mathbf{2}}\dot{\mathbf{C}} = \mathbf{F}^T\mathbf{DF} \tag{3.38}$$

3.2.5 Stress and Stress measures

Stress is the force per unit area. Just as the strain, it can be defined in the deformed or the undeformed state. We consider an element of a material body shown in figure 3.7 which is subject to resultant forces $d\overline{\mathbf{T}}$ and $d\mathbf{T}$ in the initial and final configurations, respectively. In Figure (3.7a) the force vector $d\overline{\mathbf{T}}$ is shown for an initial surface element dA_0, with normal $\mathbf{n}_o$ directing perpendicular to the surface element dA_0. And the force vector $d\mathbf{T}$ for a current

(final) surface element dA, with normal $\mathbf{n}$ directing perpendicular to the surface element dA is shown in figure (3.7b).

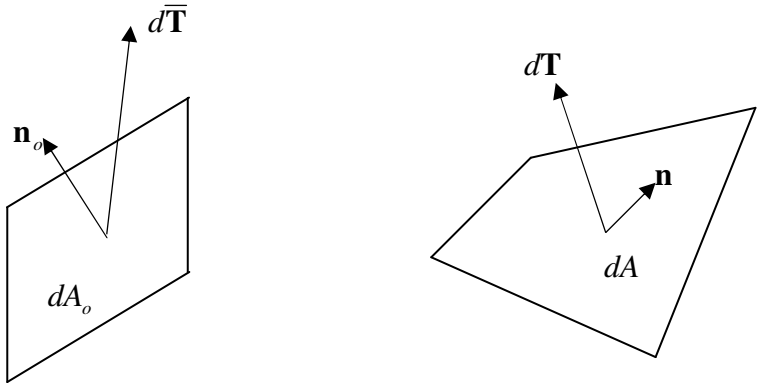

(a) Initial Configuration

(b)Final Configuration

Figure 3.6 Force vectors and surfaces with normal in the initial and final configuration

The Cauchy stress $\boldsymbol{\sigma}$, which is the most useful measures of stress, is defined by the actual force on the deformed surface. Hence it is also called the true stress. It is an objective tensor, which is symmetric when distributed moments or couple stresses are absent.

From Nanson's formula,

$$\mathbf{n}dA = \mathbf{J}\,\mathbf{F}^{-T}\mathbf{n}_0\,dA_0 \tag{3.39a}$$

which can be written as $$\mathbf{n}dA = \mathbf{J}\mathbf{F}^{T}\boldsymbol{\sigma}\mathbf{n}_o dA \tag{3.39b}$$

we find the following definition:

$$\mathbf{P}(\mathbf{x}) = \mathbf{J}(\mathbf{x})\boldsymbol{\sigma}(\varphi_t(\mathbf{X}))\mathbf{F}^{-T}(\varphi_t(\mathbf{X})) \tag{3.39c}$$

where $\mathbf{P}(\mathbf{x})$ is called the (First) Piola-Kirchhoff Stress and $\mathbf{J}$ is the determinant of the deformation gradient $\mathbf{F}$ as discussed earlier.

Equation (3.39c) allows us to write $$d\overline{\mathbf{T}} = \mathbf{S}\ \mathbf{n}_o dA_o \tag{3.39d}$$

The stress $\mathbf{S}$ is called the second Piola-Kirchhoff stress and it is a purely reference object. The product $\mathbf{S}\mathbf{n}_o$ represents traction. It means the stress by referencing the force acting on areas to the magnitude of these areas in their undeformed configuration. It is neither a pure spatial nor

reference object. Such an object can be constructed by performing a pull-back of the spatial Cauchy tress tensor $\boldsymbol{\sigma}$ to the reference configuration:

$$\begin{aligned}\mathbf{S}(x) &= \mathbf{J}(x)\mathbf{F}^{-1}(\varphi_t(X)\boldsymbol{\sigma}(\varphi_t(X)\mathbf{F}^{-T}(\varphi_t(X) \\ &= \mathbf{F}^{-1}(\varphi_t(X)\mathbf{p}(x)\end{aligned} \tag{3.39e}$$

To consider changes of a body from an initial state to a current state, a lagrangian view is used because strain is usually measured from the former state. That corresponding to the Green-Lagrange strain is the second Piola-Kirchhoff symmetric stress tensor, often abbreviated to "PK2 stress" (equation 3.39e). The three-dimensional component expression of this tensor in Cartesian coordinates is

$$\mathbf{S} = \begin{bmatrix} S_{11} & S_{12} & S_{13} \\ S_{21} & S_{22} & S_{23} \\ S_{31} & S_{32} & S_{33} \end{bmatrix} \tag{3.40}$$

The relation between the Cauchy stress and the Piola-Kirchhoff stresses are,

$$\begin{aligned}\boldsymbol{\sigma} = \mathbf{J}^{-1}\mathbf{F}.\mathbf{P} \quad &\Leftrightarrow \quad \mathbf{P} = \mathbf{J}\mathbf{F}^{-1}.\boldsymbol{\sigma} \\ \boldsymbol{\sigma} = \mathbf{J}^{-1}\mathbf{F}.\mathbf{S}.\mathbf{F}^{T} \quad &\Leftrightarrow \quad \mathbf{S} = \mathbf{J}\mathbf{F}^{-1}\boldsymbol{\sigma}\mathbf{F}^{-T}\end{aligned} \tag{3.41}$$

For small deformations all stress measures coincide with the Cauchy stress. In plasticity it is convenient to split the stress tensor into two parts, one called the spherical stress tensor and the other the stress deviator tensor. The spherical stress tensor H_{ij} is the tensor whose elements are given by $\sigma_m \delta_{ij}$, where σ_m is the mean stress, i.e.

$$H_{ij} = \sigma_m \delta_{ij} = \begin{bmatrix} \sigma_m & 0 & 0 \\ 0 & \sigma_m & 0 \\ 0 & 0 & \sigma_m \end{bmatrix} \tag{3.42}$$

and $$\sigma_m = \frac{1}{3}(\sigma_1 + \sigma_2 + \sigma_3) \tag{3.43}$$

Since σ_m is the same in all directions, it can be considered to act as a hydrostatic stress. From experimental observations of metal alloys, it is shown that the mean, hydrostatic, or spherical pressure on the process of shape changing is negligible [3]. Therefore, in plastic flow

considerations, one considers only the difference between the stress tensor and the spherical stress tensor. This is termed the stress deviator tensor, given by p_{ij}, where

$$p_{ij} = \sigma_{ij} - S_{ij} = \begin{bmatrix} \sigma_{11} - \sigma_m & \sigma_{12} & \sigma_{13} \\ \sigma_{21} & \sigma_{22} - \sigma_m & \sigma_{23} \\ \sigma_{31} & \sigma_{32} & \sigma_{33} - \sigma_m \end{bmatrix} \tag{3.44}$$

Every stress measures used must be complementary (work conjugate) to the strain measures used. i.e., an increment of strain multiplied by the current stress must be a valid infinitesimal increment in work per unit of volume of material. Therefore, the work conjugate strain measure related to the above stress measure is the rate of lagrangian strain, $\dot{\mathbf{E}}$ previously defined. Now, the power P per unit initial volume is

$$P = \mathbf{S} : d\mathbf{E} \tag{3.45}$$

and the increment of work is, with $d\mathbf{E} = \dot{\mathbf{E}}\, dt$,

$$dW = \mathbf{S} : d\mathbf{E} \tag{3.46}$$

A transformation from one stress measure to another can be readily done. The measures are related according to

$$\mathbf{S} = J\mathbf{F}^{-1}\boldsymbol{\sigma}(\mathbf{F}^{-1})^T \qquad or \qquad \boldsymbol{\sigma} = J^{-1}\mathbf{F}\mathbf{S}\mathbf{F}^T \tag{3.47}$$

The above mentioned stress and strain measures are commonly used.

3.3. Fundamentals of Metal Plasticity

The adjective “plastic” comes from a Greek word meaning “to shape”. If we take the weak (Cauchy) definition of an elastic body as one in which the strain at any point of the body is completely determined by the current stress at the point, then an obvious definition of a plastically deformed body is one in which there is something else, besides the current stress, which determines the strain. That “something else” may be thought of, for example, as the past history of the stress at the point.

The theory of plasticity makes use of some fundamental concepts: the yield criterion defining the limit; the flow rule describing the relationship between stresses and strains once the material has become plastic; and the consistency condition which prevents stresses from exceeding the yield

limit. From experimental observations made on metal alloys it is found out that shape changes occur in the plastic shaping process. In metal plasticity the theory necessary to describe plastic flow is particularly simple since metals are generally incompressible, and insensitive to the influence of hydrostatic pressure.

3.3.1 The yield criterion

A material yields when it exhibits an irreversible straining which is sustained once a certain level of the stress distribution is reached. A yield criterion indicates for which combination of stress components transition from elastic (recoverable) to plastic (permanent) deformations occurs. In one-dimension yielding occurs when the uniaxial stress reaches the value of the yield stress σ_Y in tension, i.e. at $\sigma = \sigma_Y$. When does 'yielding' occurs in multi-axial stress states? The answer is given with phenomenological theories called 'yield criteria'. Here only the two most important yield criteria for isotropic materials will be discussed.

Since plasticity is the study of materials under stresses exceeding the yielding point, one needs to understand the concept of yield surface for a more expanded view of the subject. The yield surface is defined in the stress space as the separator convex surface between elastic and plastic regions. Any point within the region will cause no permanent deformation upon unloading. No points are considered outside the surface, but inside and on it only. When a point is considered on the surface, three different conditions are possible to occur: unloading, neutral loading, and loading. If unloading, the state of stress will go back into the surface again, causing it to move back to the elastic domain. In this condition, plasticity will not occur. If neutral loading occurs, the state of stress will move on the yield surface, causing no plasticity to occur. In plastic loading with perfect plasticity, the state of stress can only be altered by redistribution between the different stress components.

3.3.1.1 The von-Mises yield criterion

According to the von-Mises yield criterion, in a general multi-dimensional stress state, yielding occurs when the von-Mises equivalent stress becomes equal to the yield stress σ_Y in tension, i.e. yield occurs when:

$$\sigma_{EQ} = \sigma_Y$$

where σ_{EQ} is an equivalent stress defined, in terms the principal components and in terms of the stress components in the 1, 2,and 3 coordinate systems respectively, by

$$\sigma_{EQ} = \frac{1}{2}\sqrt{(\sigma_1 - \sigma_2)^2 + (\sigma_2 - \sigma_3)^2 + (\sigma_3 - \sigma_1)^2}$$

$$= \frac{1}{\sqrt{2}}\sqrt{(\sigma_{11} - \sigma_{22})^2 + (\sigma_{22} - \sigma_{33})^2 + (\sigma_{33} - \sigma_{11})^2 + 6(\tau_{12}^2 + \tau_{23}^2 + \tau_{31}^2)} \tag{3.48}$$

where σ_i is a principal stress and σ_{ij}, τ_{ij} are stress components. Note that the two equations above are equivalent (i.e. the right hand side of the second equation of Equation (3.48) is invariant – does not change as we 'rotate' the stress components from one coordinate system to another).

As expected (and by an obvious design of the von-Mises criterion), for uniaxial tension the von-Mises yield criterion predicts that yielding occurs when:

$$\sigma_{EQ} = \sigma_1 = \sigma_y \tag{3.49}$$

The von-misses yield criterion is better and more accurate because it considers all the three principal shear stresses, i.e., the maximum shear stress and the two lesser shear stresses.

3.3.1.2 The Tresca (the Maximum shear stress) criterion

According to Tresca, in the general multi-dimensional stress state, yielding occurs when:

$$\tau_{\max} = \kappa \qquad \text{Where } \kappa \text{ is the yield stress in shear} \tag{3.50}$$

Recall that:

$$\tau_{\max} = \frac{\sigma_{\max} - \sigma_{\min}}{2}$$
$$= \max\left(\frac{1}{2}|\sigma_1 - \sigma_2|, \frac{1}{2}|\sigma_2 - \sigma_3|, \frac{1}{2}|\sigma_3 - \sigma_1|\right) \tag{3.51}$$

The yield stress κ in shear is not independent of the yield stress σ_Y in uniaxial tension. To compute their relation, we have to apply the Tresca criterion to uniaxial tension. For this case, $\sigma_1 \neq 0$ and $\sigma_2 = \sigma_3 = 0$. So we can write:

$$\tau_{\max} = \frac{\sigma_{\max} - \sigma_{\min}}{2} = \frac{\sigma_1 - 0}{2} = \frac{\sigma_1}{2} = \kappa \tag{3.52}$$

From this we can conclude that in uniaxial tension yielding occurs when $\sigma_1 = 2\kappa$, i.e.

$$\text{For the Tresca criterion:} \qquad \kappa = \frac{\sigma_Y}{2} \tag{3.53}$$

Using the above expression, we can summarize the Tresca yield criterion as follows:

$$\text{In a general stress state yielding occurs when:} \quad \tau_{max} = \frac{\sigma_{max} - \sigma_{min}}{2} = \kappa = \frac{\sigma_Y}{2} \tag{3.54}$$

3.3.2 Hardening

Metals exhibit some degree of hardening as an accompaniment to plastic straining. In general this means that the shape and size of the yield surface changes during plastic loading. These changes may be rather arbitrary and extremely difficult to describe accurately. Therefore, hardening is often described by a combination of two specific types of hardening, namely isotropic hardening and kinematic hardening see figure (3.7). For the von Mises criterion isotropic hardening implies an increase in the yield strength during plastic loading such that the yield criterion may be written as [21]

$$f(\sigma) - \sigma_0(\alpha) = 0 \tag{3.55}$$

Where f is loading function and α ,which has a positive value, is a hardening parameter. The stress can be related to the strain by the introduction of a tangent modulus E_t as

$$d\sigma = E_t d\varepsilon \tag{3.56}$$

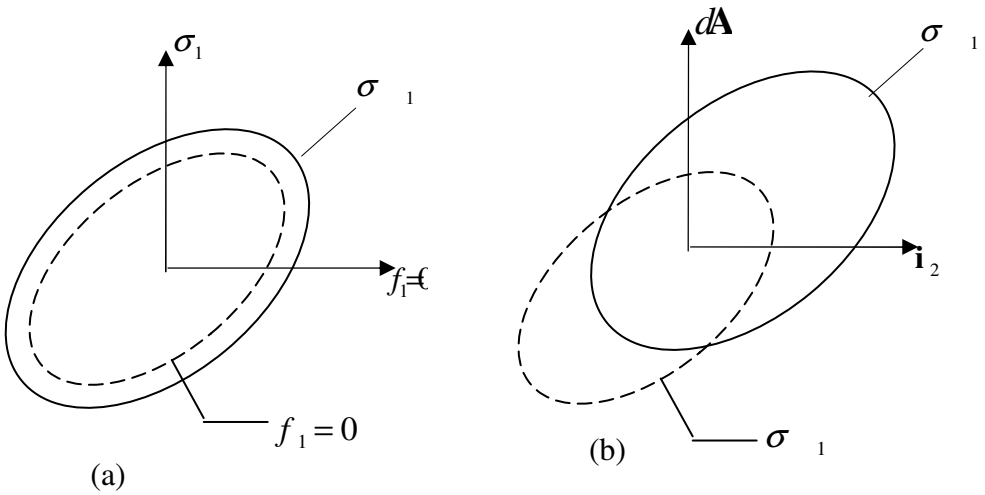

Figure 3.7 (a) Isotropic (b) Kinematic Hardening

The representation of the total strain as the sum of the elastic and plastic strain leads to

$$d\sigma = E_t(d\varepsilon^e + d\varepsilon^p) \tag{3.57}$$

For the elastic part of the strain increment Hook's law is used to give

$$d\sigma = E_t(\frac{d\sigma}{E} + d\varepsilon^P) \tag{3.58}$$

This relates the stress increment to the plastic strain increment by

$$(\frac{1}{E_t} - \frac{1}{E})d\sigma = d\varepsilon_p \tag{3.59}$$

Assuming isotropic hardening, an increase in stress above the elastic limit is equivalent to an increase in yield stress, and hence

$$\frac{d\sigma}{d\varepsilon^p} = \frac{d\sigma_0}{d\varepsilon^p} = H$$

$$\text{Where} \qquad H = \frac{E_t}{1 - E_t/E} \tag{3.60}$$

This means that α in equation (3.55) should be replaced by ε^p. In multidimensional case, however, some equivalent plastic strain must be used. For the von Mises criterion a suitable equivalent plastic strain is [21]

$$d\varepsilon^p_{eq} = \sqrt{\frac{2}{3}\left[(d\varepsilon^p_1)^2 + (d\varepsilon^p_2)^2 + (d\varepsilon^p_3)^2\right]} \tag{3.61}$$

Since isotropic hardening is irreversible, once the material has experienced a certain degree of hardening the yield limit is shifted permanently. It is easily included into the elasto-plastic stress-strain relation by considering the appropriate consistency condition. The consistency condition states that during plastic loading the change in stress, if any, occurs tangent to the yield surface. And this results in

$$\frac{\partial f}{\partial \sigma} d\sigma - \frac{\partial \sigma_0}{\partial \alpha} d\alpha = 0 \tag{3.62}$$

This conditions leads to the following elasto-plastic constitutive relation

$$d\boldsymbol{\sigma} = \left(\mathbf{D^e} - \frac{\mathbf{D^e} \dfrac{\partial g}{\partial \boldsymbol{\sigma}} \left(\dfrac{\partial f}{\partial \boldsymbol{\sigma}} \right)^T \mathbf{D^e}}{\mathbf{H} + \left(\dfrac{\partial f}{\partial \boldsymbol{\sigma}} \right)^T \mathbf{D^e} \dfrac{\partial g}{\partial \boldsymbol{\sigma}}} \right) d\varepsilon \tag{3.63}$$

where $\mathbf{D^e}$ is the elastic constitutive matrix.

3.3.3 Incremental Elastic-plastic Stress-Strain Relations

The basic premise in the formulation of all elastic-plastic constitutive models is that certain materials are capable of undergoing small plastic (permanent) strains as well as small elastic (recoverable) strains during each loading increment (Baladi and Akers 1981). This may be expressed mathematically as

$$d\varepsilon_{ij} = d\varepsilon_{ij}^e + d\varepsilon_{ij}^p \tag{3.64}$$

Where $d\varepsilon_{ij}$ = components of the total strain increment tensor,

$d\varepsilon_{ij}^e$ = components of the elastic strain increment tensor, and

$d\varepsilon_{ij}^p$ = components of the plastic strain increment tensor.

This equation simply states that the total strain increment is equal to the sum of the elastic and plastic strain increments.

The loading or yield function f for a general work- or strain-hardening elasto-plastic model may be rewritten as [21]:

$$f(\sigma_{ij}, \alpha) = F(\sigma_{ij}) - K(\varepsilon) = 0 \tag{3.65}$$

where (in matrix format) σ_{ij} is the vector of normal and shear stresses and α is the hardening parameter that controls the expansion of the yield surface.

Equation 3.56 may be differentiated to give:

$$df = \frac{\partial f}{\partial \sigma_{ij}} d\sigma_{ij} + \frac{\partial f}{\partial \alpha} d\alpha \tag{3.66}$$

Or, in another form

$$a_{ij}^T d\sigma_{ij} - A d\lambda = 0 \tag{3.67}$$

$$\text{where} \quad a_{ij}^T = \frac{\partial f}{\partial \boldsymbol{\sigma}} = \frac{\partial f}{\partial \sigma_{ij}} \quad \text{and} \quad A = -\frac{1}{d\lambda} = \frac{\partial f}{\partial \alpha} d\alpha \tag{3.68}$$

Owen and Hinton refer to the vector a_{ij} as the flow vector. The scalar A will be identified as the plastic hardening modulus.

Drucker (1951) has shown that the plastic strain increment tensor for a work-hardening material may be written as

$$d\varepsilon_{ij}^p = \begin{cases} d\lambda \dfrac{\partial f}{\partial \sigma_{ij}} & \text{if} \quad f = 0 \quad \text{and} \quad \dfrac{\partial f}{\partial \sigma_{ij}} d\sigma_{ij} > 0 \\ 0 & \text{if} \quad f < 0 \quad \text{or} \quad \dfrac{\partial f}{\partial \sigma_{ij}} d\sigma_{ij} \le 0 \end{cases} \tag{5.69}$$

The term $d\lambda$ is a positive factor of proportionality that is nonzero only when plastic deformations occur.

In its most general form, the elastic strain increment tensor may be expressed as

$$d\varepsilon_{ij}^e = C_{ijkl} d\sigma_{kl} \tag{3.70}$$

where C_{ijkl} = the material response function, which may be a function of stress.

By substituting for both the elastic and plastic strain increments, i.e., using the matrix equivalents of Equations 3.69 and 3.70, the following expression is obtained:

$$d\boldsymbol{\varepsilon} = \mathbf{D}^{-1} d\boldsymbol{\sigma} + d\lambda \frac{\partial f}{\partial \boldsymbol{\sigma}} \tag{3.71}$$

Where **D** is the matrix of elastic material constants and the inverse of the material response function. After multiplying Equation 3.71 by a_{ij}^T one obtains:

$$\mathbf{a}^T \mathbf{D}\, d\boldsymbol{\varepsilon} = \mathbf{a}^T d\boldsymbol{\sigma} + \mathbf{a}^T \mathbf{D}\, \mathbf{a}\, d\lambda \tag{3.72}$$

This may be refined further by eliminating $\mathbf{a}^T d\boldsymbol{\sigma}$ with the use of Equation 3.71 to produce:

$$\mathbf{a}^T \mathbf{D} d\boldsymbol{\varepsilon} = \left[\mathbf{A} + \mathbf{a}^T \mathbf{D} \mathbf{a}\right] d\lambda \tag{3.73}$$

where $\mathbf{A} = \dfrac{\mathbf{a}^T \mathbf{D}}{d\lambda}$

This leads to an expression for the scalar term $d\lambda$:

$$d\lambda = \frac{\mathbf{a}^T \mathbf{D}\, d\boldsymbol{\varepsilon}}{\left[\mathbf{A} + \mathbf{a}^T \mathbf{D}\, \mathbf{a}\right]} \tag{3.74}$$

This term gives the magnitude of the plastic strain increment vector. Having defined an expression for $d\lambda$, it may be substituted into Equation 3.71 to give:

$$\mathbf{D}^{-1} d\boldsymbol{\sigma} = \left\{1 - \frac{\mathbf{d}_D^T\, \mathbf{a}}{\mathbf{A} + \mathbf{d}_D^T\, \mathbf{a}}\right\} d\boldsymbol{\varepsilon} \tag{3.75}$$

where $\mathbf{d}_\mathbf{D}^\mathbf{T} = \mathbf{a}^T \mathbf{D}$

Multiplying both sides of Equation 3.75 by D gives:

$$d\boldsymbol{\sigma} = \left\{\mathbf{D} - \frac{\mathbf{D}\mathbf{a}\mathbf{d}_D^T}{\mathbf{A} + \mathbf{d}_D^T \mathbf{a}}\right\} d\boldsymbol{\varepsilon} \tag{3.76}$$

This is an expression for the elastic-plastic incremental stress-strain relation. If we substitute $\mathbf{d}_\mathbf{D}^\mathbf{T} = \mathbf{a}^T \mathbf{D}$, then the elastic-plastic constitutive matrix $\mathbf{D}^{ep}$ may be expressed as:

$$\begin{aligned} \mathbf{D}^{ep} &= \frac{d\boldsymbol{\sigma}}{d\boldsymbol{\varepsilon}} \\ &= \left\{\mathbf{D} - \frac{\mathbf{D}\mathbf{a}\mathbf{a}^T \mathbf{D}}{\mathbf{A} + \mathbf{a}^T \mathbf{D}\mathbf{a}}\right\} \end{aligned} \tag{3.77}$$

3.4 Frame Indifference

An important concept to be considered in the formulation of constitutive theories in metal forming is that of frame indifference, alternatively referred to as objectivity.

When we write constitutive laws in metal forming problems, in their most general forms, we seek to express tensorial quantities, such as stress and stress rate, in terms of kinematic tonsorial quantities, most commonly strain and strain rate. The basic physical idea behind frame indifference is that this constitutive relationship should be unaffected by any rigid body motion the material may be undergoing at the instant in question. Mathematically we describe this situation by defining an alternative reference frame that is rotating and translating with respect to the coordinate system in which we pose the problem. For our constitutive description to make sense, the tensorial quantities we use in it (stress, stress rate, strain, and strain rate) should simply transform according to the laws of tensor calculus when subjected to this transformation. If a given quantity does this we say it is material frame indifferent, and if it does not we say it is not properly invariant.

Consider again a motion $\varphi(\mathbf{X},t)$. We imagine ourselves to be viewing this motion from another reference frame, denoted in the following by *, which can be related to the original spatial frame via

$$\mathbf{x}^* = \mathbf{c}(t) + \mathbf{Z}(t)\mathbf{x} \tag{3.78}$$

where $\mathbf{x} = \varphi(\mathbf{X},t)$. In equation (3.78) $\mathbf{c}(t)$ is a relative rigid body translation between the original frame and observer *, while a relative rotation is produced by the proper orthogonal tensor **Z**(t). To observer * the motion appears as defined by

$$\mathbf{x}^* = \varphi^*(\mathbf{X},t) = \mathbf{c}(t) + \mathbf{Z}(t)\varphi(\mathbf{X},t) \tag{3.79}$$

Then for the * frame, we can define an appropriate deformation gradient:

$$\mathbf{F}^* = \frac{\partial}{\partial \mathbf{X}}\varphi^* = \mathbf{Z}\frac{\partial}{\partial \mathbf{X}}\varphi(\mathbf{X}) = \mathbf{ZF} \tag{3.80}$$

and a spatial velocity gradient $\mathbf{L}^*$:

$$\begin{aligned}\mathbf{L}^{*} = \dot{\mathbf{F}}^{*}\mathbf{F}^{*-1} &= \frac{d}{dt}(\mathbf{ZF})(\mathbf{ZF})^{-1} \\ &= (\mathbf{ZLZ}^{T} + \dot{\mathbf{Z}}\mathbf{Z}^{T})\end{aligned} \tag{3.81}$$

For $\mathbf{L}$ to be objective, it would transform according to the laws of tensor transformation between the two frames, so that only the first term on the right-hand side of equation (3.36) would be present. Clearly $\mathbf{L}$ is not objective.

Examining the rate of deformation tensor, on the other hand, we can find:

$$\begin{aligned}\mathbf{D}^{*} &= \frac{1}{2}\left(\mathbf{L}^{*} + (\mathbf{F}^{*})^{T}\right) \\ &= (\mathbf{ZLZ}^{T} + \dot{\mathbf{Z}}\mathbf{Z}^{T} + \mathbf{ZL}^{T}\mathbf{Z}^{T} + \mathbf{Z}\dot{\mathbf{Z}}^{T}) \\ &= \frac{1}{2}\mathbf{Z}\left(\mathbf{L} + \mathbf{L}^{T}\right)\mathbf{Z}^{T} = \mathbf{ZDZ}^{T}\end{aligned} \tag{3.82}$$

which shows that **D** is objective**.**

Therefore, we have a spatial rate-of-strain object, **D**, that is objective. The question arises about whether corresponding reference measures of rate are objective. It turns out that such material rates are automatically objective, since they do not change when superimposed rotations occur spatially. Considering, for example, the right Cauchy-Green tensor **C**:

$$\mathbf{C}^{*} = (\mathbf{F}^{*})^{T}\mathbf{F}^{*} = (\mathbf{ZF})^{T}\mathbf{ZF} = \mathbf{F}^{T}\mathbf{Z}^{T}\mathbf{ZF} \tag{3.83}$$

In view of equation (3.83) it is obvious that

$$\mathbf{C}^{*} = \mathbf{C} \tag{3.84}$$

Turning our attention to stress rates, let us examine the material time derivative of the Cauchy stress **T**:

$$\dot{\mathbf{T}} = \left[\frac{d}{dt}(\mathbf{T}\cdot\varphi_{t})\right]\cdot\varphi_{t}^{-1} = \left(\frac{\partial\mathbf{T}}{\partial t} + \mathbf{u}\cdot\nabla\mathbf{T}\right) \tag{3.85}$$

Now **T** is itself objective by its very definition as a tensorial quantity. Thus we can write

$$\mathbf{T} = \mathbf{ZTZ}^{T} \tag{3.86}$$

Computing the material time derivative of equation (3.86) we find

$$\dot{\mathbf{T}} = \dot{\mathbf{Z}}\mathbf{TZ}^{T} + \mathbf{Z}\dot{\mathbf{T}}\mathbf{Z}^{T} + \mathbf{ZT}\dot{\mathbf{Z}}^{T} \tag{3.87}$$

Since the first and third terms on the right-hand side of equation (3.87) do not, in general, cancel, we see that the material time derivative of the Cauchy stress is not objective. It, therefore, becomes critical, when a constitutive description requiring a stress rate is to be formulated, to

consider a frame indifferent measure of stress rate. The subject of objective rates is a controversial one in continuum mechanics. By far the most common choice in plasticity theory is the *Jaumann rate* or *corotational derivative*, which is the time derivative with respect to a corotating reference frame (Neale, 1981).

Now let us consider the Jaumann rate which rely on roughly the same physical idea: rather than taking the derivative of the Cauchy stress itself, we rotate the object from the spatial frame before taking the time derivative, so that the reference frame in which the time derivative is taken is the same for all frames related by the transformation equation (3.78). The Jaumann rate of stress, which we denote here as $\hat{\mathbf{T}}$, definition is given as follows:

$$\hat{\mathbf{T}} = \dot{\mathbf{T}} - \mathbf{WT} + \mathbf{TW} \tag{3.88}$$

where **W** and **T** are the spin and Cauchy stress tensors, respectively.

We can verify that this rate of stress is truly objective by direct calculation, by considering the object as it would appear to observer *:

$$\hat{\mathbf{T}}^* = \dot{\mathbf{T}}^* - \mathbf{W}^*\mathbf{T}^* + \mathbf{T}^*\mathbf{W}^* \tag{3.89}$$

After some calculation we arrive at

$$\hat{\mathbf{T}}^* = \mathbf{Z}\left[\dot{\mathbf{T}} - \mathbf{WT} + \mathbf{TW}\right]\mathbf{Z}^T = \mathbf{Q}\hat{\mathbf{T}}\mathbf{Q}^T \tag{3.90}$$

Which ensures us that, indeed, $\hat{\mathbf{T}}$ is objective.

CHAPTER FOUR

4. METAL FORMING PROBLEM FORMULATION

In forming processes, a piece of material called a work piece is formed into a specific shape by employing tools. The formed material is called the work piece, and the manner in which it is supported determines the type of the forming process. The forming is achieved trough the interaction between the work piece and the tools. The interaction forces are the contact forces which consist of normal components which prevent the objects from interpenetrating and tangential components, which are also known as the frictional components. The forming process hinges on the transfer of these forces from the work piece to the tool, and vice versa. Thus we need to determine these forces as accurately as possible if we wish to simulate the problem correctly.

In this section, implementation of a FEM analysis for finite elasto-plastic deformations and frictionless contact in metal forming processes is presented. The analysis of a continuum described in the previous chapter involves seeking the solution to equations governing the balance of linear momentum (equilibrium) and the conservation of energy, subject to appropriate initial and boundary conditions. In metal forming, there is a thermo-mechanical system which can be algorithmically divided into two sub-problems that are highly coupled, the mechanical sub problem (balance of momentum) and the thermal sub problem (energy conservation). Each of these sub problems is generally non-linear (geometric and/or material). In this thesis we consider an isothermal, isotropic problem; i.e., the deformation gradient due to temperature change is neglected and the material properties are independent of direction. The mechanical sub problem can be further divided into three main problems which represent distinct physical aspects of the deformation process, namely the kinematic, the constitutive and the frictionless-contact problems.

4.1 The Constitutive Problem

The constitutive model used in any analysis of metal forming process must represent properly the complex deformation and elasto-plastic properties of the material. The elasto-plastic constitutive model used in this thesis is that developed by Zabaras and Arif [2]. In the description of large elasto-plastic deformations, the multiplicative decomposition of the deformation gradient tensor $\mathbf{F}$ into its elastic $\mathbf{F}^e$ and plastic part $\mathbf{F}^p$ is assumed. The model is developed in stress-free intermediate configuration, and then all the constitutive relationships are transformed to the deformed configuration.

In the deformed configuration the following additive decomposition of the Almansi strain tensor $\mathbf{e}$ into the elastic and plastic parts, $\mathbf{e}^e$ and $\mathbf{e}^p$, respectively, is obtained:

$$\mathbf{e} = \mathbf{e}^e + \mathbf{e}^p \tag{4.1}$$

The Almansi strain tensor, and its elastic and plastic parts, $\mathbf{e}$, $\mathbf{e}^e$ and $\mathbf{e}^p$, can be expressed by the deformation gradient tensor $\mathbf{F}$ and its elastic $\mathbf{F}^e$ and plastic $\mathbf{F}^p$ parts in the following form [1]:

$$\begin{aligned}
\mathbf{e}^e &= \frac{1}{2}\left(\mathbf{I} - \left(\mathbf{F}^e\right)^{-T}\left(\mathbf{F}^e\right)^{-1}\right) \\
\mathbf{e}^p &= \frac{1}{2}\left(\left(\mathbf{F}^e\right)^{-T}\left(\mathbf{F}^e\right)^{-1} - \mathbf{F}^{-T}\mathbf{F}^{-1}\right) \\
\mathbf{e} &= \frac{1}{2}\left(\mathbf{I} - \mathbf{F}^{-T}\mathbf{F}^{-1}\right)
\end{aligned} \tag{4.2}$$

This indicates that the constitutive model consists of evolution equations for the Cauchy stress $\mathbf{T}$ and an internal scalar (or tensorial state variable), *s,* called the isotropic deformation resistance. Assuming a hypoelastic form of elasticity, the Jaumann rate, $\overset{\Delta}{\mathbf{T}}$, of the Cauchy stress is given as a linear isotropic function of the elastic rate of deformation, $\mathbf{D}^e$, which is here assumed to be the difference of the total, $\mathbf{D}$, and plastic, $\mathbf{D}^p$, deformation rates, respectively. Using the continuum mechanics notation of Zabaras [21] , we can write the following evolution equation:

$$\hat{\mathbf{T}} = \ell^e[\mathbf{D} - \mathbf{D}^p] \tag{4.1}$$

With the elastic isotropic moduli ℓ^e defined as

$$\ell^e = 2G\Im + \left(K - \frac{2}{3}G \right) \mathbf{I} \otimes \mathbf{I} \tag{4.2}$$

and where G and K are the shear and bulk moduli, respectively, and $\Im$ and $\mathbf{I}$ denote unit fourth and second order tensors, respectively. In this thesis, the symbol '[ ]' is reserved for the dot product between any fourth order tensor and any second order tensor, '$\bullet$' Is used for the dot product of any two second order tensors and '$\otimes$' is used for the dyadic product of two same order tensors.

A flow rule describing the plastic rate of deformation is defined as follows [2]:

$$\mathbf{D}^p = \sqrt{\frac{3}{2}} \dot{\overline{\varepsilon}}^p \mathbf{N}^p (\mathbf{T}', \tilde{\sigma}) \tag{4.3}$$

The unit direction $\mathbf{N}^p$ of the plastic rate of deformation is given using the normality rule

$$\mathbf{N}^p (\mathbf{T}', \tilde{\sigma}) = \sqrt{\frac{3}{2}} \frac{\mathbf{T}'}{\tilde{\sigma}} \tag{4.4}$$

where $\mathbf{T}'$ is the deviatoric part of the Cauchy stress and the equivalent stress is defined as

$$\tilde{\sigma} = \sqrt{\frac{2}{3} \mathbf{T}'.\mathbf{T}'} \tag{4.4}$$

In addition, the equivalent plastic strain rate is prescribed as a function of the current values of equivalent stress and state variable

$$\dot{\tilde{\varepsilon}}^p = f(\tilde{\sigma}, s) \tag{4.5}$$

To complete the flow rule for rate-dependent plasticity, the evolution equation of a scalar state variable takes the form

$$\begin{aligned} \dot{s} &= g(\tilde{\sigma}, s) \\ g(\tilde{\sigma}, s) &= h(s) \dot{\tilde{\varepsilon}}^p \end{aligned} \tag{4.6a}$$

where h(s) denotes a positive hardening function.

The selection of both functions $g(\tilde{\sigma}, s)$ and $f(\tilde{\sigma}, s)$ is based on phenomenological theories usually related to micromechanics. Equations 4.4 and 4.6 can also be written as

$$\begin{aligned} \tilde{\sigma}_{n+1} - \tilde{\sigma}_n + 3\mu \Delta t f(\tilde{\sigma}_{n+1}, s_{n+1}) &= 0 \\ s_{n+1} - s_n - \Delta t g(\tilde{\sigma}_{n+1}, s_{n+1}) &= 0 \end{aligned} \tag{4.6b}$$

Let us assume that at time t_n, the configuration $\mathbf{B}_n$ of the body and the pair of variables ($\mathbf{T}_n$, S_n) are known. At time $t_{n+1} = t_n + \Delta t$, the continuum is assumed to occupy the know configuration B_{n+1}. Then the problem is to determine the state ($\mathbf{T}_{n+1}, s_{n+1}$) at each material point in B_{n+1}, based on the given constitutive relations. From now on, $\mathbf{F}_{n+1}$ will denote the relative deformation gradient of the configuration B_{n+1} with respect to the configuration B_n ($\mathbf{F}_n = \mathbf{I}$).

4.1.1 Review of objectivity requirements

Two motions $\mathbf{x}(\mathbf{X}, t)$ and $\mathbf{x}^*(\mathbf{X}, t)$ are called objectively equivalent if and only if

$$\mathbf{x}^*(\mathbf{X}, t) = \mathbf{Z}(t)(\mathbf{x}(\mathbf{X},t)-\mathbf{0})+\mathbf{c}(t) \tag{4.7}$$

where $\mathbf{0}$ is a fixed point in space and the rigid body rotation $\mathbf{Z}(t)$ and translation $\mathbf{c}(t)$ are functions of time alone, of which $\mathbf{Z}(t)$ is subject to

$$\mathbf{Z}^T\mathbf{Z} = \mathbf{I} \quad \text{and} \quad \det \mathbf{Z} = 1 \tag{4.8}$$

Now, it can be shown that

$$\begin{aligned}
\mathbf{F}^* &= \frac{\partial \mathbf{x}^*}{\partial \mathbf{X}} = \mathbf{Z}\mathbf{F} \\
\mathbf{L}^* &= \dot{\mathbf{F}}^*\mathbf{F}^{*-1} = \dot{\mathbf{Z}}\mathbf{Z}^T + \mathbf{Z}\mathbf{L}\mathbf{Z}^T \\
\mathbf{D}^* &= \mathbf{Z}\mathbf{D}\mathbf{Z}^T \\
\mathbf{W}^* &= \dot{\mathbf{Z}}\mathbf{Z}^T + \mathbf{Z}\mathbf{W}\mathbf{Z}^T
\end{aligned} \tag{4.9}$$

where **F, D**, **W** and **L** represent the deformation gradient, rate of deformation, spin and velocity gradients in the $\mathbf{x}(\mathbf{X},t)$ motion, respectively and **F***, **D***, **W*** and **L*** represent the corresponding star quantities, respectively. In summary, a tensorial quantity is said to be objective or material frame-indifferent, if in any two objectively equivalent motions it obeys the appropriate tensor transformation law as given below for a vector **a**, second order tensor **B** and fourth order tensor $\boldsymbol{\xi}$:

$$\begin{aligned}
\mathbf{a}^* &= \mathbf{Z}\mathbf{a} \\
\mathbf{B}^* &= \mathbf{Z}\mathbf{B}\mathbf{Z}^T \\
\boldsymbol{\xi}^* &= \mathbf{Z}(\mathbf{Z}\boldsymbol{\xi}(\ )^T)\mathbf{Z}^T
\end{aligned} \tag{4.10}$$

Rotational –neutralized form of the constitutive model

Let us define the incremental rotation tensor **Q**(t), as the solution of the following initial value Problem:

$$\begin{aligned} &\dot{\mathbf{Q}}(t)\mathbf{Q}(t)^T = \mathbf{W}(t) \qquad t_n \le t \le t_{n+1} \\ &\mathbf{Q}(t) = \mathbf{I} \end{aligned} \tag{4.11}$$

where the spin tensor **W** is defined as the antisymmetric part of the velocity gradient **L**.

The following bar transformations, the stress-free intermediate configurations, of **x**, **F**, **A** (any second order symmetric tensor), and **Θ** (any fourth order isotropic tensor) are also defined as

$$\begin{aligned} &\overline{\mathbf{x}} = \mathbf{Q}^T\mathbf{x} \\ &\overline{\mathbf{F}} = \mathbf{Q}^T\mathbf{F} \\ &\overline{\mathbf{D}} = \mathbf{Q}^T\mathbf{D}\mathbf{Q} \\ &\overline{\mathbf{A}} = \mathbf{Q}^T\mathbf{A}\mathbf{Q} \\ &\overline{\mathbf{\Theta}} = \mathbf{Q}^T[\mathbf{Q}^T\mathbf{\Theta}\mathbf{Q}]\mathbf{Q} \end{aligned} \tag{4.12}$$

These pull back (rotation-neutralized) quantities (equation 4.12) with **Q** would be used to define a convenient framework to perform the integration of the constitutive model defined by equations (4.1) - (4.6).

Following the previous definitions, the pull back Cauchy stress with **Q** can be defined as

$$\overline{\mathbf{T}} = \mathbf{Q}^T\mathbf{T}\mathbf{Q} \tag{4.13}$$

Then, equation (4.1) takes the following simplified form:

$$\dot{\overline{\mathbf{T}}} = \mathbf{Q}^T\hat{\mathbf{T}}\mathbf{Q} = \overline{\ell}^e[\overline{\mathbf{D}}^e] = \overline{\ell}^e[\overline{\mathbf{D}} - \overline{\mathbf{D}}^p] \tag{4.14}$$

With

$$\begin{aligned} &\overline{\mathbf{D}}^p = \sqrt{\frac{3}{2}}\dot{\tilde{\varepsilon}}^p\overline{\mathbf{N}}^p(\overline{\mathbf{T}}', \tilde{\sigma}) \\ &\overline{\mathbf{N}}^p(\overline{\mathbf{T}}', \tilde{\sigma}) = \sqrt{\frac{3}{2}}\frac{\overline{\mathbf{T}}'}{\tilde{\sigma}} \\ &\tilde{\sigma} = \sqrt{\frac{2}{3}\mathbf{T}'.\mathbf{T}'} \\ &\dot{\tilde{\varepsilon}}^p = (\tilde{\sigma}, s) \end{aligned} \tag{4.15}$$

where for material obeying isotropic elasticity $\overline{\ell}^e = \ell^e$.

Finally, the evolution equation for the state variable (s) remains the same as in equation (4.6).

4.1.2 Generalized mid-point rule

To derive the generalized mid-point integration rule, we can start from the following objective identity:

$$\overline{\mathbf{T}}_{n+1} = \mathbf{T}_n + \int_{t_n}^{t_{n+1}} \dot{\overline{\mathbf{T}}} dt \tag{4.16}$$

thus, by using equation (4.14), equation (4.16) can be written as:

$$\overline{\mathbf{T}}_{n+1} = \mathbf{T}_n + \int_{t_n}^{t_{n+1}} \ell^e \left[\overline{\mathbf{D}}\right] dt - \int_{t_n}^{t_{n+1}} \ell^e \left[\overline{\mathbf{D}}^p\right] dt \tag{4.17}$$

Using the generalized mid-point rule to calculate the two integrals on the right side of the equation above, we can write

$$\overline{\mathbf{T}}_{n+1} = \mathbf{T}_n + \ell^e \left[\Delta\overline{\mathbf{E}} - \Delta\overline{\mathbf{E}}^p\right] \tag{4.18}$$

where the strain increments $\Delta\overline{\mathbf{E}}$ and $\Delta\overline{\mathbf{E}}^p$ are defined as

$$\begin{aligned} \Delta\overline{\mathbf{E}} &= \overline{\mathbf{D}}_{\mathbf{n}+\alpha}\Delta t \\ \Delta\overline{\mathbf{E}}^p &= \overline{\mathbf{D}}^p{}_{\mathbf{n}+\beta}\Delta t \end{aligned} \tag{4.19}$$

where α *and* β are constants and with $0 \le (\alpha, \beta) \le 1$, and $\overline{\mathbf{D}}_{\mathbf{n}+\alpha}$ *and* $\mathbf{D}_{\mathbf{n}+\beta}{}^p$ are defined as the total and plastic rate of deformation at some intermediate configurations $\mathbf{B}_{n+\alpha}$ *and* $\mathbf{B}_{n+\beta}$ between $\mathbf{B}_n$ *and* $\mathbf{B}_{n+1}$ respectively. As will be discussed later, such a generalized two parameter mid-point rule includes a scheme that is second order accurate in the integration of both the total rate of deformation and the plastic rate of deformation $(\alpha = 0.5 \, and \; \beta = 0.5)$, and a scheme which is second order accurate in the integration of the total rate of deformation, while still maintaining the efficiency of the radial return method $(\alpha = 0.5 \, and \; \beta = 1)$.

Finally, upon calculation of $\overline{\mathbf{T}}_{n+1}$ from equation (4.18), we can calculate the stress $\mathbf{T}_{n+1}$ as

$$\mathbf{T}_{n+1} = \mathbf{Q}_{\mathbf{n+1}} \overline{\mathbf{T}}_{n+1} \mathbf{Q}^T{}_{\mathbf{n+1}} \tag{4.20}$$

To effectively use the above algorithm in order to calculate the stress $\mathbf{T}_{n+1}$ corresponding to a given $\mathbf{F}_{n+1}$, we should assume an objective interpolation scheme for the calculation of the rate of deformation $\overline{\mathbf{D}}_{n+\alpha}$ and the rotation tensor $\mathbf{Q}_{n+1}$, and also a scheme for the iterative calculation

of $\overline{\mathbf{D}}^{p}_{\mathbf{n}+\beta}$. The first two of these issues are undertaken in the next section, while a discussion of the last one follows.

Calculation of the plastic rate of deformation $\overline{\mathbf{D}}^{p}_{\mathbf{n}+\beta}$ requires the knowledge of the material state ($\mathbf{T}_{n+\beta}, s_{n+\beta}$). Assuming an iterative approach, one can calculate the right side of equation (4.19) using the following approximations for $\overline{\mathbf{T}}_{n+\beta}$ and $s_{n+\beta}$:

$$\begin{aligned} s_{n+\beta} &= s_n + \beta \dot{s}_{n+\beta} \Delta t \\ \dot{s}_{n+\beta} &= g(\tilde{\sigma}_{n+\beta}, s_{n+\beta}) \\ \mathbf{T}_{n+\beta} &= (1-\beta)\mathbf{T}_n + \beta \overline{\mathbf{T}}_{n+1} \end{aligned} \tag{4.21}$$

where $\overline{\mathbf{T}}_{n+1}$ is calculated through an iterative process. Note that the generalized mid-point rule for the calculation of the plastic strain increment $\Delta\overline{\mathbf{E}}^{p}$ may be considered as a return mapping algorithm which corrects the elastic predictor $\overline{\mathbf{T}}^{trial}_{n+1}$ along a flow direction evaluated at the mid-point ($\overline{\mathbf{T}}_{n+\beta}, s_{n+\beta}$), where

$$\overline{\mathbf{T}}^{trial}_{n+1} = T_n + \ell^e \left[\Delta\overline{\mathbf{E}}_{n+\alpha}\right] \tag{4.22}$$

4.2 Kinematic approximations

Equations (4.18)-(4.19) will be incrementally objective when for the motion x* (**X**, t) defined earlier (equations (4.7) – (4.10)), the algorithm predicts that

$$\mathbf{T}^{*}_{n+1} = \mathbf{Z}_{\mathbf{n+1}} \mathbf{T}_{n+1} \mathbf{Z}^{T}_{\mathbf{n+1}} \tag{4.23}$$

and

$$S^{*}_{n+1} = S_{n+1} \tag{4.24}$$

To derive a family of incrementally objective integration schemes based on the generalized mid-point rule proposed earlier, an approximation of $\overline{\mathbf{D}}_{n+\alpha}$ and $\mathbf{Q}_{n+1}$ are required. This interpolation scheme must be such that

$$\overline{\mathbf{D}}^{*}_{n+\alpha} = \overline{\mathbf{D}}_{n+\alpha} \tag{4.25a}$$

$$\text{and} \quad \mathbf{Q}^{*}_{n+1} = \mathbf{Z}_{n+1} \mathbf{Q}_{n+1} \tag{4.25b}$$

Indeed, from equations (4.18), (4.19), (4.21) and (4.25) it can be concluded that

$$\overline{\mathbf{T}}^{*}{}_{n+1} = \overline{\mathbf{T}}_{n+1} \tag{4.26}$$

or using the definition of the bar transformed tensors

$$\mathbf{Q}^{*}_{\mathbf{n+1}}{}^{T}\mathbf{T}^{*}{}_{n+1}\mathbf{Q}^{*}{}_{n+1} = \mathbf{Q}_{n+1}{}^{T}\mathbf{T}_{n+1}\mathbf{Q}_{n+1} \tag{4.27}$$

which, using equation (4.25), leads to equation (4.24).

It is then our task to generate interpolation schemes which satisfy equations (4.25) for any rotation **Z**(t) defined such that $\mathbf{Z}(t_n) \equiv \mathbf{Z}_n = \mathbf{I}$. Since the deformation gradients are given in the beginning $(\mathbf{F}_n = \mathbf{I})$ and end ($\mathbf{F}_{n+1}$) of the time step, our goal is to derive an interpolation scheme of the following form:

$$\overline{\mathbf{D}}_{n+\alpha} = \hat{\overline{\mathbf{D}}}(\mathbf{F}_{n+1}, \alpha)$$

with $$\hat{\overline{\mathbf{D}}}_{n+\alpha}(\mathbf{I}, \alpha) = 0 \tag{4.28a}$$

and $$\mathbf{Q}_{n+1} = \hat{\overline{\mathbf{Q}}}(\mathbf{F}_{n+1})$$

with $$\hat{\overline{\mathbf{Q}}}_{n+\alpha}(\mathbf{U}_{n+1}) = 0 \tag{4.28a}$$

Certain restrictions have to be imposed on the functions $\hat{\overline{\mathbf{D}}}_{n+\alpha}$ and $\hat{\overline{\mathbf{Q}}}_{n+\alpha}$ in order to satisfy the objectivity constrains given by equations (4.25). Since these two equations are true for any proper rotation **Z**, let us select $\mathbf{Z}_{n+1} = \mathbf{R}^{T}_{n+1}$ where the rotation, $\mathbf{R}_{\mathbf{n+1}}$ is defined from the polar decomposition of $\mathbf{F}_{\mathbf{n+1}}$, i.e. $\mathbf{F}_{n+1} = \mathbf{R}_{n+1}\mathbf{U}_{n+1}$ .Then equations (4.28a, b) give

$$\hat{\overline{\mathbf{D}}}_{n+\alpha}(\mathbf{F}_{n+1}, \alpha) = \hat{\overline{\mathbf{D}}}_{n+\alpha}(\mathbf{R}_{n+1}\mathbf{U}_{n+1}, \alpha) = \hat{\overline{\mathbf{D}}}_{n+\alpha}(\mathbf{U}_{n+1}, \alpha) \tag{4.29a}$$

and

$$\hat{\overline{\mathbf{Q}}}_{n+\alpha}(\mathbf{F}_{n+1}) = \mathbf{R}_{n+1}\hat{\overline{\mathbf{Q}}}_{n+\alpha}(\mathbf{R}^{T}{}_{n+1}\mathbf{F}_{n+1}, \alpha) = \mathbf{R}_{n+1} \tag{4.29b}$$

Equations (4.29a) and (4.29b) define the final required interpolation forms. Here, $\hat{\overline{\mathbf{D}}}_{n+\alpha}$ is a function only of the right stretch tensor at the end of time step l $\mathbf{U}_{n+1}$ and α while $\hat{\overline{\mathbf{Q}}}_{n+\alpha}$ is equal

to the known rotation tensor $\mathbf{R}_{n+\alpha}$. A derivation of the present interpolation scheme to $\hat{\bar{\mathbf{D}}}_{n+\alpha}$ is now given. The rotation-neutralized configuration at time $t_{n+\alpha}$ (see Figure 1) is assumed as

$$\bar{\mathbf{x}}_{n+\alpha} = (1-\alpha)\bar{\mathbf{x}}_n + \alpha\bar{\mathbf{x}}_{n+1} \tag{4.30}$$

where the rotation – neutralized configuration at time t_{n+1} is approximated as

$$\bar{\mathbf{x}}_{n+1} = \mathbf{x}_n + \Delta t\dot{\bar{\mathbf{x}}}_{n+\alpha} \tag{4.31}$$

With the configuration B_n selected as the reference configuration (i.e. $\bar{\mathrm{F}}_n = I$), we can derive from equation (4.30) that

$$\bar{\mathbf{F}}_{n+\alpha} = (1-\alpha)\mathbf{I} + \alpha\bar{\mathbf{F}}_{n+1} \tag{4.32}$$

From equation (4.31), one can derive that

$$\bar{\mathbf{L}}_{n+\alpha} = \frac{1}{\Delta t}(\bar{\mathbf{F}}_{n+1} - \mathbf{I})\bar{\mathbf{F}}^{-1}{}_{n+\alpha} \tag{4.33}$$

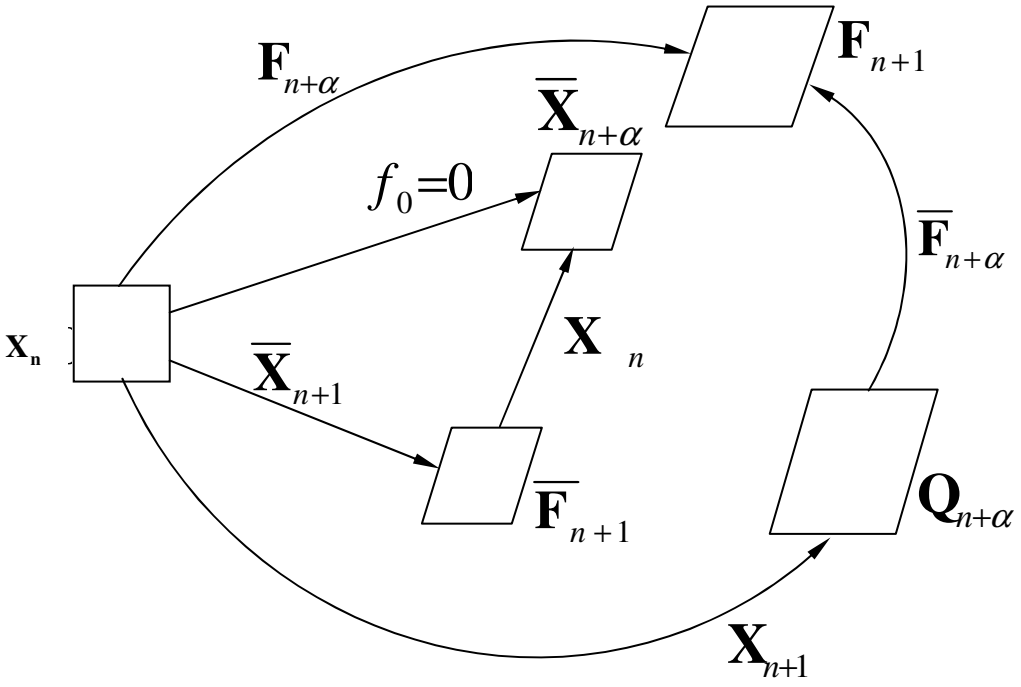

Figure 4.1 Schematic of a deforming depicting the 'rotation-neutralized' states as described by the assumed kinematic approximations

Following equation (4.29b), the rotation $\mathbf{Q}_{n+1} = \mathbf{R}_{n+1}$ which modifies equations (4.32) and (4.33) to the following form [2]:

$$\overline{\mathbf{F}}_{n+\alpha} = (1-\alpha)\mathbf{I} + \alpha\mathbf{U}_{n+1} \tag{4.34a}$$

$$\overline{\mathbf{L}}_{n+\alpha} = \overline{\mathbf{D}}_{n+\alpha} = \frac{1}{\Delta t}(\mathbf{U}_{n+1} - \mathbf{I})\overline{\mathbf{F}}^{-1}{}_{n+\alpha} \tag{4.34b}$$

From the above equations it becomes clear that the proposed integration scheme falls in the category of equations (4.29a) and (4.29b), and so it is an objective scheme for any value of α. Out of the several combinations of α and β, it is found that for a wide range of strain increments the most efficient and accurate algorithm is the one with $\alpha = 0.5$ and $\beta = 1$ [2]. Thus, it is quite interesting to observe that the present interpolation for $\alpha = 0.5$ takes the following form:

$$\overline{\mathbf{D}}_{n+\frac{1}{2}} = \frac{2}{\Delta t}(\mathbf{U}_{n+1} - \mathbf{I})(\mathbf{U}_{n+1} + \mathbf{I})^{-1} \tag{4.35}$$

This form has been proposed independently by Weber et al. More specifically, Nagtegaal and Veldpaus proposed that

$$\overline{\mathbf{D}}_{n+\alpha} = \frac{1}{\Delta t}\ln(\mathbf{U}_{n+1}) \tag{3.36}$$

This was modified by Weber et al using a pade approximation of $\ln(\mathbf{U}_{n+1})$. In the end, they independently arrived at the approximation given by equation (4.35). Also note that, for $\alpha = 0$, $\Delta\overline{\mathbf{E}}_{n+\alpha}\left(= \overline{\mathbf{D}}_{n+\alpha}\Delta t\right)$ becomes the incremental Biot strain, while for $\alpha = 1$, $\Delta\overline{\mathbf{E}}_{n+\alpha}$ takes a form similar to an Eulerian strain.

4.3 Variational Formulation and Solution Procedure

Let us suppose that the configuration $\mathbf{B}_n$ of the body at time $t = t_n$ is known and under equilibrium. Then the incremental quasi-static boundary value problem at time $t = t_{n+1}$ is to find the incremental (with respect to configuration $\mathbf{B}_n$) displacement field $\mathbf{u}(\mathbf{x}_n, t_{n+1}) \equiv \mathbf{u}_{n+1}$. The equilibrium equation is expressed in the reference configuration $\mathbf{B}_n$ as:

$$\nabla_n \cdot \mathbf{S}_n + \mathbf{f}_n = 0 \qquad \forall \mathbf{x} \in \mathbf{B}_n$$

where $\mathbf{S}$ is the Piola-Kirchoff I stress and $\mathbf{f}$ is the internal body forces.

The weak form of the above equation is written as:

$$\mathbf{G}\left(\mathbf{u}_{n+1}, \tilde{\mathbf{u}}(\mathbf{x}_n)\right) = 0 \tag{4.37b}$$

or $$\mathbf{G}(\mathbf{u}_{n+1}, \tilde{\mathbf{u}}(\mathbf{x}_n)) = \int_{\mathbf{B_n}} \mathbf{S}_{n+1} \cdot \frac{\partial \tilde{\mathbf{u}}}{\partial \mathbf{x}_n} d\mathbf{V} - \int_{\partial \mathbf{B}_{n+1}} \hat{\mathbf{t}} \cdot \tilde{\mathbf{u}}\, ds - \int_{\mathbf{B_{n+1}}} \hat{\mathbf{b}} \cdot \tilde{\mathbf{u}}\, d\nu = 0 \tag{4.36b}$$

for each test vector field $\tilde{\mathbf{u}}(\mathbf{x}_n)$, is zero on the portion of the boundary where kinematic boundary conditions are applied. The above equation is a mixed form of the principle of virtual work. The internal work is expressed in the reference configuration $\mathbf{B}_n$ using the Piola-Kirchhoff I stress, $\mathbf{S}_{n+1} = (\det \mathbf{F}_{n+1})\mathbf{T}_{n+1}\mathbf{F}_{n+1}^{-T}$, while the external work is expressed in the current configuration where the applied surface tractions, $\hat{\mathbf{t}}$, and body forced, $\tilde{\mathbf{b}}$,are given.

In order to solve the above set of non-linear equations for the incremental displacement field, $\mathbf{u}(\mathbf{x}_n, t_{n+1})$, an iterative scheme must be used. In this thesis a Newton-Raphson scheme is adopted, which requires linearization of equation (4.36) about the last obtained solution for U_{n+1}.

Denoting the estimate of $\mathbf{u}_{n+1}$ at the k^{th} iteration as $\mathbf{u}_{n+1}^{k}$, one can write equation (4.36) in linearized form as

$$\mathbf{G}(\mathbf{u}_{\mathbf{n+1}}^{\mathbf{k-1}}, \tilde{\mathbf{u}}(\mathbf{x}_n)) = \frac{\partial \mathbf{G}}{\partial \mathbf{u}_{n+1}}\Big|_{u=u^{k-1}} \cdot (\mathbf{u}_{n+1}^{k}, \mathbf{u}_{n+1}^{k-1}) = 0 \tag{4.37}$$

The above equation can be used for the calculation of $\mathbf{u}_{n+1}^{k}$, given $\mathbf{u}_{n+1}^{k-1}$. The derivative of $\mathbf{G}$ with respect to $\mathbf{u}_{n+1}$ is calculated at the present (prescribed) value $\mathbf{u}_{n+1}^{k-1}$, and is known ass the global Jacobian. To calculate this, we can take the variation of equation (4.36) with respect to $\mathbf{u}_{n+1}$, as shown below:

$$d\mathbf{G}\left(\mathbf{u}_{n+1}, \tilde{\mathbf{u}}(\,\mathbf{x}_n\,)\right) = d\left(\int_{\mathbf{B}_n} d\mathbf{S}_{n+1} \cdot \frac{\partial \tilde{\mathbf{u}}}{\partial \mathbf{x}_n} d\mathbf{V}\right) - d\left(\int_{\partial \mathbf{B}_{n+1}} \hat{\mathbf{t}} \cdot \tilde{\mathbf{u}} ds - \int_{\mathbf{B}_n} \hat{\mathbf{b}} \cdot \tilde{\mathbf{u}} dv\right) \tag{4.38}$$

In this thesis the contribution of body forces to the internal stiffness matrix are neglected. For the linearization of the internal work term we strictly follow the procedure of Zabaras and Arif [5]. Using the definition of Piola-Kirchhoff I stress, $\mathbf{S}_{n+1} = (\det \mathbf{F}_{n+1})\mathbf{T}_{n+1}\mathbf{F}_{n+1}^{-T}$, we can show that

$$\mathbf{dS}_{n+1} = d(\det \mathbf{F}_{n+1})\mathbf{T}_{n+1}\mathbf{F}_{n+1}^{-T} + (\det \mathbf{F}_{n+1})d\mathbf{T}_{n+1}\mathbf{F}_{n+1}^{-T} + (\det \mathbf{F}_{n+1})\mathbf{T}_{n+1}\mathbf{dF}_{n+1}^{-T} \tag{4.39}$$

The main part of the following analysis is to express all differentials in the equation above in terms of $d\mathbf{F}_{n+1}$, which will then be expressed in terms of $\mathbf{du}_{n+1}$.

Using the identities

$$d(\det \mathbf{F}_{n+1}) = (\det \mathbf{F}_{n+1})tr(d\,\mathbf{F}_{n+1}\mathbf{F}_{n+1}^{-1}) \tag{4.40a}$$

$$\mathbf{F}_{n+1}^{-T} = -\mathbf{F}_{n+1}^{-T}d\,\mathbf{F}_{n+1}\mathbf{F}_{n+1}^{-T} \tag{4.40b}$$

Equation (4.39) can be further simplified as

$$\mathbf{dS}_{n+1} = (\det \mathbf{F}_{n+1})\left\{tr(d\,\mathbf{F}_{n+1}\mathbf{F}_{n+1}^{-1})\mathbf{T}_{n+1} + d\mathbf{T}_{n+1} - \mathbf{T}_{n+1}\mathbf{F}_{n+1}^{-T}d\mathbf{F}_{n+1}^{T}\right\}\mathbf{F}_{n+1}^{-T} \tag{4.41}$$

The calculation of $d\mathbf{T}_{n+1}$ must be consistent with the integration scheme used earlier for the calculation of $\overline{\mathbf{T}}_{n+1}$. With variation of equation (4.20) and after some tensor algebra we can show that

$$d\mathbf{T}_{n+1} = \left[d\mathbf{R}_{n+1}\mathbf{R}_{n+1}^{T}\right]\overline{\mathbf{T}}_{n+1} + \mathbf{R}_{n+1}d\overline{\mathbf{T}}_{n+1}\mathbf{R}_{n+1}^{T} + \mathbf{T}_{n+1}\left[\mathbf{R}_{n+1}d\mathbf{R}_{n+1}^{T}\right] \tag{4.42}$$

To complete the linearization process in the equation above, it remains to calculate

$$d\mathbf{R}_{n+1}\mathbf{R}_{n+1}^{T}(= -\mathbf{R}_{n+1}d\mathbf{R}_{n+1}^{T}) \quad and \quad d\overline{\mathbf{T}}_{n+1}$$

Taking the variation of the relative deformation gradient $\mathbf{F}_{n+1}(= \mathbf{R}_{n+1}\mathbf{U}_{n+1})$, we can finally derive

$$d\mathbf{R}_{n+1}\mathbf{R}_{n+1}^{T} = d\mathbf{F}_{n+1}\mathbf{F}_{n+1}^{-1} - \mathbf{R}_{n+1}(d\mathbf{U}_{n+1}\mathbf{U}_{n+1}^{-1})\mathbf{R}_{n+1}^{T} \tag{4.43}$$

To compute $d\mathbf{U}_{n+1}$ in terms of $d\mathbf{F}_{n+1}$, we can use the identity

$$\mathbf{U}_{n+1}\mathbf{U}_{n+1} = \mathbf{F}_{n+1}^{T}\mathbf{F}_{n+1}$$

to derive that

$$d\mathbf{U}_{n+1} + \mathbf{U}_{n+1}^{-1}d\mathbf{U}_{n+1}\mathbf{U}_{n+1} = 2\mathbf{U}_{n+1}^{-1}sym\left[\mathbf{F}_{n+1}^{T}d\mathbf{F}_{n+1}\right] \tag{4.44}$$

Here "sym" refers to the symmetric part of the tensor.

Introducing Biot's strain, $\mathbf{E}_{n+1}^{B} = \mathbf{U}_{n+1} - \mathbf{I}$, we have

$$\mathbf{U}_{n+1}^{-1} = (\mathbf{E}_{n+1}^{B} + \mathbf{I})^{-1} = \mathbf{I} - \mathbf{E}_{n+1}^{B} + \mathbf{O}((\mathbf{E}_{n+1}^{B})^{2}) \tag{4.45}$$

Substitution of equation (4.45) in to equation (4.44) gives

$$d\mathbf{E}_{n+1}^{B} - \mathbf{E}_{n+1}^{B}d\mathbf{E}_{n+1}^{B} + d\mathbf{E}_{n+1}^{B}\mathbf{E}_{n+1}^{B} + \mathbf{O}((\mathbf{E}_{n+1}^{B})^{2}) + d\mathbf{U}_{n+1} = 2\mathbf{U}_{n+1}^{-1}sym\left\{\mathbf{F}_{n+1}^{T}\mathbf{F}_{n+1}\right\} \tag{4.46}$$

Taking the transpose of equation (4.46) and adding to equation (4.46), the following linearized approximation of $d\mathbf{U}_{n+1}$ is obtained:

$$d\mathbf{U}_{n+1} = sym\left[\mathbf{U}_{n+1}^{-1} sym\left\{\mathbf{F}_{n+1}^{T}\mathbf{F}_{n+1}\right\}\right] + \mathbf{O}(\,(\mathbf{E}_{n+1}^{B})^{2}\,) \tag{4.47}$$

Substitution of equation (4.47) in to equation (4.43) gives the following approximation:

$$\begin{aligned} d\mathbf{R}_{n+1}\mathbf{R}_{n+1}^{T} &= -\mathbf{R}_{n+1}d\mathbf{R}_{n+1}^{T} \\ &= d\mathbf{F}_{n+1}\mathbf{F}_{n+1}^{-1} - \mathbf{R}_{n+1}sym\left[\mathbf{U}_{n+1}^{-1}sym\left\{\mathbf{F}_{n+1}^{T}\mathbf{F}_{n+1}\right\}\right]\mathbf{U}_{n+1}^{-1}\mathbf{R}_{n+1}^{T} + \mathbf{O}(\,(\mathbf{E}_{n+1}^{B})^{2} \end{aligned} \tag{4.48}$$

To complete the calculation of the right hand side of equation (4.42) in terms of $d\mathbf{F}_{n+1}$, we must calculate $d\overline{\mathbf{T}}_{n+1}$.

From the constitutive part, we have

$$d\overline{\mathbf{T}}_{n+1} = \overline{\mathfrak{I}}^{ep}\left[d\Delta\overline{\mathbf{E}}\right] \tag{4.49}$$

$\Delta\overline{\mathbf{E}}$ is defined from equation (4.19) and the calculation of the consistent elasto-plastic moduli $\overline{\mathfrak{I}}^{ep}$ will be will be undertaken later. As discussed earlier, it will be necessary to express $\Delta\overline{\mathbf{E}}$ in terms of $d\mathbf{F}_{n+1}$. From equation (4.33) and using the definition of $\mathbf{E}_{n+1}^{B}$, the following approximation of $\Delta\overline{\mathbf{E}}$ is obtained:

$$\Delta\overline{\mathbf{E}} = \mathbf{E}_{n+1}^{B}\left[\mathbf{I} - \alpha\,\mathbf{E}_{n+1}^{B} + \mathbf{O}(\mathbf{E}_{n+1}^{B})^{2}\right] \tag{4.50}$$

The differential of equation (4.50) can be shown to take the form

$$d\Delta\overline{\mathbf{E}} = \left(\mathbf{I} - \alpha\mathbf{E}_{n+1}^{B}\right)d\mathbf{U}_{n+1}\left(\mathbf{I} - \alpha\mathbf{E}_{n+1}^{B}\right) + \mathbf{O}(\mathbf{E}_{n+1}^{B})^{2} \tag{4.51}$$

which, using equations (4.33), (4.47) and the definition of $\mathbf{E}_{n+1}^{B}$,is modified as

$$d\Delta\overline{\mathbf{E}} = \overline{\mathbf{F}}_{n+1}^{-1}sym\left[\mathbf{U}_{n+1}^{-1}sym\left\{\mathbf{F}_{n+1}^{T}\mathbf{F}_{n+1}\right\}\right]\overline{\mathbf{F}}_{n+\alpha}^{-1} \tag{4.52}$$

Finally, substitution of equation (4.42), (4.48) and (4.49) in equation (4.41) leads the following form:

$$d\mathrm{G} = \int_{B_n}\left\{\begin{array}{r} \mathrm{R}_{n+1}\left(\overline{\mathfrak{I}}^{ep}\left[d\Delta\overline{\mathrm{E}}\right]\right)\mathrm{R}_{n+1}^{T} + (d\mathrm{R}_{n+1}\mathrm{R}_{n+1}^{T})\mathrm{T}_{n+1} + \mathrm{T}_{n+1}(\mathrm{R}_{n+1}d\mathrm{R}_{n+1}^{T}) \\ -(\det\mathrm{F}_{n+1})\left\{tr(d\,\mathrm{F}_{n+1}\mathrm{F}_{n+1}^{-1})\mathrm{T}_{n+1} + d\mathrm{T}_{n+1} - \mathrm{T}_{n+1}\mathrm{F}_{n+1}^{-T}d\mathrm{F}_{n+1}^{T}\right\}\mathrm{F}_{n+1}^{-T} \end{array}\right\} \tag{4.53}$$

This equation shows that the incremental internal nodal work consists of two distinct parts. However, the nodal forces can also be extracted from the equation.

1. The first term involves the incremental stress ($d\overline{\mathbf{T}}_{n+1}$) and thus depends on the material response and leads to what is called the *material tangent stiffness matrix* which we

denote by $\mathbf{K}^{mat}$. This term reflects material response, it changes with deformation since B_n depends on $\mathbf{F}_{n+1}$.

2. The other terms involve the current state of stress ($\mathbf{T}_{n+1}$) and accounts for rotation of the stress with the motion. This term is called the *geometric stiffness* because it represents the geometric nonlinearities associated with rotation of the stress. It is also called the *initial stress matrix* to indicate the role of the existing state of stress. It is denoted by $\mathbf{K}^{geo}$.

4.4 The Contact Problem

Contact problems fall into two general classes: rigid-to-flexible and flexible-to-flexible. In rigid-to-flexible contact problems, one or more of the contacting surfaces are treated as rigid (with a much higher stiffness relative to the deformable body/bodies contacted). In general, any time a soft material comes in contact with a hard material, the problem may be assumed to be rigid-to-flexible. Many metal forming problems fall into this category. In flexible-to-flexible contact problems, both (or all) contacting bodies are deformable. (i.e., have similar stiffness). An example of flexible-to-flexible analysis is the case of bolted flanges. In this thesis rigid-to-flexible contact of metal forming is studied. The work piece is considered to be flexible and that of the dies are considered to be rigid.

Contact problems, in metal forming, are among the most difficult nonlinear problems because the response in contact problems is not smooth. The displacements normal to the contact interface are discontinuous in time when contact occurs. These characteristics of contact problems introduce significant difficulties in the time integration of the governing equations and impair the performance of numerical algorithms.

A typical forming process employs one or more tools with which a work-piece is deformed in to a desired shape, from which we can conclude that there exists an interaction between different solid components during the process. Once the modeling of contact problems is

considered, two research areas can be distinguished, namely the constitutive modeling of contact and development of numerical methods for contact problems. Therefore, the appropriate choice of methodologies and algorithms is crucial in the successful treatment of contact problems. Techniques such as regularization are highly useful in obtaining robust solution procedures.

4.4.1 Frictionless Contact Description

Two bodies that come in contact are depicted in Figure 1. Contact algorithms in general purpose software can treat the interaction of many bodies, but for purposes of simplicity, we limit ourselves to two bodies, the die and the work-piece. Let's denote the configurations of the two bodies by Ω^A and Ω^B, for the work piece and the die, respectively, and the union of the two bodies by Ω. The boundaries of the bodies are denoted by Γ^A and Γ^B. Although the two bodies are interchangeable with respect to their mechanics, it is sometimes useful to express the equations in terms of one of the bodies, which is called the master. Body A (the work piece) is designated as the master, body B (the die) as the slave. To distinguish field variables that are associated with a particular body, we append a superscript A or B; when neither of these superscripts appears, the field variable applies to the union of the two bodies. Thus the displacement field **u(X, t)** refers to the displacement field in both bodies, whereas $\mathbf{u^A(X, t)}$ refers to the displacement in body **A**.

As indicated in figure 4.2, the reference configurations of the die and the work piece are represented by the open sets Ω^A and Ω^B. The bodies undergo motions denoted $\varphi_t^{(A)}$ and $\varphi_t^{(B)}$, which cause them to contact and produce interactive forces during some portion of the time interval **H**= [0.T]. These motions can be expressed via the following mappings:

$$\varphi^{(i)} : \overline{\Omega}^{(i)} \times \mathbf{H} \to \mathbf{R}^{n_d}, \qquad i = 1,2 \tag{4.54}$$

$\overline{\Omega}^{(i)}$ indicates the closer of $\Omega^{(i)}$, or the union of the open set with its boundary. It is assumed for simplicity that $\Omega^{(i)}$ (i=1, 2) correspond spatially to the initial positions of the bodies, and that

these reference configurations are such that if the bodies contact at t=0, no interactive forces are produced.

For any time $t \in \mathbf{H}$, the configuration obtained by fixing the time argument of $\Omega^{(i)}$ is denoted as $\Omega_t^{(i)}$, $i = 1,2$. Following a frequently used convention, geometric objects and tensor quantities defined on $\varphi_t^{(i)}(\Omega^i)$ will be referred to as spatial objects, while quantities defined on the reference states $\Omega^{(i)}$ will be referred to as material objects.

Accordingly, material points of $\Omega^{(A)}$ are denoted as $\mathbf{X}^{(A)}$, and material point of $\Omega^{(B)}$ are denotedas $\mathbf{X}^{(B)}$

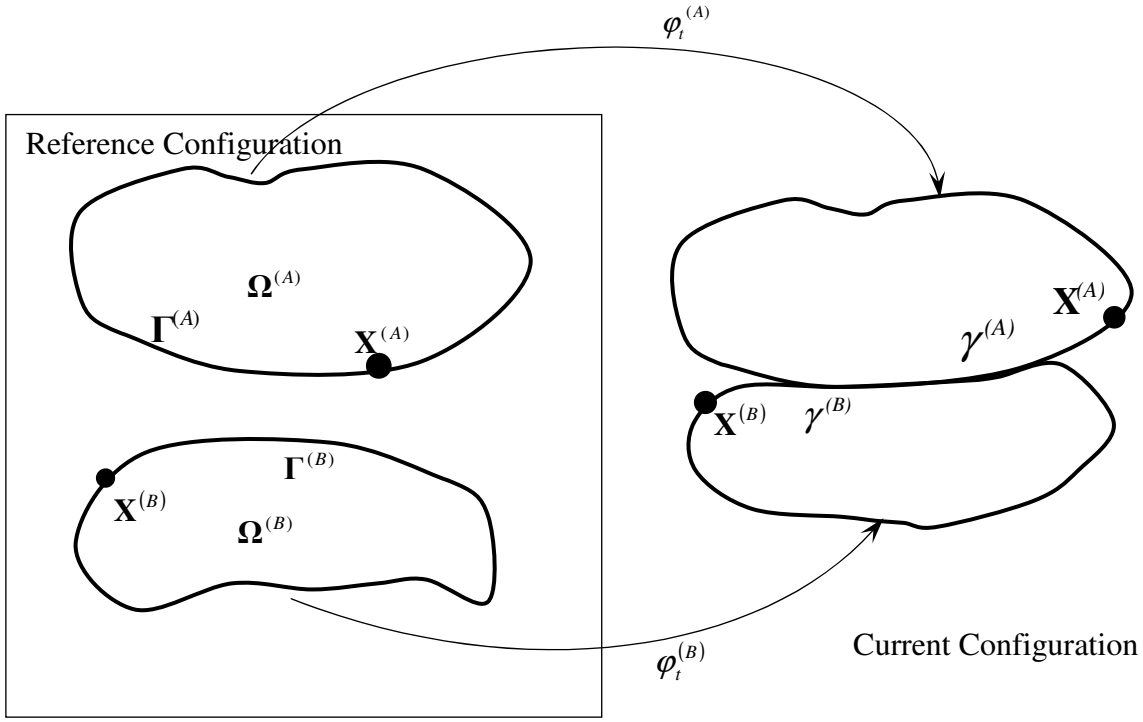

Figure 4.2 Notation for the finite deformation Contact in metal forming

The contact interface consists of the intersection of the surfaces of the two bodies and is denoted by Γ^C .

$$\Gamma^C = \Gamma^A \cap \Gamma^B \tag{4.44}$$

This contact interface consists of the two physical surfaces of the two bodies which are in contact. In those cases, Γ^C refers to the master surface. Moreover, although the two bodies may be in contact on several disjoint interfaces, we designate their union by a single symbol Γ^C . The contact interface is a function of time, and its determination is an important part of the solution of the contact problem.

The dimension of the contact surface Γ^C is one lower than the number of space dimensions. Thus, for a 2D problem, Γ^C is a curve, and for a 3D problem Γ^C is a surface. Furthermore, without loss of generality we assume that Γ^C is simply connected. As a consequence of the connectivity, all the points in Γ^C can be continuously mapped onto a unique point in $\Re^{n_d-1}$ and vice versa. The mapping in itself is not unique.

In construction the equations, it is convenient to express vectors in terms of local components of the contact surface. A local coordinate system is set up at each point of the master contact surface as shown in Figure 4.3. At each point, we can construct unit vectors tangent to the surface of the master body $\hat{\mathbf{e}}_1^A \equiv \hat{\mathbf{e}}_x^A$ *and* $\hat{\mathbf{e}}_2^A \equiv \hat{\mathbf{e}}_x^A$. The normal for body A is given by

$$\mathbf{n}^A = \hat{\mathbf{e}}_1^A \times \hat{\mathbf{e}}_2^A \tag{4.45}$$

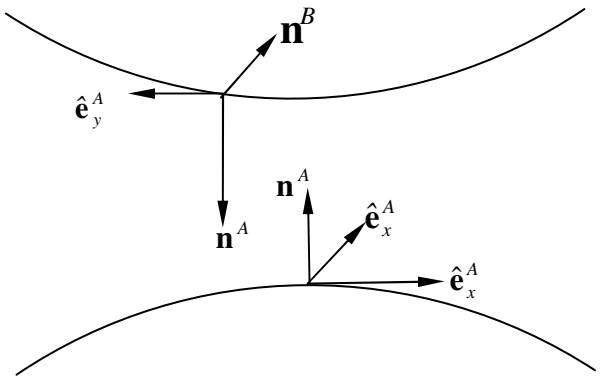

Figure4.3 Contact interface showing local unit vectors

The dimension of the contact surface $\Gamma^{(i)}$ is one lower than the number of space di-mensions. Thus, for a 2D problem, $\Gamma^{(i)}$ is a curve, and for a 3D problem $\Gamma^{(i)}$ is a surface. Furthermore, without loss of generality we assume that $\Gamma^{(i)}$ is simply connected. As a consequence of the connectivity, all the points in $\Gamma^{(i)}$ can be continuously mapped onto a unique point in $\mathbf{R}^{n_{d-1}}$ and vice versa. The mapping in itself is not unique.

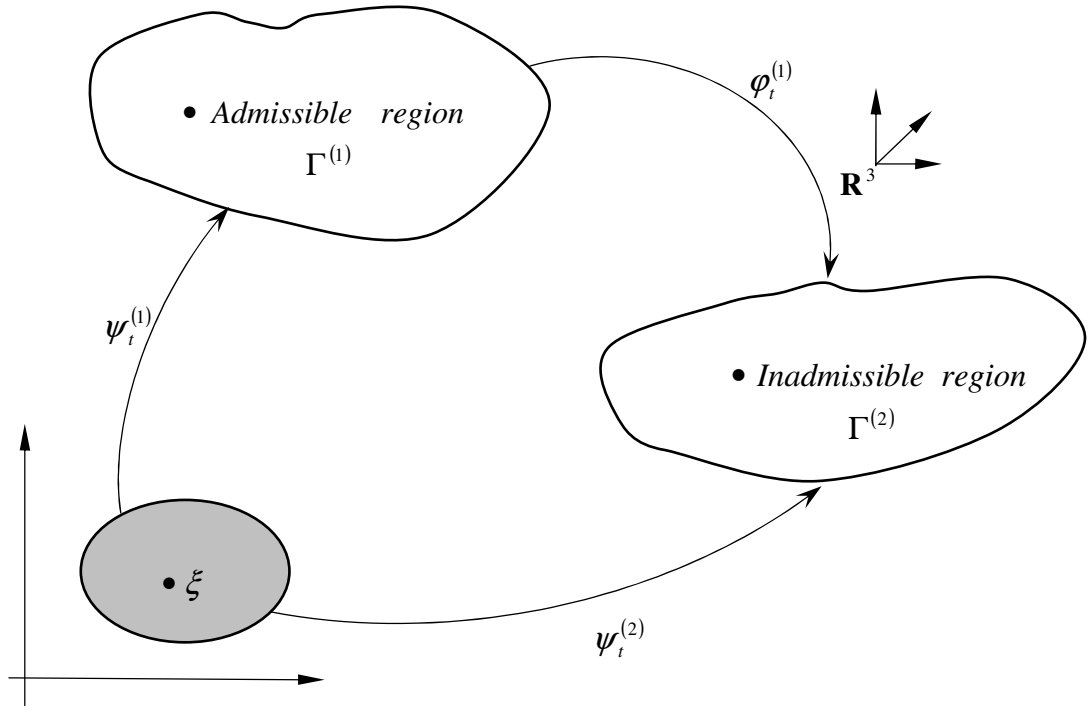

Figure4.4 Parameterization of contact surfaces

On the contact surface

$$\mathbf{n}^A = -\mathbf{n}^B \tag{4.46}$$

that is, the normal of the two bodies are in opposite directions.

The displacement fields can be expressed in the local coordinates of the contact surface by

$$\mathbf{u}^A = \mathbf{u}_N^A \mathbf{n}^A + \hat{u}_\alpha^A \hat{\mathbf{e}}_\alpha^A = u_N^A \mathbf{n}^A + \mathbf{u}_T^A \tag{4.47a}$$

$$\mathbf{u}^B = \mathbf{u}_N^B \mathbf{n}^A + \hat{u}_\alpha^B \hat{\mathbf{e}}_\alpha^A = u_N^A \mathbf{n}^B + \mathbf{u}_T^A \tag{4.47b}$$

As can be seen in the above, the components are expressed in terms of the local coordinate system of the master surface. The normal displacements are given by

$$u_N^A = \mathbf{u}^A \cdot \mathbf{n}^A \qquad u_N^B = \mathbf{u}^B \cdot \mathbf{n}^A \tag{4.48}$$

The two bodies, the die and the work piece, are governed by the standard field equations: conservation of mass, momentum and energy, a strain measure, and the constitutive equations as discussed before. Contact adds the following conditions: the bodies can not interpenetrate and the tractions must satisfy momentum conservation on the interface. Furthermore, the normal traction across the contact interface cannot be tensile. We classify the requirements on the displacements as kinematic conditions and the requirements on the tractions as kinetic conditions.

4.4.2 Contact constraints

In this section, contact constraints are discussed, which are constraints for impenetrability and tractions. These constraints pair the traction in normal direction with the normal displcement. Stated in another way, the impenetrability condition simply states that two bodies can not occupy the same space at the same time and the compressive interaction requirement excludes the possible adhesion of contacting bodies. This capacity to separate at the slightest pull is sometimes emphasized by referring to the problem under consideration as unilateral contact problem. In expressing these constraints, it is convenient to choose one contact surface as slave (contactor) and the other as master (target). Here, Γ^A is chosen as master and Γ^B as slave.

4.4.2.1 Impenetrability Condition

In a continuum model, it is not allowed that two points occupy the same location in space. For the interior points within an object, this is taken care of by choosing appropriate candidate functions for the solution of the problem. For multiple bodies this problem reduces to stating that no boundary point of the first body may penetrate the other.

The impenetrability condition for a pair of bodies can be stated as

$$\Omega^A \cap \Omega^B = 0 \tag{4.49}$$

That is, the intersection of the two bodies is the null set. In other words, the two bodies are not allowed to overlap, which can also be viewed as a compatibility condition. The impenetrability condition is highly nonlinear for metal forming problems, and in general cannot be expressed as an algebraic or differential equation in terms of the displacements.

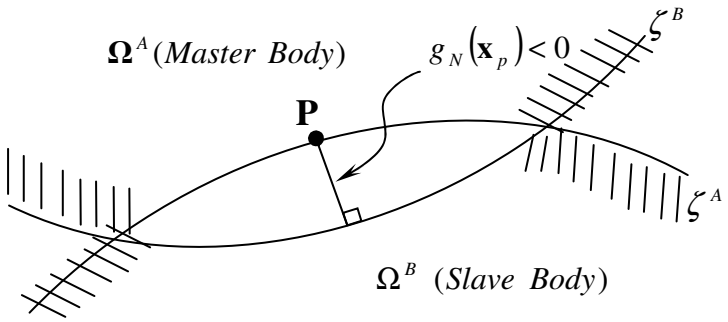

Figure 4.5 Interpenetration of point P on body slave B defined as orthonormal projection from master body A

In many implementations of contact, as can be seen in figure 4.4, the impenetrability condition is relaxed [5], i.e. a certain amount of interpenetration is permitted. When the points of two contact areas have interpenetrated, it is useful to write the interpenetration $g_N(\zeta^\alpha, t)$ in the form of an explicit equation. Consider a situation such as shown in Figure 4.4, where point P has penetrated body A.

The interpenetration is defined as the minimum distance from point P on body B to a point on body A. The distance between P and any point on A is given by

$$\begin{aligned} l_{AB} &= \left\| \mathbf{x}^B(\zeta, t) - \mathbf{x}^A(\bar{\zeta}, t) \right\| \\ &\equiv \left[(x^B - x^A)^2 + (y^B - y^A)^2 + (z^B - z^A)^2 \right]^{\frac{1}{2}} \end{aligned} \tag{4.50}$$

The referential coordinates ζ^A and ζ^B pertains to bodies A and B, respectively. The interpenetration $g_N(\zeta,t)$ is then defined as the *minimum distance* of point P to the surface of work piece when point P has penetrated the die:

$$g_N\left(\zeta^B,t\right)=\min_{\zeta^A}\left\|\mathbf{x}^B\left(\zeta^B,t\right)-\mathbf{x}^A\left(\zeta^A,t\right)\right\| \tag{4.51a}$$

$$\text{if}\quad \left[\mathbf{x}^B\left(\zeta^B,t\right)-\mathbf{x}^A\left(\zeta^A,t\right)\right]\cdot\mathbf{n}^A\le 0 \tag{4.51b}$$

$$\text{Otherwise}\quad g_N\left(\zeta^B,t\right)=0 \tag{4.51c}$$

According to this definition, $g_N\left(\zeta^B,t\right)$ is positive when interpenetration occurs and vanishes when the bodies have not interpenetrated.

To evaluate the $g_N\left(\zeta^B,t\right)$, the referential coordinate ζ^A which minimizes the interpenetration must be found, i.e. we must find location of the point $\mathbf{x}^A\left(\zeta^A,t\right)$on the work piece which corresponds to the stationary point of the distance, so we take the derivative of l_{AB} with respect to ζ^A and set the result to zero. This yield

$$\begin{aligned}\frac{\partial l_{AB}}{\zeta^\alpha}&=\frac{\mathbf{x}^B\left(\zeta^B,t\right)-\mathbf{x}^A\left(\zeta^A,t\right)}{\left\|\mathbf{x}^B\left(\zeta^B,t\right)-\mathbf{x}^A\left(\zeta^A,t\right)\right\|}\cdot\frac{\partial\mathbf{x}^A\left(\zeta^A,t\right)}{\partial\zeta^\alpha}\\&=\mathbf{e}\cdot\mathbf{a}_\alpha=0\end{aligned} \tag{4.52}$$

where $\alpha=A,B$ and $\mathbf{a}_\alpha$ is given by

$$\mathbf{a}_\alpha=\frac{\partial\mathbf{x}^A\left(\zeta^A,t\right)}{\partial\zeta^\alpha}=x,_\alpha^A \tag{4.53}$$

and $\mathbf{e}=\dfrac{\mathbf{x}^B-\mathbf{x}^A}{\left\|\mathbf{x}^B-\mathbf{x}^A\right\|}$, so $\mathbf{e}$ is a unit vector from the work piece to the die surface. The last term in the above shows that the distance is minimum, i.e. the derivative vanishes, when $\mathbf{e}$ is orthogonal to the two tangent vectors $\mathbf{a}_\alpha$. This implies that $\mathbf{e}$ is normal to the surface of the work piece. Thus $\mathbf{x}^A\left(\zeta^A,t\right)$ is the orthogonal projection of the point P with coordinates $\mathbf{x}^B$ onto the work piece.

For the case of metal forming problems, the subject of the thesis, we can define the range of deformation space as admissible and non admissible. Here using this definition, in this thesis the non admissible range is the space which is occupied by the die and the rest is the admissible one.

Implication of nonconvexity

One difficulty with the definition of equation (4.51) is that the projection may not be unique. This can occur when the admissible region boundary by Γ^A is nonconvex, as depicted in figure 4.4. In other words, it is possible that more than one point of Γ^A will accomplish the minimization of equation (4.51).

In practice, however, this problem is not o major consequence. This is true for two reasons. First, it is really only local convexity that is of concern in gap determination. When even this weaker condition is violated, the number of points achieving the minimization is generally small in the discrete case. Of these, usually only the worst offender of the constraints (equation 4.51a) needs to be considered and corrected. Second, with regard to the kinematic descriptions discussed earlier, the key point with regard to the projection is its normality to the master (work piece) surface, which will hold for many local minimizer of the distance in equation (4.51). Thus, although the potential lack of uniqueness must be accounted for in contact detection, it poses little difficulty with regard to contact formulation.

4.4.2.2 Traction Conditions.

The tractions must observe the balance of momentum across the contact interface. Since the interface has no mass, this requires that the sum of the tractions on the two bodies vanish.

$$\mathbf{t}^A + \mathbf{t}^B = 0 \tag{4.54}$$

And $$\mathbf{t}^{(i)} = \mathbf{P}^{(i)}(\mathbf{X},t)\mathbf{N}^{(i)}(\mathbf{X},t) \tag{4.55}$$

Where $\mathbf{P}^{(i)}(\mathbf{X},t)$ and $\mathbf{N}^{(i)}(\mathbf{X},t)$ are the first Piola–Kirchhoff stress tensor and reference normal vector determined at the particular contactor point $\mathbf{X}$ respectively.

The tractions on the surfaces of the two bodies are defined by Cauchy's law

$$\begin{aligned} \mathbf{t}^A &= \boldsymbol{\sigma}^A \cdot \mathbf{n}^A \\ \mathbf{t}^B &= \boldsymbol{\sigma}^B \cdot \mathbf{n}^B \end{aligned} \quad \text{or} \quad \begin{aligned} t_i^A &= \sigma_{ij}^A \cdot n_j^A \\ t_i^B &= \sigma_{ij}^B \cdot n_j^B \end{aligned} \tag{4.56}$$

The normal tractions are defined by

$$\begin{aligned} \mathbf{t}_N^A &= \mathbf{t}^A \cdot \mathbf{n}^A \\ \mathbf{t}_N^B &= \mathbf{t}^A \cdot \mathbf{n}^A \end{aligned} \quad \text{or} \quad \begin{aligned} \mathbf{t}_N^A &= t_j^A \cdot n_j^A \\ \mathbf{t}_N^B &= t_j^B \cdot n_j^A \end{aligned} \tag{4.57}$$

The normal components, like all local components on the contact surface, refer to the work piece. The momentum balance condition on the normal tractions can be obtained by taking a dot product of Equation (4.54) with the normal vector $\mathbf{n}^A$, which gives

$$\mathbf{t}_N^A + \mathbf{t}_N^B = 0 \tag{4.58}$$

We do not consider any adhesion between the contact surfaces in the normal direction, soothe normal tractions can not be tensile; the normal tractions must be compressive, although the normal tractions can also vanish. This can be stated as

$$t_N \equiv t_N^A(\mathbf{x},t) = -t_N^B(\mathbf{x},t) \le 0 \tag{4.59}$$

4.4.2.3 Constitutive Contact Laws

The constitutive contact laws relate the kinematic and static contact variables discussed before. In general, these laws can be formulated using both the spatial and nominal contact tractions. However, in metal forming, it seems that a physically acceptable and natural way is to derive or postulate these laws in the spatial description and later to transform them to the material description.

In fact, the whole contact problem can be reduced to a boundary based problem, by demanding that the signed distance of any point on the first body is non-negative with respect to the other, where the signed distance between a point and a boundary is defined as in the previous section. That is, the normal gap between a point and a boundary is positive when interpenetration occurs and vanishes when the bodies have not interpenetrated.

Conditions (4.51) and (4.59) can be combined to:

$$\begin{aligned} & g_N(\mathbf{x},t) \geq 0 \\ & t_N \leq 0 \\ & g_N(\mathbf{x},t) \cdot t_N = 0 \end{aligned} \tag{4.60}$$

The first condition, in equation 4.60, states that no penetration may occur. Hence, this is the form in which the impenetrability constraint is cast. Using this, the normal traction can be characterized. The second condition states that the contact normal traction should be compressive. Finally, the third condition states a complementarity condition. It is called the *unitary contact condition*. This equation also expresses the fact that the contact forces do no work. That this condition must hold on the contact surface can be seen as follow: when the bodies are in contact and remain in contact, $g_N(\mathbf{x},t) = 0$, whereas when contact ceases, $g_N(\mathbf{x},t) \leq 0$ but the normal traction must vanish, so the product always vanishes. It will also be seen that this is a *Kuhn-Tucker condition* when a Lagrange multiplier approach is used, for the normal traction is then equivalent to a Lagrange multiplier, and the unitary condition states that product of the Lagrange multiplier an the constraint on the velocities vanishes.

4.5 The Weak Form of Contact

The weak formulation of contact is obtained from the strong formulation of contact by applying the principle of virtual work. The strong form is given by the constraints given in equation (4.60) and an equilibrium model. The equilibrium model presented here is a quasi-static one, although no additional difficulty is to be encountered if a dynamic model would be used.

The model is commonly given as:

$$\begin{aligned} & \nabla \cdot \boldsymbol{\sigma}^i = 0 \qquad in \quad \boldsymbol{\Omega} \\ & \boldsymbol{\sigma}^i.\mathbf{n} = \tilde{\mathbf{t}}^i \qquad in \quad \boldsymbol{\Gamma}_\sigma^i \quad \text{, Neumann boundary} \\ & \mathbf{u}^i = \tilde{\mathbf{u}}^i \qquad in \quad \boldsymbol{\Gamma}_u^i \quad \text{, Dirichlet boundary} \end{aligned} \tag{4.61}$$

In the equilibrium equation $\boldsymbol{\sigma}^i$ is the Cauchy stress tensor in body i and $\mathbf{f}^i$ represents the body forces acting on body i. There is furthermore boundary conditions prescribed on $\boldsymbol{\Gamma}_\sigma^i$, which is that part of the boundary on which tractions are prescribed. The prescribed tractions are $\tilde{\mathbf{t}}^i$.

Also boundary conditions are prescribed on $\boldsymbol{\Gamma}_u^i$, which is that part of the boundary on which displacements are prescribed. The prescribed displacements are given by $\tilde{\mathbf{u}}^i$.

4.5.1 Forming the Contact Integrals

If the equilibrium equation holds, then upon taking the inner-product with some arbitrary weighing function $\mathbf{w}^i$, which is interpreted as virtual displacements, it follows that:

$$\left[\nabla \cdot \boldsymbol{\sigma}^i + \mathbf{f}^i\right] \cdot \mathbf{w}^i = 0 \tag{4.62}$$

To see that this is true, choose for $\mathbf{w}^i$ consecutively $\mathbf{e}_1, \mathbf{e}_2$ and $\mathbf{e}_3$ to regain the equilibrium equations.

Integrating the above equation yields:

$$\int_\Omega \left[\nabla \cdot \boldsymbol{\sigma}^i + \mathbf{f}^i\right] \cdot \mathbf{w}^i d\Omega = 0 \tag{4.63}$$

Integrating the previous equation by parts by applying the divergence theorem, yields:

$$\begin{aligned} \int_\Omega \left[\boldsymbol{\sigma}^i : \nabla \mathbf{w} - \mathbf{f}^i \cdot \mathbf{w}^i\right] d\Omega - \int_{\Gamma_\sigma^i} \tilde{\mathbf{t}}^i \cdot \mathbf{w}^i d\Gamma \\ - \int_{\Gamma_u^i} \left[\boldsymbol{\sigma}^i \cdot \mathbf{n}^i\right] \cdot \mathbf{w}^i d\Gamma - \int_{\Gamma_c^i} \mathbf{t}^i \cdot \mathbf{w}^i d\Gamma = 0 \end{aligned} \tag{4.64}$$

Introducing the compatibility condition $\mathbf{w}^i = 0 \,\text{on}\, \Gamma_u^i$, does not change the solution of the original problem. It will however cause the integral over the prescribed displacement boundary to vanish. By using the following shorthand:

$$\mathbf{G}^i\left(\mathbf{u}^i, \mathbf{w}^i\right) = \int_\Omega \left[\boldsymbol{\sigma}^i : \nabla \mathbf{w}^i - \mathbf{f}^i \cdot \mathbf{w}^i\right] d\Omega - \int_{\Gamma_\sigma^i} \tilde{\mathbf{t}}^i \cdot \mathbf{w}^i d\Gamma, \tag{4.65a}$$

$$\mathbf{G}_c^i\left(\mathbf{u}^i, \mathbf{w}^i\right) = -\int_{\Gamma_c^i} \mathbf{t}^i \cdot \mathbf{w}^i d\Gamma \tag{4.65b}$$

We can also write

$$\mathbf{G}^i\left(\mathbf{u}^i, \mathbf{w}^i\right) - \mathbf{G}_c^i\left(\mathbf{u}^i, \mathbf{w}^i\right) = 0 \tag{4.66}$$

Up until this point, nothing was really done to obtain the work conjugate pairs as was suggested in the introduction. To obtain these, an *interpretation* is to be made on the meaning of $\mathbf{w}^i$. On the one hand, $\mathbf{w}^i$ are often interpreted as virtual displacements. The interpretation of the above weak equations is then that of virtual work.

4.5.2 Weak Form with Virtual Work

Here frictionless contact is considered. We restrict the following developments to the case where all traction or displacement components are prescribed on a traction or displacement boundary, respectively. The contact surface is neither traction nor a displacement boundary. Thus the total boundary of work piece A is given by

$$\boldsymbol{\Gamma}^A = \boldsymbol{\Gamma}_\sigma^A \cup \boldsymbol{\Gamma}_u^A \cup \boldsymbol{\Gamma}^c \tag{4.67a}$$

$$\boldsymbol{\Gamma}_\sigma^A \cap \boldsymbol{\Gamma}_u^A = 0, \quad \boldsymbol{\Gamma}_u^A \cup \boldsymbol{\Gamma}^c = 0 \ \textit{and} \ \ \boldsymbol{\Gamma}_\sigma^A \cap \boldsymbol{\Gamma}^c = 0 \tag{4.67a}$$

Similar relations hold for slave body B.

In order to derive the weak form of the contact problem in metal forming, we use the Lagrange multiplier approach as regularization method for the impenetrability conditions. While alternative approaches are available (Penalty technique, augmented Lagrangian method, cross constrain method, etc), the Lagrange method is very popular despite the disadvantage that it is needed to set up a nodal and element topology for the Lagrange multipliers. However, there are no user-set parameters and the contact constraints can be met almost exactly when nodes are contiguous.

A common approach to imposing the contact constraints is by means of Lagrange multipliers. We will follow the description given by T. Belytschko (1998). Let the Lagrange multiplier trial functions $\lambda(\zeta^\alpha, t)$ and the corresponding test functions be in the following spaces

$$\begin{aligned} &\lambda(\zeta^\alpha, t) \in J^+, J^+ = \{\lambda(\zeta^\alpha, t) / \ \lambda \in c^{-1}, \lambda \geq 0 \ on \ \Gamma^c\} \ \ and \\ &\delta\lambda(\zeta^\alpha, t) \in J^-, J^- = \{\delta\lambda(\zeta^\alpha, t) / \ \delta\lambda \in c^{-1}, \delta\lambda \geq 0 \ on \ \Gamma^c\} \end{aligned} \tag{4.68}$$

The weak form is:

$$if \ \ \delta\mathbf{G}_L(\mathbf{u}, \delta\mathbf{u}, \lambda, \delta\lambda) \equiv \delta\mathbf{G} + \delta\mathbf{G}_C \geq 0 \qquad \forall \delta\mathbf{u} \in U_0, \forall \delta\lambda \in, J^- \tag{4.69}$$

$$\text{Then} \qquad \delta\mathbf{G}_C = \int_{\Gamma^C} \delta(\lambda g_N) d\Gamma \tag{4.70}$$

Where $\boldsymbol{\Gamma}_C$ is the part of the boundary which potentially comes in contact with die. This weak form is equivalent to the momentum equation, the traction boundary conditions and the following contact interface conditions: impenetrability (4.51) and momentum balance on

normal tractions (4.59). The restriction of the normal interface fraction to be compressive will result from the constraints on the trial set of Lagrange multipliers.

The term $\mathbf{G}^i\left(\mathbf{u}_{n+1}^i, \delta\mathbf{u}^i\right)$ is given as

$$\delta G_L^i = \int_\Omega \left(\delta u_i \sigma_{ji} - (\rho b_i - \rho \dot{u}_i)\right) d\Omega - \int_{\Gamma_C^i} \delta u_i \bar{t}_i d\Gamma = 0 \tag{4.71}$$

All integrals in the above apply to the union of both bodies, i.e. $\Omega^A = \Omega_\sigma^A \cup \Omega_\sigma^B$, $\mathbf{\Gamma}_c = \mathbf{\Gamma}_\sigma^A \cup \mathbf{\Gamma}_\sigma^B$. The first step is to integrate the internal virtual work by parts and apply Gauss's theorem:

$$\begin{aligned} &\int_\Omega \left(\delta u_i \sigma_{ji}\right)_{,j} d\Omega = \int_{\Gamma_\sigma^i} \delta u_i \sigma_{ji} n_j d\Gamma + \int_{\Gamma_c^i} (\delta u_i^A t_i^A + \delta u_i^B t_i^B) d\Gamma = 0 \\ &\Rightarrow \int_\Omega \nabla \sigma_{ji} d\Omega \delta u_i = \int_{\Gamma_\sigma^i} \delta u_i \sigma_{ji} n_j d\Gamma + \int_\Omega \delta u_{i,j} \sigma_{ji} d\Omega \\ &\qquad\qquad + \int_{\Gamma_c^i} (\delta u_i^A t_i^A + \delta u_i^B t_i^B) d\Gamma = 0 \end{aligned} \tag{4.72}$$

We have used the fact that the integral over the displacement boundary $\mathbf{\Gamma}_u$ vanishes because $\delta u_i = 0$ on $\mathbf{\Gamma}_u$ and Cauchy's law (equation 4.57) has been applied to obtain the expressions in the last integral. The first integral on the right hand side of the above applies to both the master and slave bodies. The contact surface integral appears for each body when Gauss's theorem is applied, so to express the result as a single integral, the field variables associated with the two bodies have been specifically indicated the superscripts A and B.

The integrand of the second integral on the RHS of the above is now broken up in to components normal and tangential to the contact surface. In indicial notation this gives

$$\delta u_N^A t_i^A = \delta u_N^A t_N^A + \delta \hat{u}_t^A \hat{t}_t^A \tag{4.73}$$

Where t_N is the normal tractions between the contacting bodies; and

t_t is tangential traction between the contacting bodies.

Substituting Equations (4.72) and (4.73) in to equation (4.71) gives

$$\begin{aligned} \delta G_L = &\int_\Omega \left(\delta u_i \sigma_{ji} - (\rho b_i - \rho \dot{u}_i)\right) d\Omega - \int_{\Gamma_t^i} \delta u_i (\sigma_{ji} n_j - \bar{t}_i) d\Gamma + \\ &\int_{\Gamma_C^i} (\delta u_N^A t_N^A + \delta u_N^B t_N^B + \delta \hat{u}_t^A \hat{t}_t^A + \delta \hat{u}_t^B \hat{t}_t^B) d\Gamma = 0 \end{aligned} \tag{4.74}$$

Now consider Equation (4.70)

$$\begin{aligned}\delta G_C &= \int_{\Gamma_C} \delta(\lambda g_N) d\Gamma \\ &= \int_{\Gamma_C} (\delta\lambda g_N + \delta g_N \lambda) d\Gamma \\ &= \int_{\Gamma_C} (\delta\lambda g_N + \lambda(\delta u_N^A - \delta u_N^B) d\Gamma\end{aligned} \tag{4.75}$$

Combining Equations (4.74) and (4.75) yields

$$\begin{aligned}\delta G_L = \int_\Omega \left(\delta u_i \sigma_{ji} - (\rho b_i - \rho \dot{u}_i)\right) d\Omega - \int_{\Gamma_t^i} \delta u_i (\sigma_{ji} n_j - \bar{t}_i) d\Gamma + \\ \int_{\Gamma_C^i} (\delta u_N^A (t_N^A + \lambda) + \delta u_N^B (t_N^B + \lambda) + \delta\lambda g_N) d\Gamma = 0\end{aligned} \tag{4.76}$$

5. FINITE ELEMENT IMPLEMENTATION

In this chapter, the metal forming problem is solved using the finite element method. The analysis of metal forming processes leads to a nonlinear problem where the iterative solution procedure can become very slow or may even diverge [38]. The non-linearities observed can be categorized as geometrical non-linearities, material non-linearities due to plastic deformation, and contact mode changes. In a static finite element program, high mesh resolution can cause convergence problems, especially for large deformable elements [34]. But a sufficiently fine mesh must be generated so that reasonable results are captured. According to K. C. Ho et al. [39], in order to obtain optimal and reliable convergence, it is essential that the rigid tool surface representation be smooth.

The above mentioned nonlinearities make the metal forming problem more complicated and hence equations that describe the solution must incorporate conditions which are not fully known until the solution is found. Therefore the solution can not be obtained in a single step of analysis. Rather we must take several steps, update the iterative solutions after each step, and repeat it until convergence test is satisfied.

Theoretically, the iteration may begin with either contact iteration or elasto-plastic iteration and go on till the contact status of all contact nodes does not change and there is no increase in new failure points. In practice, it seems to work better that the procedure begins with contact iteration. The corresponding iterative procedure in a load step is illustrated in Figure 5.2.

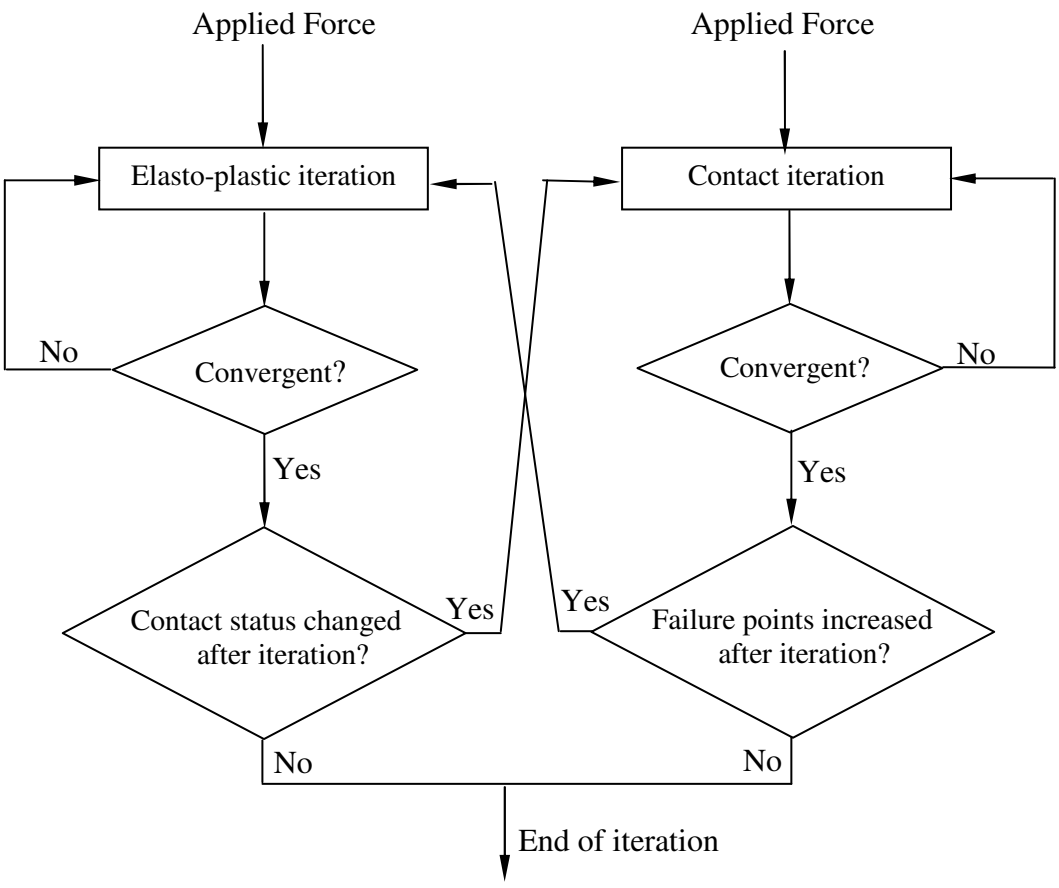

Figure 5.1 Iterative procedure

5.1 Incompressibility condition

With the previous weak formulation, the incompressibility condition $\Theta = tr(\boldsymbol{\varepsilon}) = 1$ can be introduced by a proper choice of the energy function $\mathbf{U}(\Theta)$. However the energy function $\mathbf{U}(\Theta)$ must satisfy the following two conditions.

- $\mathbf{U}(\Theta) \geq 0$. This condition is imposed by the fact that the energy must be positive or zero function.
- $\mathbf{U}(\Theta) = 0 \equiv \Theta = 1$. This condition is required by the incompressibility condition.

It is known that standard displacement-based finite element methods are known to behave poorly for nearly incompressible elasto-plastic media, like metal forming exhibiting volumetric locking

effect and failing to correctly reproduce ultimate loads in limit state analyses. Well-known finite element processes which overcome these difficulties include the family of $\overline{B}$ elements [10], enhanced-assumed strain (EAS) elements [41] or high-order mixed displacement–pressure formulations [10]. In this thesis, we consider an alternative approach based on the stabilization of a mixed displacement–pressure low-order finite element formulation.

In this thesis we are dealing with elasto-plasticity. Hence, a residual-driven iterative scheme is needed. Therefore, at step (n+1) we have the following volumetric–deviatoric split of the constitutive equations discussed in chapter 4:

$$\int_{\Omega} \mathbf{B}^T \mathbf{T}_{n+1} d\Omega = \mathbf{F}_{n+1}^{ext} \tag{5.1a}$$

$$\int_{\Omega} \tilde{\mathbf{N}}^T \mathbf{1}^T \left(\boldsymbol{\varepsilon}_{n+1} - \boldsymbol{\varepsilon}_{n+1}^p \right) d\Omega - \int_{\Omega} \tilde{\mathbf{N}}^T \frac{p_{n+1}}{K} d\Omega = 0 \tag{5.1b}$$

Equation (5.1a) represents the general constitutive equations and equation (5.1b) is representation of the volumetric–deviatoric split of the constitutive equations discussed in chapter four. Pressure shape functions are denoted by $\tilde{\mathbf{N}}$, and $\mathbf{B}$ is the standard strain–displacement operator including spatial derivatives of displacement shape functions and $\mathbf{1}$ is the vectorial representation of Kronecker's delta δ_{ij}. Applying a full implicit integration scheme for plastic strains the constitutive equation can be expressed in its integrated form (as given in chapter 4) at step (n+1), as:

$$\mathbf{T}_{n+1} = \overline{\mathbf{D}} \left[\boldsymbol{\varepsilon}_{n+1} - \boldsymbol{\varepsilon}_{n+1}^p) \right] + \mathbf{I} p_{n+1} \tag{5.2}$$

where $\overline{\mathbf{D}}$ is the deviatoric projection of the elastic constitutive matrix $\mathbf{D}$ defined as:

$$\overline{\mathbf{D}} = \mathbf{D}(\mathbf{I} - \frac{1}{3}\mathbf{1}\mathbf{1}^T) \tag{5.3}$$

and

$$\boldsymbol{\varepsilon}^p{}_{n+1} = \boldsymbol{\varepsilon}_n^p + \Delta\gamma_{n+1} f(\mathbf{T}_{n+1})$$

where γ is the plastic multiplier.

The stress correction is expressed as

$$\Delta\mathbf{T}_{n+1} = \overline{\mathbf{D}}\left(\Delta\boldsymbol{\varepsilon} - \Delta\gamma\mathbf{r}_{n+1} - \Delta\gamma_{n+1}\frac{\partial\mathbf{r}_{n+1}}{\partial\mathbf{T}}\Delta\mathbf{T} \right) + \mathbf{I}\Delta p \tag{5.4}$$

Rearranging the terms we get

$$\Delta\mathbf{T} = \overline{\mathbf{D}}^{*}\left(\Delta\boldsymbol{\varepsilon} - \Delta\gamma\mathbf{r}\right) + \overline{\mathbf{C}}^{*}\Delta p \tag{5.5}$$

with auxiliary matrices

$$\begin{aligned} \overline{\mathbf{D}}^{*} &= \mathbf{A}^{-1}\overline{\mathbf{D}}, \\ \overline{\mathbf{C}}^{*} &= \mathbf{A}^{-1}\mathbf{1}, \end{aligned} \tag{5.6}$$

and $$\mathbf{A}^{-1} = \left(\mathbf{1} + \Delta\gamma_{n+1}\frac{\partial\mathbf{r}_{n+1}}{\partial\mathbf{T}} \right)$$

The increment of plastic multiplier $\Delta\gamma$ appearing in Equation (5.5) can be expressed through total strain and mean pressure increments via consistency condition $\dot{f} = 0$, that is $\left(\frac{\partial f_{n+1}}{\partial\mathbf{T}_{n+1}}\right)^{T}\Delta\mathbf{T} = 0$, which yields

$$\Delta\gamma = \frac{\left(\frac{\partial f_{n+1}}{\partial\mathbf{T}_{n+1}}\right)^{T}\overline{\mathbf{D}}^{*}\Delta\varepsilon + \left(\frac{\partial f_{n+1}}{\partial\mathbf{T}_{n+1}}\right)^{T}\overline{\mathbf{C}}^{*}\Delta p}{\left(\frac{\partial f_{n+1}}{\partial\mathbf{T}_{n+1}}\right)^{T}\overline{\mathbf{D}}^{*}\mathbf{r}} \tag{5.7}$$

Introducing $\Delta\gamma$ into equation (5.5) we get the final form of the stress correction $\Delta\mathbf{T}$:

$$\Delta\mathbf{T} = \left(\overline{\mathbf{D}}^{*} - \frac{\overline{\mathbf{D}}^{*}\mathbf{r}\left(\frac{\partial f_{n+1}}{\partial\mathbf{T}_{n+1}}\right)^{T}\overline{\mathbf{D}}^{*}}{\left(\frac{\partial f_{n+1}}{\partial\mathbf{T}_{n+1}}\right)^{T}\overline{\mathbf{D}}^{*}\mathbf{r}} \right)\Delta\varepsilon + \left(\overline{\mathbf{C}}^{*} - \frac{\overline{\mathbf{D}}^{*}\mathbf{r}\left(\frac{\partial f_{n+1}}{\partial\mathbf{T}_{n+1}}\right)^{T}\overline{\mathbf{C}}^{*}}{\left(\frac{\partial f_{n+1}}{\partial\mathbf{T}_{n+1}}\right)^{T}\overline{\mathbf{D}}^{*}\mathbf{r}} \right)\Delta p \tag{5.8}$$

which we can express in compact form as:

$$\begin{aligned} &\Delta\mathbf{T} = \overline{\mathbf{D}}^{\mathbf{uu}}\Delta\boldsymbol{\varepsilon} + \overline{\mathbf{D}}^{\mathbf{up}}\Delta p \\ &or \\ &\Delta\mathbf{T} = \overline{\mathbf{D}}^{\mathbf{uu}}\mathbf{B}\Delta u + \overline{\mathbf{D}}^{\mathbf{up}}\tilde{\mathbf{N}}\Delta\mathbf{p} \end{aligned} \tag{5.9}$$

Hence the final form of the linearized equation takes the following form, at step (n+1) and iteration (i+1):

$$\int_{\Omega} \overline{\mathbf{D}}^{uu}\mathbf{B}\Delta\mathbf{u}d\Omega + \int_{\Omega} \overline{\mathbf{D}}^{up}\tilde{\mathbf{N}}\Delta\mathbf{p}d\Omega = \mathbf{F}_{n+1}^{ext} - \int \mathbf{B}^T\mathbf{T}_{n+1}d\Omega \tag{5.10}$$

During the iterative process, the accumulated values of the displacement and the pressure are updated as follows:

$$\begin{aligned} \Delta\mathbf{u}_{n+1} &= \Delta\mathbf{u}_{n+1} + \Delta\mathbf{u}, \\ \Delta\mathbf{p}_{n+1}^{i+1} &= \Delta\mathbf{p}_{n+1}^{i} + \Delta\mathbf{p}, \\ \Delta\boldsymbol{\lambda}_{n+1}^{i+1} &= \Delta\boldsymbol{\lambda}_{n+1}^{i} + \Delta\boldsymbol{\lambda}, \end{aligned} \tag{5.11}$$

Here, $\Delta\mathbf{p}_{n+1}^{i+1}$ can be viewed as the mean pressure of the stress increment $\Delta\mathbf{T}_{n+1}^{i+1}$ if and only if the step converges. During the iterations, $\Delta\mathbf{p}_{n+1}^{i+1}$ does not always coincide with the hydrostatic part of the hydro static-deviatoric split of the stress increment tensor [29], i.e. it may not be exactly the mean of the stress increment.

The linearized form of the pressure constitutive equation is expressed in the form:

$$\int_{\Omega} \tilde{\mathbf{N}}^T\mathbf{1}^T\left(\Delta\boldsymbol{\varepsilon} - \Delta\gamma\mathbf{r} - \Delta\gamma_{n+1}\frac{\partial\mathbf{r}}{\partial\mathbf{T}}\Delta\mathbf{T}\right)d\Omega - \int_{\Omega} \tilde{\mathbf{N}}^T\frac{\Delta p}{\mathbf{K}}d\Omega = \mathbf{R}_{\theta,n+1}^{i} \tag{5.12}$$

with the residual term $\mathbf{R}_{\theta,n+1}^{i}$ expressed as follows:

$$\mathbf{R}_{\theta,n+1}^{i} = -\int_{\Omega} \tilde{\mathbf{N}}^T\left(\mathbf{1}^T\left(\boldsymbol{\varepsilon}^{i}{}_{n+1} - \boldsymbol{\varepsilon}_{n+1}^{p,i}\right) - \Delta\gamma\mathbf{1}^T\frac{\partial\mathbf{r}}{\partial\mathbf{T}}\Delta\mathbf{T} - \frac{p^{i}{}_{n+1}}{K}\right)d\Omega \tag{5.13a}$$

If we restrict our consideration to the Drucker–Prager model then the term $\Delta\gamma_{n+1}\mathbf{1}^T\frac{\partial\mathbf{r}}{\partial\mathbf{T}}\Delta\mathbf{T}$ disappears and the simplified expression of equation (5.13a) will have the form:

$$\mathbf{R}_{\theta,n+1}^{i} = -\int_{\Omega} \tilde{\mathbf{N}}^T\left(\mathbf{1}^T\left(\boldsymbol{\varepsilon}^{i}{}_{n+1} - \boldsymbol{\varepsilon}_{n+1}^{p,i}\right) - \frac{p^{i}{}_{n+1}}{K}\right)d\Omega \tag{5.13b}$$

$$\mathbf{R}_{\theta,n+1}^{i} = \int_{\Omega} \tilde{\mathbf{N}}^T\left(\mathbf{1}^T - \frac{\mathbf{1}^T\mathbf{r}\left(\frac{\partial f}{\partial\mathbf{T}_{n+1}}\right)^T\overline{\mathbf{D}}^{*}}{\left(\frac{\partial f}{\partial\mathbf{T}_{n+1}}\right)^T\overline{\mathbf{D}}^{*}\mathbf{r}}\right)\Delta\boldsymbol{\varepsilon}d\Omega - \int_{\Omega} \tilde{\mathbf{N}}^T\left(\frac{1}{K} + \frac{\mathbf{1}^T\mathbf{r}\left(\frac{\partial f}{\partial\mathbf{T}_{n+1}}\right)^T\overline{\mathbf{C}}^{*}}{\left(\frac{\partial f}{\partial\mathbf{T}_{n+1}}\right)^T\overline{\mathbf{D}}^{*}\mathbf{r}}\right)\tilde{\mathbf{N}}\Delta\mathbf{p}d\Omega \tag{5.14}$$

or in compact form

$$\int_{\Omega} \tilde{\mathbf{N}}^T\overline{\mathbf{D}}^{\mathbf{pu}}\mathbf{B}\Delta\Delta\mathbf{d}\Omega + \int_{\Omega} \tilde{\mathbf{N}}^T\overline{\mathbf{D}}^{\mathbf{pp}}\tilde{\mathbf{N}}\Delta\mathbf{p}\,d\Omega = \mathbf{R}_{n+1}^{i} \tag{5.15}$$

In the case of J2-Plasticity (von Mises), $\overline{\mathbf{D}}^{\mathbf{pu}}$ is reduced to $\mathbf{1}^{\mathbf{T}}$ and $\overline{\mathbf{D}}^{\mathbf{pp}}$ reduces to $\frac{1}{K}$ as $\mathbf{r}$ is orthogonal to $\mathbf{1}$ and therefore $\mathbf{1}^{\mathbf{T}}\mathbf{r} = 0$.

By grouping Equations (5.10) and (5.15), we get:

$$\begin{bmatrix} \mathbf{K}_{uu} & \mathbf{K}_{up} \\ \mathbf{K}_{pu} & \mathbf{K}_{pp} \end{bmatrix} \begin{Bmatrix} \Delta\mathbf{u} \\ \Delta\mathbf{p} \end{Bmatrix} = \begin{Bmatrix} \mathbf{F}^{u} \\ \mathbf{F}^{p} \end{Bmatrix} \tag{5.16}$$

with the left-hand side:

$$\begin{aligned} \mathbf{K}_{uu} &= \int_{\Omega} \mathbf{B}^{T} \overline{\mathbf{D}}^{uu} \mathbf{B} d\Omega, \\ \mathbf{K}_{up} &= \int_{\Omega} \mathbf{B}^{T} \overline{\mathbf{D}}^{up} \tilde{\mathbf{N}} d\Omega, \\ \mathbf{K}_{uu} &= \int_{\Omega} \tilde{\mathbf{N}}^{T} \overline{\mathbf{D}}^{pu} \mathbf{B} d\Omega, \\ \mathbf{K}_{uu} &= \int_{\Omega} \tilde{\mathbf{N}}^{T} \overline{\mathbf{D}}^{pp} \tilde{\mathbf{N}} d\Omega \end{aligned} \tag{5.17}$$

and the right-hand side:

$$\begin{aligned} \mathbf{F}_{u} &= \mathbf{F}_{n+1}^{ext} - \int_{\Omega} \mathbf{B}^{T} \mathbf{T}_{n+1}^{i} d\Omega, \\ \mathbf{F}_{p} &= \mathbf{R}_{\theta,n+1}^{i} \end{aligned} \tag{5.18}$$

The second line of equation (5.16) is the multiplied by -1 in order to achieve positive-definiteness:

$$\begin{bmatrix} \mathbf{K}_{uu} & \mathbf{K}_{up} \\ -\mathbf{K}_{pu} & -\mathbf{K}_{pp} \end{bmatrix} \begin{Bmatrix} \Delta\mathbf{u} \\ \Delta\mathbf{p} \end{Bmatrix} = \begin{Bmatrix} \mathbf{F}^{u} \\ -\mathbf{F}^{p} \end{Bmatrix} \tag{5.19}$$

5.2. Stabilization techniques

Stabilized methods are generalized Galerkin methods where terms are added to enhance the stability of the method. Those terms are typically functions of the residuals of the Lagrange equations multiplied by a differential operator acting on the weight space, and evaluated element-wise. Therefore, we have to add appropriate terms to the matrix equation (5.19) in order to enhance its stability. These terms take the form:

$$\sum_{e=1}^{n_{el}} \int_{\Omega e} \left(\mathbf{L}^T \mathbf{T}(\mathbf{W}^h, \mathbf{q}^h)\right)^T \tau \left(\mathbf{L}^T \mathbf{T}(\mathbf{u}^h, \mathbf{p}^h) + \mathbf{f}\right) d\Omega \tag{5.20}$$

where, $\boldsymbol{\tau}$ is a stabilization factor matrix, with $\boldsymbol{\tau} = \tau \mathbf{I}$ and τ is defined as:

$$\tau = \frac{\vartheta^e (h^e)}{2K}$$

ϑ^e is a dimensionless scalar factor and h^e is a characteristic length of the element and K is the element's material shear modulus.

The weighting part and the residual part of equation (5.20) will now be addressed separately. In the elasto-plastic case, the weighting part of the stabilization term (equation (5.20)) can be written as:

$$\mathbf{L}^T \mathbf{T}(\mathbf{W}^h, \mathbf{q}^h) = \mathbf{L}^T \left(\overline{\mathbf{D}}(\boldsymbol{\varepsilon}(\mathbf{w}^h) - \boldsymbol{\varepsilon}^p(\mathbf{w}^h, \mathbf{q}^h)) + \mathbf{1}\mathbf{q}^h\right) \tag{5.21}$$

We modify the standard (Galerkin/least-squares) GLS scheme by dropping the plastic contribution, avoiding therefore linearization of the weighting part of the stabilizing terms, and the weighting term $\mathbf{L}^T \mathbf{T}(\mathbf{w}^h, \mathbf{q}^h)$ is replaced by the $\mathbf{P}(\mathbf{w}^h, \mathbf{q}^h)$

$$\mathbf{P}(\mathbf{w}^h, \mathbf{q}^h) = \mathbf{L}^T \overline{\mathbf{D}} \mathbf{B}\mathbf{w} + \mathbf{L}^T \mathbf{1} \tilde{\mathbf{N}} \mathbf{q} = \mathbf{L}_p^{el} \mathbf{w} + \mathbf{L}_p^{el} \mathbf{q} \tag{5.22}$$

Expressing the residual part of the stabilizing term at step (n+1), iteration (n+1):

$$\mathbf{T}_{n+1}^{i+1}(\mathbf{u}^h, p^h) + \mathbf{f} = \mathbf{L}^T (\mathbf{T}_{n+1}^{i+1}, \Delta \mathbf{T}) + \mathbf{f} = \mathbf{R}_{T,n+1}^{i} + \Delta \mathbf{R} + \mathbf{f} \tag{5.23}$$

where the incremental constitutive equation (5.9) can be used in order to derive an expression for

$$\Delta \mathbf{R}_T = \mathbf{L}^T (\overline{\mathbf{D}}^{uu} \mathbf{B} \Delta \boldsymbol{\Delta} + \overline{\mathbf{D}}^{up} \tilde{\mathbf{N}} \Delta \mathbf{p}) \tag{5.24}$$

and therefore

$$\begin{aligned} \mathbf{R}_{T,n+1}^{i+1} &= \mathbf{R}_{T,n+1}^{i} + \mathbf{L}^T \overline{\mathbf{D}}^{uu} \mathbf{B} \Delta \boldsymbol{\Delta} + \mathbf{L}^T \overline{\mathbf{D}}^{up} \tilde{\mathbf{N}} \Delta \mathbf{p} \\ &= \mathbf{R}_{T,n+1}^{i} + \mathbf{G}_u^{ep} \Delta \mathbf{u}_{n+1}^{i+1} + \mathbf{G}_p^{ep} \Delta \mathbf{p}_{n+1}^{i+1} \end{aligned} \tag{5.25}$$

Collecting weighting and residual parts of the stabilizing term leads to

$$\sum_{e=1}^{n_{el}} \int_{\Omega^e} (\mathbf{G}_u^{el} \mathbf{w} + \mathbf{G}_p^{el} \mathbf{q})^T \boldsymbol{\tau} (\mathbf{R}_{T,n+1}^{i} + \mathbf{G}_u^{ep} \Delta \mathbf{u} + \mathbf{G}_p^{ep} \Delta \mathbf{p} + \mathbf{f}) d\Omega \tag{5.26}$$

Adding these terms to the matrix equation (5.19) we end up with the following system of equations:

$$\begin{bmatrix} \mathbf{K}_{uu} + \mathbf{K}'_{uu} & \mathbf{K}_{up} + \mathbf{K}'_{up} \\ -\mathbf{K}_{pu} + \mathbf{K}'_{pu} & -\mathbf{K}_{pp} + \mathbf{K}'_{pp} \end{bmatrix} \begin{Bmatrix} \Delta \mathbf{u} \\ \Delta \mathbf{p} \end{Bmatrix} = \begin{Bmatrix} \mathbf{F}^u + \mathbf{F}'_u \\ -\mathbf{F}^p + \mathbf{F}'_p \end{Bmatrix} \tag{5.27}$$

where

$$\mathbf{K}'_{uu} = \sum_{e=1}^{n_{el}} \int_{\Omega^e} \mathbf{G}_u^{el} \boldsymbol{\tau} \mathbf{G}_p^{ep} \mathbf{d}\Omega, \qquad \mathbf{K}'_{up} = \sum_{e=1}^{n_{el}} \int_{\Omega^e} \mathbf{G}_u^{el,T} \boldsymbol{\tau} \mathbf{G}_p^{ep} \mathbf{d}\Omega,$$

$$\mathbf{K}'_{pu} = \sum_{e=1}^{n_{el}} \int_{\Omega^e} \mathbf{G}_p^{el,T} \boldsymbol{\tau} \mathbf{G}_u^{ep} \mathbf{d}\Omega, \qquad \mathbf{K}'_{pp} = \sum_{e=1}^{n_{el}} \int_{\Omega^e} \mathbf{G}_p^{el,T} \boldsymbol{\tau} \mathbf{G}_p^{ep} \mathbf{d}\Omega\Omega \tag{5.28}$$

$$\mathbf{F}'_u = \sum_{e=1}^{n_{el}} \int_{\Omega^e} \mathbf{G}_u^{el,T} \boldsymbol{\tau} (\mathbf{R}_{T,n+1}^i + \mathbf{f}) \mathbf{d}\Omega, \quad \mathbf{F}'_p = \sum_{e=1}^{n_{el}} \int_{\Omega^e} \mathbf{G}_p^{el,T} \boldsymbol{\tau} (\mathbf{R}_{T,n+1}^i + \mathbf{f}) \mathbf{d}\Omega$$

The scheme of the iterative solution of equation (5.27) is given below.

Loop 1: Incremental loading

2-Point prediction

Loop 2: Newton Iteration, *i=1, 2,3,…*

Compute **[K]** and **R** (**R** is he residual)

if $\left\|\mathbf{R}(\mathbf{u}^i)\right\| < \hat{\varepsilon}$ // $\hat{\varepsilon}$ is the saturation parameter.

Terminate Newton Iteration

else

$\Delta\mathbf{u} = \mathbf{-K}(\mathbf{u}^i)^{-1}\mathbf{R}(\mathbf{u}^i)$ // Linearized System Solution

$\mathbf{u}^{(ewton)} = \mathbf{u}^i + \Delta\mathbf{u}$ // Full Newton Step

Loop 3: Line Search, $\alpha = 1, 1/2, 1/4, \ldots$

if $\left\|\mathbf{R}((1-\alpha)\mathbf{u}^i + \alpha\mathbf{u}^{newton})\right\| < \left\|\mathbf{R}(\mathbf{u}^i)\right\|$

$\mathbf{u}^{i+1} = (1-\alpha)\mathbf{u}^i + \alpha\mathbf{u}^{newton}$

Terminate Line Search

Figure 5.2 Algorithm of Nonlinear System Solver

5.3 Solution Procedure

The finite element method is accompanied by a large number of numerical procedures such as: numerical integration, numerical algorithms for solving nonlinear problems. In this thesis we mention briefly some of these methods which play an important role in the analysis of the metal forming problem. Since we will use MATLAB, we limit our presentation to numerical methods related to this code. Here, the following shape functions are used for displacement field modeling.

$$
\begin{aligned}
N_1(\xi,\eta) &= \frac{1}{4}(1-\xi)(1-\eta) \\
N_2(\xi,\eta) &= \frac{1}{4}(1+\xi)(1-\eta) \\
N_3(\xi,\eta) &= \frac{1}{4}(1+\xi)(1+\eta) \\
N_4(\xi,\eta) &= \frac{1}{4}(1-\xi)(1+\eta)
\end{aligned}
\tag{5.29}
$$

where ξ *and* η are the local coordinates of the node *i* as is shown in Figure 5.1.

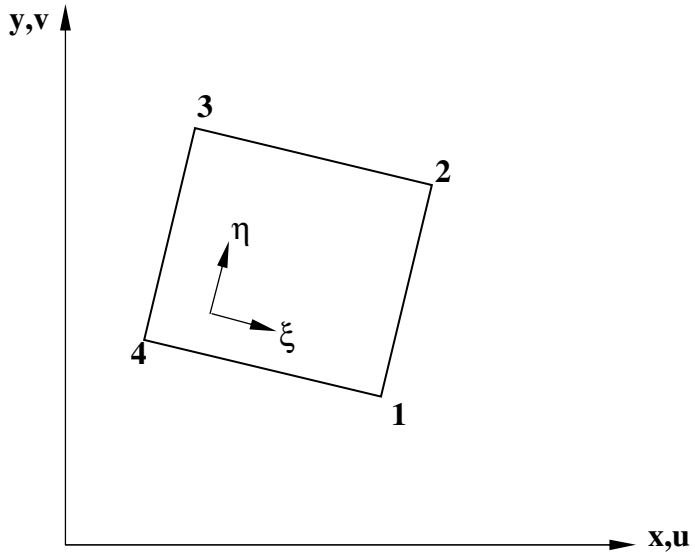

Figure 5.3 Two dimensional constant strain triangular finite

The procedure is a 2×2 Gauss-type integration. Here we distinguish two types of integrals: volume integrals and surface integrals. A volume integral on the element *e* is calculated as follows

$$\begin{aligned}\int_{\Omega^e} f(\mathbf{x}_1,\mathbf{x}_2)d\Omega &= \int_{-1}^{+1}\int_{-1}^{+1} f(\xi,\eta)J_e d\xi d\eta \\ &= \sum_{i=1}^{2}\sum_{j=1}^{2} f(\xi,\eta)Jw_i w_j\end{aligned} \tag{5.30}$$

where ξ *and* η are the Gauss point coordinates and w_i and w_j are the Gauss weights.*J* is the surface Jacobian [1]

$$\begin{aligned}J &= \begin{vmatrix} \dfrac{\partial x_1}{\partial \xi} & \dfrac{\partial x_1}{\partial \eta} \\ \dfrac{\partial x_2}{\partial \xi} & \dfrac{\partial x_2}{\partial \eta} \end{vmatrix} = \left| \frac{\partial \mathbf{x}}{\partial \xi} \times \frac{\partial \mathbf{x}}{\partial \eta} \right| \\ &= \sqrt{\mathbf{VW} - \mathbf{Z}^2}\end{aligned} \tag{5.31}$$

in which

$$\mathbf{V} = \frac{\partial \mathbf{x}}{\partial \xi}\cdot\frac{\partial \mathbf{x}}{\partial \xi}, \quad \mathbf{W} = \frac{\partial \mathbf{x}}{\partial \eta}\cdot\frac{\partial \mathbf{x}}{\partial \eta}, \quad \textit{and} \quad \mathbf{Z} = \frac{\partial \mathbf{x}}{\partial \xi}\cdot\frac{\partial \mathbf{x}}{\partial \eta} \tag{5.32}$$

The unit normal to the surface of the element *e* is

$$\mathbf{n} = \frac{1}{J}\left(\frac{\partial \mathbf{x}}{\partial \xi}\times\frac{\partial \mathbf{x}}{\partial \eta}\right) \tag{5.32}$$

5.4 Iterative algorithm

Solving equation (5.27) implies calculation of the tangent stiffness matrix $\mathbf{K}^{\tan}$ at every iteration. This iteration method is called full Newton-Raphson. This is very expensive in the finite element analysis and therefore a modified procedure is usually used. One way is to use the tangent matrix from the first time step. This method is called the initial stress method and it usually leads to more iterations as the solution advances in time. The contact algorithm is based on the Lagrange multiplier method with augmentation steps in order to increase the accuracy and efficiency of the algorithm.

In the updated Lagrangian FEM formulation, sequences of incremental problems are defined from time t_n to t_{n+1}; n=0, 1, 2… Within each time increment, as discussed in chapter 3 and 4, the deformation problem is further divided into three incremental sub-problems: (1) the constitutive problem, (2) the kinematic problem and (3) the contact problem.

In the constitutive incremental problem, we calculate $(\mathbf{T}_{n+1}, s_{n+1}, \mathbf{F}^p_{n+1})$ given the incremental deformation gradient $\mathbf{F}^{trial}$ from t_n to t_{n+1} and $(\mathbf{T}_n, s_n, \mathbf{F}^p_n)$. In the kinematic problem, one calculates the incremental displacements from t_n to t_{n+1} given the triad $(\mathbf{T}, s, \mathbf{F}^p)$ at t_{n+1}. In the contact sub-problem, given the configuration $\mathbf{B}_{n+1}$, the die location and shape at t_{n+1}, as well as estimates of the contact tractions from a previous time step or Newton iteration, we have to compute (update) regions of contact as well as the contact traction component λ_N. The overall solution method for the large deformation problem with contact can be divided in to two main steps. The first one is solving of the principle of virtual work relations for the incremental displacements. Then the next step is updating of the stresses and state variables based on the incremental displacements calculated before.

In the algorithm below, *k* refers to the augmentation index and *j* refers to the Newton–Raphson iteration index. The terms $\mathbf{G}$ and $\mathbf{G}_C$ in the kinematic problem refer to the principle of virtual work and contributions from the internal work/non-contact related boundary terms and contact terms, respectively [28].

1. Initialization:

   $\lambda_N^{(0)} = \lambda_{N_n}$

   $\Delta\lambda_T^{(0)} = 0$

   $k = 0$

2. Solve for the incremental displacement $\mathbf{u}^{(k)} = \mathbf{x}_{n+1}^{(k)} - \mathbf{x}_n$ which is the converged estimate of $\mathbf{u}_j^{(k)} = \mathbf{x}_{n+1,j}^{(k)} - \mathbf{x}_n$:

   $$\tilde{\mathbf{G}}(\mathbf{u}_j^{(k)}, \tilde{\mathbf{u}}) = \mathbf{G}(\mathbf{u}_j^{(k)}, \tilde{\mathbf{u}}) + \mathbf{G}_C(\mathbf{u}_j^{(k)}, \tilde{\mathbf{u}}) = 0$$

Here, the above equation is non-linear and is solved iteratively [28]. A Newton–Raphson algorithm is used to solve this system and the computation of the linearized stiffness matrix and residual is dependent on the solution of the kinematic, constitutive and contact sub-problems. The solution of this non-linear equation predicts estimates of the body configuration $\mathbf{B}^{k}{}_{n+1,j}$ at t_{n+1} and finally the converged solution $\mathbf{B}^{k}{}_{n+1}$.

The contact traction $\lambda^{k}_{j\text{-}1}$ used in the solution of the linearized principle of virtual work (based on the estimate $\mathbf{B}^{k}_{(n+1),(j-1)}$) is calculated as follows:

Normal traction:

$$\lambda_N = \lambda^{k}_{N}$$

Tangential traction:

Compute trial state:

$$\lambda_T^{trial} = \lambda_{T_n} + \Delta\lambda_T^{k}$$

$$\Pi^{trial} = \left\|\lambda_T^{trial}\right\| - \mu\lambda_N$$

Radial return update:

IF $\left(\Pi^{trial} \le 0\right)$

THEN $\lambda_T = \lambda_T^{trial}$ $(stick)$

ELSE

$$\lambda_T = \mu\lambda_N \frac{\lambda_T^{trial}}{\left\|\lambda_T^{trial}\right\|} \quad (slip)$$

Complete contact traction description:

$$\lambda^{k}_{j-1} = \lambda_N \mathbf{v}(\bar{\mathbf{y}}) - \lambda_T \boldsymbol{\tau}_1(\bar{\mathbf{y}})$$

3. Check for contact constraints satisfaction:

IF $g(\mathbf{x}^{(k)}_{n+1}) \le TOL_g$

CONVERGED

ELSE

AUGMENT ($\forall \mathbf{x}_n \in \boldsymbol{\Gamma}$)

$$\lambda_N^{(k+1)} = \lambda_T^{(k)}$$

$$\lambda_N^{trial} = \lambda_{T_n} + \Delta\lambda_T^{(k)}$$

$$\Pi^{trial} = \left\| \lambda_N^{trial} \right\| - \mu\lambda_N^{(k+1)}$$

IF $\left(\Pi^{trial} \le 0\right)$

THEN

$$\Delta\lambda_T^{(k+1)} = \Delta\lambda_T^{(k)}$$

ELSE

$$\Delta\lambda_T^{(k+1)} = \mu\Delta\lambda_N^{(k+1)} \frac{\lambda_T^{(trial)}}{\left\| \lambda_T^{(trial)} \right\|} - \lambda_{T_n}$$

END

k=k+1

GO TO STEP2

END

4. Post-process operation:

   Use the converged solution of the configuration $\mathbf{B}_{n+1}$ to update the triad ($\mathbf{T}, s, \mathbf{F}^p$) as well as the contact traction component (λ_N) at time t_{n+1}.

The three sub-problems (constitutive, kinematic and contact) are solved in an iterative manner.

CHAPTER SIX

6. NUMERICAL EXAMPLE AND DISCUSSION OF RESULTS

6.1 Axisymmetric open-die forging

Open die forging is a process in which products are made through repeated, incremental plastic deformations of a work piece using dies of relatively simple shapes. It is commonly used to reduce large ingots or billets into square or round bars of smaller dimension, or for forging large high-value parts with limited geometric complexity. In a typical open die forging system the work piece is held by a forging manipulator that positions it between the dies of the press. In contrast to the more common closed die forging process, the dies only deform a limited region of the work piece surface, so that many programmed forming increments are needed to bring the work piece to its final shape.

Open die forging is of interest for theoretical studies as a model process since it represents a basic process which can be varied in many ways to analyze different types of forming problems. In addition to a large segment of the industry depends primarily on the predominant application of open die forging processes. Parts produced using this process includes forging ingots, large and bulky forgings, preforms for finished forgings, etc.

The actual problem can be described schematically as shown in figure 6.1. Here the work piece is placed on the fixed lower die and the desired shape will be imparted to the work piece by the downward movement of the moveable upper die. In this thesis the one which is indicated in part (b), uniform deformation of the billet without friction, is considered.

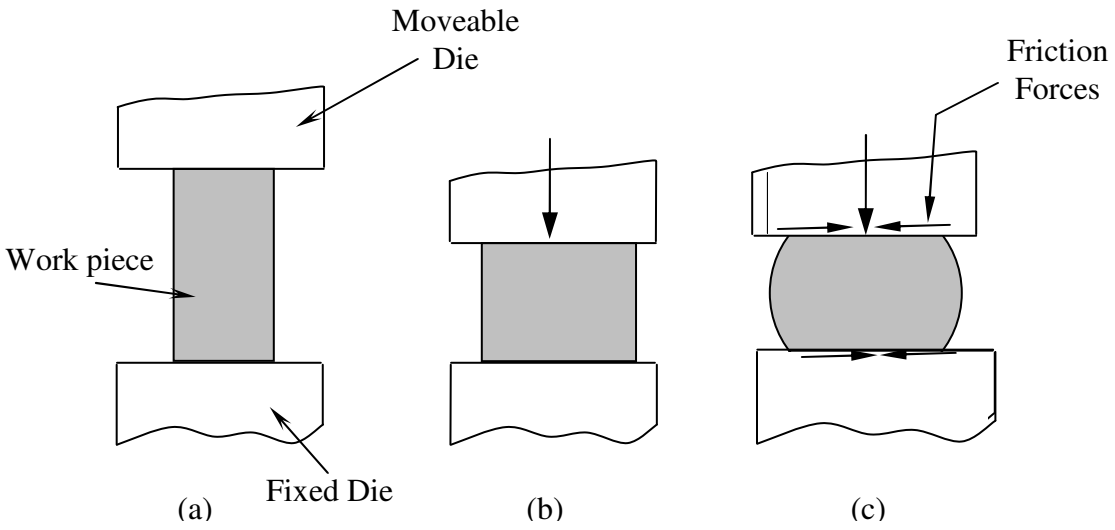

Figure 6.1 (a) Solid cylindrical billet between two flat dies. (b) Uniform deformation of the billet without friction. (c) Deformation with friction.

In order to minimize the complexity of the problem and to get results close to what is obtained in practice with minimum computational cost, we have made assumptions that are relevant to the given problem. Thus, the assumptions considered during the formulation of the problem and the material models used for the implementation of the formulation using the finite element method are described below.

- Dies are assumed to be rigid and will not experience any deformation.
- Contact between die and work piece is taken as frictionless.
- The displacements are two dimensional.
- The process is considered to be isothermal.
- The work piece material is isotropic.
- The process is assumed to be quasi-static.

6.2 Material model

In this section, we will present a rate-dependent plasticity model proposed by Anand [35]. This rate-dependent model differs from the rate-independent model in that there is no explicit yield condition, and no loading/unloading criterion is used. Instead, plastic flow is assumed to take place at all non-zero stress values, although at law stresses the rate of plastic flow may be immeasurably small. Further, the equivalent plastic strain rate needs to be prescribed by an appropriate constitutive function in the rate-dependent model.

Here are two basic futures in Anand's model applicable to isotropic rate-dependent constitutive model for metals.

I. There is no explicit yield surface; rather the instantaneous response of the material is dependent on its current state.
II. A single scalar internal variable "*s*", called the *deformation resistance*, is used to represent the isotopic resistance to inelastic flow of the material.

The specifics of this constitutive equation are the flow equation

$$f(\tilde{\sigma}, s) = \dot{\tilde{\varepsilon}}^{p} = Ae^{-\frac{Q}{R\theta}}[\sinh(\xi\frac{\tilde{\sigma}}{s})]^{\frac{1}{m}} \tag{6.1}$$

and the evolution equation:

$$g(\tilde{\sigma}, s) = \dot{s} = h_o\left|1-\frac{s}{s^*}\right| f(\tilde{\sigma}, s) \tag{6.2}$$

Equation (6.2) allows modeling of both strain hardening and strain softening.

with

$$s^* = \tilde{s}\left(\frac{\dot{\tilde{\varepsilon}}^{p}}{A}\right)^{b} \tag{6.3}$$

where f =effective inelastic deformation rate

$\tilde{\sigma}$ =effective Cauchy stress

s =deformation resistance

s^* =saturation value of deformation resistance

$\dot{s}$ =time derivative of deformation resistance

θ =absolute temperature

The remaining parameters are defined in Table 6.1. The inelastic strain rate in Anand's definition of material is stress dependent as well as dependent on the rate of loading. A consistent stress update procedure which is equivalent to Euler backward scheme is used to enforce the consistency condition and the evolution equation (6.2) at the end of the time step.

Table 6.1 Material Parameter Units for Anand Model [2]

	Parameter	Meaning	Units
1	s_o	Initial value of deformation resistance	Mpa
2	$\frac{Q}{R}$	Q=Activation Energy	
		R=Universal gas constant	KJ/(mole*^oK)]
3	A	Pre-exponential factor	1/second
4	ξ	Multiplier of stress	Dimensionless
5	m	Strain rate sensitivity of stress	Dimensionless
6	h_o	Hardening/softening constant	Mpa
7	$\tilde{s}$	Coefficient for deformation resistance saturation value	Mpa
8	b	Strain rate sensitivity of saturation (deformation resistance) value	Dimensionless
9	a	Strain rate sensitivity of hardening or softening	Dimensionless

Here, as an example of a large deformation metal forming problem, the open-die forging of a cylindrical 1100-Al billet is considered between parallel dies. This benchmark problem is examined with the quadrilateral elements to address incompressibility [3].

Principal Design Features of 1100-Al

1100-Al is a relatively low strength, essentially pure aluminum alloy. It is noted for excellent formability and welding characteristics along with good corrosion resistance. It cannot be hardened by heat treatment. It has also excellent forming capability by cold or hot working with commercial techniques. The chemistry data of 1100-Al is given in table 6.2 below.

Table 6.2 Chemistry data of 1100-Al [45]

Material	*Value (%)*	*Material*	*Value (%)*
Aluminum	99.6 min	Titanium	0.03 max
Copper	0.05 max	Vanadium	0.05 max
Iron	0.35 max	Manganese	0.03 max
Magnesium	0.03 max	zinc	0.05 max
Remainder Each	0.03 max	silicon	0.25 max

The specific values of the material parameters are given in table 6.3 below.

Table 6.3 Material parameters for Al 1100-O at 673 K [2]

Material Parameter	*Value*
A	$4.75\times10^{-7}\ s^{-1}$
ξ	7.0
m	0.23348
s_o	29.7 Mpa
h_o	1115.6 Mpa
$\tilde{s}$	18.92 Mpa
n	0.07049
a	1.3
μ	20.2 Mpa
k	66.0 Mpa

6.3 Finite Element Model

In this forging example, the initial cylindrical billet is 5mm in diameter and 7.5mm high. The dimensions given in Zabaras et al. were 2mm and 3mm, respectively [2]. The forging die is modeled as a rigid surface and there is no friction between the die and the workpiece, as mentioned before. The deformation is highly non-homogeneous with variable rates of straining at material points and time-varying/unsteady contact. The symmetry of the problem allows modeling one half of the geometry.

A nominal strain rate of 0.01 is applied during the forging process. Rather coarse uniform grids of 10×10 four-nodded quadrilateral finite elements are used to discretize the domain. A stabilizing parameter of $\varepsilon = 10^{-4}$ is used in the analysis.

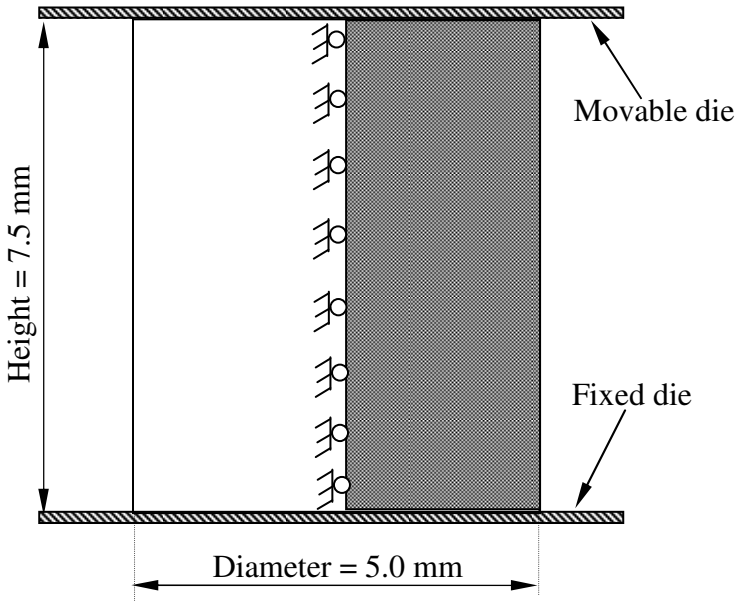

Figure 6.2 Geometry and Boundary condition for the open die forging of a cylindrical billet

The finite element decartelization involves quadrilateral elements to address incompressibility [39]. The domain of the problem is discretized by a finite element mesh and the displacement field is expressed by means of finite element shape functions. The nodal displacements along with the finite element shape functions describe the displacement field. The boundary conditions are either fixed displacements or tractions. The finite element model of the problem with respective boundary conditions is shown in the figure 6.3 [2].

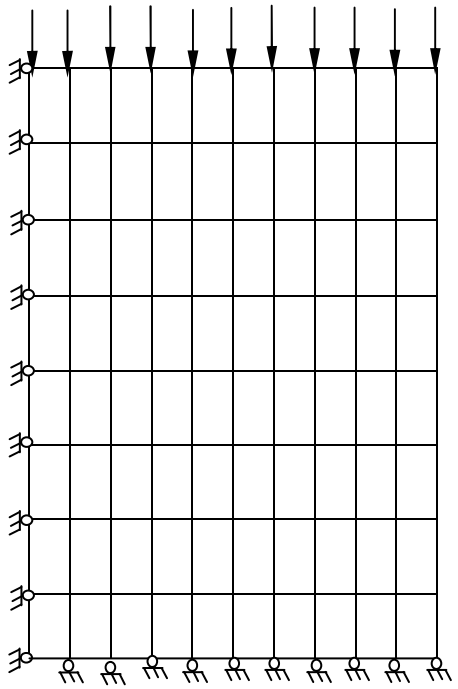

Figure 6.3 The Axisymmetric finite element model of open die forging problem

The deformed mesh after 56.3 percent height reduction is shown in figure 6.4 along with the undeformed mesh. This is obtained in 25 minutes using a fixed time step of one second. If the number of iterations is reduced, the intermediate configuration looks like that given in figure 6.5 after 300 iterations with initial assumed displacement of 0.1 times the value of the nodal displacements calculated while the element loaded elastically and assumed value of zero stress and zero internal variables. Figure 6.6 shows the contour of the equivalent plastic strain at the end of the open die forging (upsetting) process. As can be seen from the figure, the maximum equivalent plastic strain is found around the middle of the work piece and decreases to wards the

ends. This is due to the fact that, at the middle of the workpiece, there is an additive nature of the equivalent plastic strain due to the applied force at the top by the moveable die causing a downward and horizontal plastic strain components to occur and the reaction force at the bottom by the lower fixed die which produces an upward and horizontal plastic strain components. But to wards the ends, this additive nature decreases causing the equivalent plastic strain to decrease. The results are in good agreement with the numerical solutions of Zabaras et al [2].

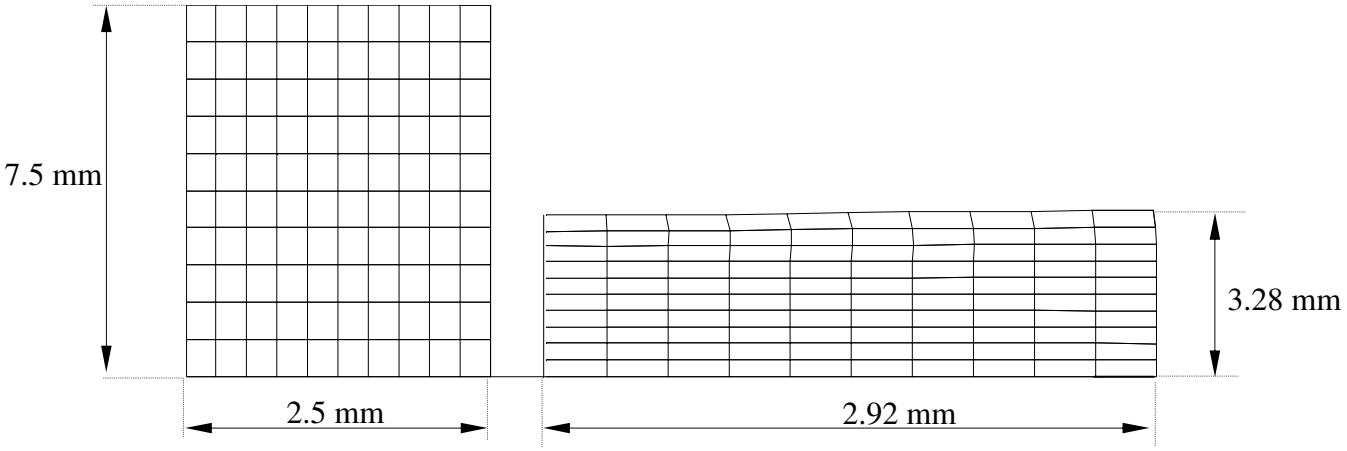

Figure 6.4 Initial and deformed meshes after 56.3 percent height reduction in axisymmetric open die forging. (Owing to the symmetry of the problem only a half of the billet is modeled).

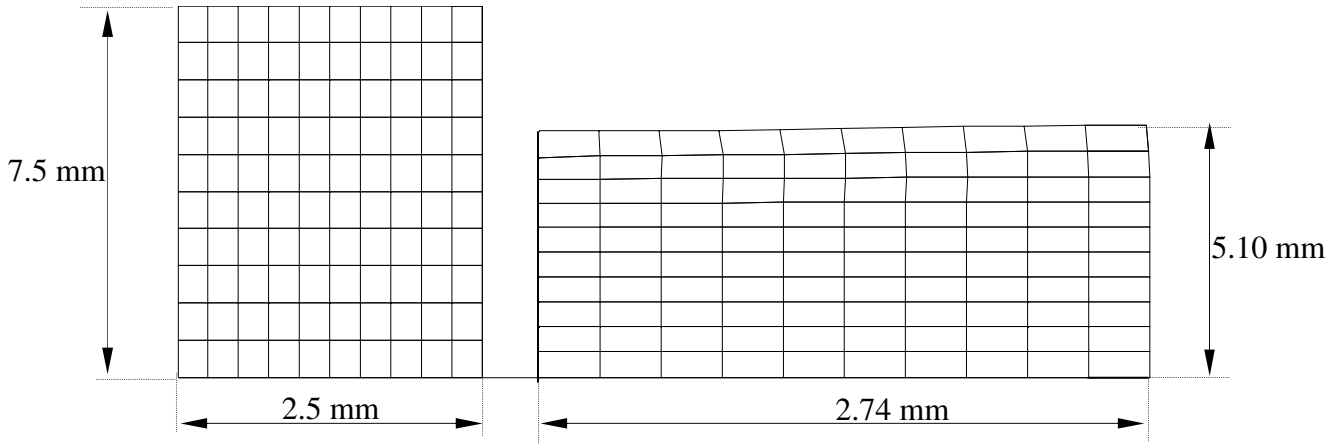

Figure 6.5 Initial and deformed configuration of the work-piece after 300 iterations with initially assumed displacement of 0.1 times the value of nodal displacements calculated while the element is loaded elastically and assumed value of zero stress and zero internal variables

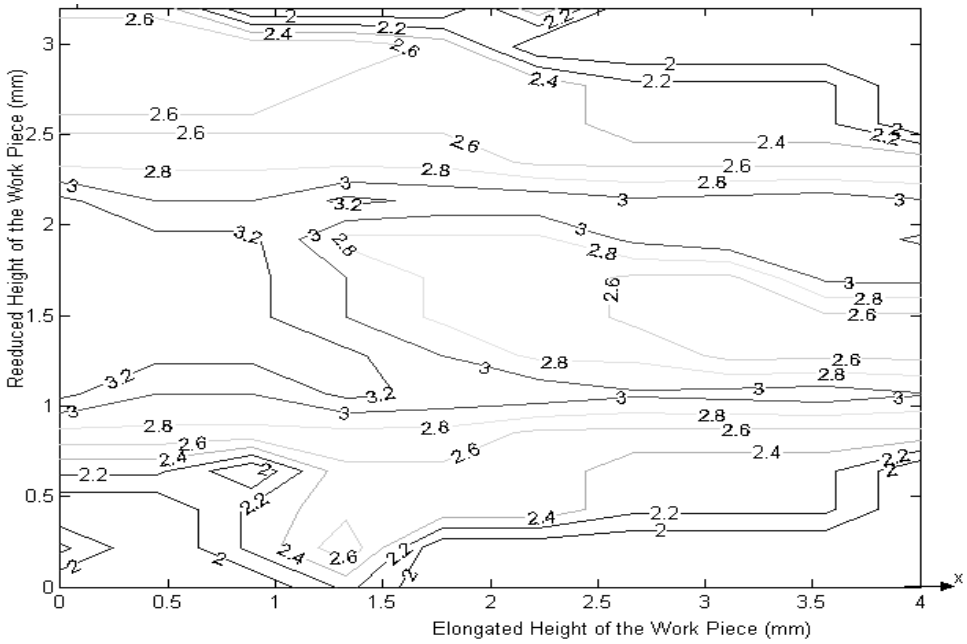

Figure 6.6 Contours of the equivalent plastic strain in the final forged product.

6.5 Summary

In this thesis, finite element implementation and evaluation of the performance of a family of objective integration schemes based on the hyperelastic-viscoplastic constitutive equations of large deformation of a metal forming process has been developed. Also the integration of the contact integral was discussed. One of the key factors that arise in this process is that of geometric incompatibility when the problem under consideration is discretised. Geometric incompatibility between the slave and master surfaces can cause the traction approximations to be inaccurate. However, incompatibility can result from non-smooth master surface, which again affects convergence of the scheme.

The hyperelastic constitutive equations and the formulation of the finite element system of equations used in the program are dealt with in this thesis. The contact boundary conditions have been dealt with using a Lagrangian multiplier method. This method is implicit, stable and accurate for relatively big time steps. It is also relatively easy to implement within the finite element program. Further more, it incorporates some of the well known constraint optimization techniques which are specifically useful for metal forming problems. The nonlinear system of equations arising from the discretized form of the principle of virtual work is solved using a Newton-Raphson method. To overcome incompressibility problems, the assumed strain method is adopted. Linearization of the principle of virtual work relation, which is useful for the computation of the tangent stiffness matrix, has been treated in detail. Also the updating procedure for the stress and state parameters using the radial return method has been discussed.

Using the developed computer code, an attempt is made to solve a specific metal forming problem under specific conditions. Also the effects of different input parameters on the correctness of the output and the convergence property of the formulation have been investigated.

Finally, in order to account for history of loading of the updated Lagrangian method, which updates the reference configurations after a successful iteration, is considered. Then the formulation is converted to a computer program written using MatLab. Finally the program is used to solve a benchmark problem, an open die forging (upsetting) problem to investigate the efficiency of the formulation.

7. CONCLUSION AND RECOMMENDATIONS

7.1 Conclusion

As can be seen from the results given in chapter 6, it is possible to find the distribution of any required parameter such as stress, equivalent plastic strain, elastic strain, internal resistance of the material, etc throughout the work-piece, which is a very important step towards the design of effective and robust metal forming process. Having the above information at hand it is possible to design the metal forming equipment such as presses and dies with high reliability and minimum cost. And the design of the formed part can be performed in such a way as to get every quality parameters within the maximum achievable tolerance throughout the work-piece. Also using this method is possible to model material properties of the work-piece with any degree of complexity to represent actual condition as much as possible. Therefore the usefulness of the method for designing of a metal forming process cannot be overemphasized.

7.2 Recommendations for Future Work

The following are suggestions for future work of this research:

- This thesis has not included friction, which is the main process governing parameter in the case of metal forming processes. Therefore to model metal forming problems, more accurately, frictional contact should be considered. Then additional considerations are necessary regarding the update of the active contact set including stick and slip areas for the Lagrange multiplier formulation.
- Furthermore this thesis has considered upsetting through Axisymmetric dies, which eliminates the need for contact searching algorithm. But to make the formulation more flexible to solve a wide variety of metal forming problems, the incorporation of contact searching algorithm is crucial.

- In this thesis an isothermal process, is assumed. Thus, consideration of thermo-mechanically coupled problems, which include the effect of heat generation during plastic deformation and heat supplied from external source are important factors for future work.

- To solve more practical and complicated problems, the program must be refined in such a way as to minimize the CPU time. This can be achieved by applying more advanced solution techniques, such as Line Search method, Quasi-Newton methods and Conjugate Gradient methods, which increase the convergence rate and reduce the possibility of divergence of the Newton Raphson iterative scheme.

BIBLIOGRAPHY

1. Zabaras N., Badrinarayanan S.M, 'A 2-d FEM code for the analysis of large deformation of hyperelastic viscoplastic solids' *Technical report* MM 93-05, 1993

2. Zabaras N., Arif AA.F.M., 'A family of integration algorithms for constitutive equations in finite deformation elasto-viscoplasticity', *Int. Journal for Numerical Methods in Engineering,* 33:59-84(1992)
3. Zabaras N., Akkaram S., 'An object oriented programming approach to the Lagrangian FEM analysis of large inelastic deformations and metal-forming processes', *Int. Journal for Numerical Methods in Engineering*, 45,399-445 (1999).
4. Zabaras N., Ganapathy subramanian S.,'A continuum sensitivity method for finite thermo-inelastic deformation with application to the design of hot forming process', *Int.Journal for Numerical Methods in Engineering*, 55, 1391-1437(1996).
5. Zabaras N., Badrinarayanan S.M., 'A Sensitivity analysis for the optimal design of metal forming process', *Computer Methods In App. Mech. & Eng'g*, 129,319-348919960
6. Zabaras N., Ganapathy subramanian S., 'Computational design of deformation process for material with ductile damage', *Computer Methods in App. Mech. & Eng'g*. 192,147-183 (2003)
7. Zabaras N., Badrinarayanan S.,' Inverse problem and technique in metal forming', *Internal Journal for Numerical Methods in engineering*, 1993
8. Bathe K.J., *Finite element procedure in engineering analysis*, Prentice Hall, Englewood Cliffs, NY, 1982
9. Y.C. Fung Y.C. *Foundation of solid mechanics*, Prentice Hall, Englewood Cliffs, NY. 1965
10. Daniel Christ, 'A mixed finite element formulation for incompressibility using linear displacement and pressure interpolations', *Diploma Thesis*, RUHRR-university Bochum,2003

11. Malvern L.E., Introduction *to the mechanics of a continuous medium*, Prentice Hall, Englewood cliffs: NY, 1969
12. Robert H.W., Jean-Loup C., *Fundamentals of metal forming*, Jony Wiley & Sons Inc.: NY. 1997
13. Lemaitre J., Chaboche J.L., *Mechanics of Solid Materials*, Cambridge Univ. press: London, 1994
14. B. Avitzur, *Metal Forming: Process and Analysis,* TATA McGraw-HILL pub. Comp. ltd.: New Delgi,1968
15. Stephen J.C., *MATLAB Programming for Engineers*, Thomson Asia Ltd.: Singapore, 2002
16. Laursen T.A., Attaway S.W., *SEACAS theory manual*, part I, II, III, 1998
17. Altan T., Douglas J.U., 'Flow stress determination for metals and its application in metal forming analysis', *Journal of Engineering for Industry*, Nov.1973
18. Atan T., Douglas J.R., 'Flow stress determination for metals at forging rate and temperatures', *Journal of Engineering for Industry*, Feb. 1975,
19. Altan T., Lee CH., 'Influence of the flow stress and friction up0on metal flow in upset forging of rings and cylinders', *Journal of Engineering for Industry*, may 1972
20. Liu J.Y., 'Upper bound solutions of axisymmetric forming problems I', *Journal of Engineering fro Industry*, May. 1964,
21. Kobayshi S., 'Upper bound solutions of axisymmetric forming problems I', *Journal of Engineering fro Industry,* Nov. 1964
22. Kobayshi S., 'Upper bound solutions of axisymmetric forming problems II', *Journal of Engineering fro Industry,* Nov. 1964
23. Kiuchi M., Avitzur B., 'Limit analysis of flow through inclined converging dies', *Journal of Engineering for Industry,* May 1980
24. Nagpal V., 'General kinematically admissible velocity fields for some axisymmetric metal forming problems', *Journal of Engineering for industry*, Nov. 1974
25. Nagpal V., Clough W.R., 'plane strain forging – a lower upper bound approach', *Journal of Engineering for industry*, Feb. 1975
26. Avitzur B., Van Tyne V.J., 'Ring forming an upper bound approach part I: flow pattern and calculation of power', *Journal of Engineering for Industry*, Aug. 1982,

27. Avitzur B., Van Tyne V.J., 'Ring forming an upper bound approach part 2: process analysis and characteristics', *Journal of Engineering for Industry*, Aug 1982,
28. Avitzur B., Van Tyne V.J. 'Ring forming an upper bound approach part 3:P constrained forging and deep drawing application', *Journal of Engineering for Industry,* Aug 1982
29. Oh S.I., Park J.J., Kobayashi S., Atan T. 'Application of fem modeling to simulate metal flow in forging a titanium alloy engine disc', *Journal of Engineering for Industry*, Nov 1983
30. Lu S.C.,; Wright P.K. 'finite element modeling of plan strain strip drawing with interface friction', *Journal of Engineering fro Industry*, May 1988
31. Iwata, K., Oskada K., Fungio S. 'Analysis of hydrostatic extrusion by fem', Journal *of Engineering for Industry*, May 1972,
32. Mehta H.S., Kobayshi S. ' Finite element analysis and experimental investigation of sheet metal stretching', *Journal of Engineering for Industry* , Aug. 1973
33. GuoJi Li., Kobayshi S. 'Rigid plastic finite element analysis of plain strain rolling', *Journal of Engineering for Industry*, Feb.1982
34. Shabaik A.H. 'Computer aided viscoplastic solution to axisymmetric extrusion through curved boundaries', *Journal of Engineering for Industry*, Nov. 1972
35. Sehgal M.M., Kobayashi S. 'plastic indentation of steel cylinders with circular punches'; *Journal of Engineering for Industry*, Nov. 1972
36. Lee C.H., Kobayshi S. 'New solution to rigid plastic deformation problem using a matrix method', *Journal of Engineering for Industry*, Aug. 1973.
37. Altan T. 'Modular analysis of geometry and stresses in closed die forging application to a structural part', *Journal of Engineering for Industry*, Nov. 1972
38. Bhattacharyya S., Majumdar A., Bvaru S.K. 'Mathematical modeling of metal extrusion process', *Journal of Engineering for Industry*, Feb. 1982,
39. Yangang B. 'An Object-Oriented Implementation of Die Design Problems in Metal Forming Process Using the REM Method ', *Masters Thesis*, Cornell University Aug 1999
40. Badrinarayan S. 'Preform and Die Design Problems in Metal Forming', *PhD Dissertation*, Cornell University, Jan. 1997
41. Sriknath A. 'A Continuum Sensitivity Analysis of Large Deformations with Applications to Metal Forming Process Design', *PhD Dissertation*, Cornell University: January 2001

42. Lee E.H. 'Elastic-plastic Deformation at finite deformation', *Journal of applied mechanics*, march 1969
43. Zabaras N., Arif A.F.M. 'On the performance of two tangent operators for finite element analysis of large deformation inelastic problems', *Int. Journal for Numerical Methods in Engineering*, 35: 369-389 (1992)
44. http://www.lightcorp.com/PDFs/industrial/AlAlloyInfo.pdf
45. Krabbenhoft K. 'Basic computational plasticity', *Technical university of Denmark,* June 2002
46. Laurent B., Taoufik S. 'Mixed finite element formulation in large deformation frictional contact problem', *Laboratoire de Mécanique des Contacts et des Solides*, CNRS-UMR 5514 INSA de Lyon, 69621 Villeurbanne Cedex, France
47. G. Rebel, K.C. Park, C.A. Felippa 'A contact formulation based on localized Lagrange multipliers: formulation and application to two-dimensional problems', *Int. Journal for Numer. Meth. In Eng'g 2002*; 54:263 –297 (DOI:10.1002/nme.426)
48. K.Y. Wang, Q.H. Qin, Y.L. Kang, J.S. Wang, C.Y. Qu. 'A direct constraint-Trefftz FEM for analyzing elastic contact problems', *Int. Journal for Numer. Meth. In Eng'g,* Published online in Wiley InterScience (www.interscience.wiley.com). DOI: 10.1002/nme.1333
49. Jianqiang M. 'A finite element approach to solve contact problems in geotechnical engineering', International Journal for Numerical and Analytical Methods in Geomechanics, 2005; 29:525 .550
50. J.S. Chen, C. Pan, C. M. O. L. Roque, H.-P. Wang. 'A Lagrangian reproducing kernel particle method for metal forming analysis', *Computational Mechanics*, 22 (1998) 289-307
51. Reese E., Jonesz and Panayiotis P. 'A yield-limited Lagrange multiplier formulation for frictional contact', *Int. Journal for Numer. Meth. In Eng'g*, 2000; 48:1127-1149
52. K.A. Fischer, P. Wriggers, 'Frictionless 2D Contact formulations for finite deformations based on the mortar method', *Computational Mechanics* (2005)36:226 –244

APPENDIX

Appendix A: Linearized moduli for rate-dependent plasticity

To derive the Linearized material moduli, we take the variation of equation (4.18) with respect to $\mathbf{u}_{n+1}$ as follows:

$$\overline{\mathbf{T}}_{n+1} = \mathbf{T}_n + \ell^e \left[\Delta\overline{\mathbf{E}} - \Delta\overline{\mathbf{E}}^p\right] \tag{A-1}$$

where from equations (4.15 and 4.19), it follows that

$$d\Delta\overline{\mathbf{E}}^p = \sqrt{\frac{3}{2}}\Delta t(\dot{\tilde{\varepsilon}}^p_{n+\beta} d\overline{\mathbf{N}}^p_{n+\beta} + d\dot{\tilde{\varepsilon}}^p_{n+\beta}\overline{\mathbf{N}}^p_{n+\beta}) \tag{A-2}$$

The equivalent plastic strain increment $\dot{\tilde{\varepsilon}}^p_{n+\beta}$ was defined in equation (4.15) from which using the chain-rule and equation (4.21), we can derive

$$d\dot{\tilde{\varepsilon}}^p_{n+\beta} = \beta\frac{\partial f}{\partial\tilde{\sigma}}\bigg|_{\mathbf{n}+\beta}\frac{\partial\tilde{\sigma}}{\partial\overline{\mathbf{T}}}\bigg|_{\mathbf{n}+\beta} .d\mathbf{T}_{n+\beta} + \frac{\partial f}{\partial s}\bigg|_{n+\beta} ds_{n+\beta} \tag{A-3}$$

where $\partial\tilde{\sigma}/\partial\overline{\mathbf{T}}$ is the flow vector for J_2 plasticity and is related to the unit vector $\overline{\mathbf{N}}^p$ as follows:

$$\frac{\partial\tilde{\sigma}}{\partial\overline{\mathbf{T}}} = \sqrt{\frac{3}{2}}\overline{\mathbf{N}}^p \tag{A-4}$$

Similarly, we can derive that

$$d\overline{\mathbf{N}}^p = \beta\frac{\partial\overline{\mathbf{N}}^p}{\partial\overline{\mathbf{T}}}\bigg|_{\mathbf{n}+\beta}[d\mathbf{T}_{n+1}] \tag{A-5}$$

Variation of equation (4.21) leads to

$$ds_{n+\beta} = \beta\Delta t d\dot{s}_{n+\beta} \tag{A-6}$$

This, using equations (4.7 and 21), leads finally to following expression for $ds_{n+\beta}$:

$$ds_{n+\beta} = \frac{\beta^2\Delta t\left\{\frac{\partial g}{\partial\tilde{\sigma}}\Big|_{\mathbf{n}+\beta}\frac{\partial\tilde{\sigma}}{\partial\overline{\mathbf{T}}}\Big|_{\mathbf{n}+\beta} .d\mathbf{T}_{n+1}\right\}}{\left\{1-\beta\Delta t\frac{\partial g}{\partial\tilde{\sigma}}\Big|_{\mathbf{n}+\beta}\right\}} \tag{A-7}$$

Finally, substituting equation (A-7) in equation (A-3 and A-4), and then equations (A-3, A-4 and A-5) in equation (A-2) and taking the common terms together yields

$$\mathrm{d}\overline{\mathbf{T}}_{\mathrm{n+1}} = \left.\frac{\partial \overline{\mathbf{T}}}{\partial \Delta \overline{\mathbf{E}}}\right|_{\mathrm{n+1}} \left[\mathrm{d}\Delta \overline{\mathbf{E}}\right] = \overline{\hat{\lambda}}^{\mathrm{ep}} \left[\mathrm{d}\Delta \overline{\mathbf{E}}\right] \tag{A-7}$$

where

$$\overline{\hat{\lambda}}^{ep} = \left[\ell^{e^{-1}} + \sqrt{\frac{3}{2}}\beta\Delta t \left\{ \sqrt{\frac{3}{2}} \left(\left.\frac{\partial f}{\partial \tilde{\sigma}}\right|_{\mathbf{n}+\beta} \frac{\beta\Delta t \left\{ \left.\frac{\partial g}{\partial s}\right|_{\mathbf{n}+\beta} \left.\frac{\partial g}{\partial \tilde{\sigma}}\right|_{\mathbf{n}+\beta} \right\}}{1 - \beta\Delta t \left.\frac{\partial g}{\partial s}\right|_{\mathbf{n}+\beta}} \right) \tilde{\mathbf{N}}^{p}_{n+\beta} \otimes \tilde{\mathbf{N}}^{p}_{n+\beta} + \dot{\tilde{\varepsilon}}^{p}_{n+\beta} \left.\frac{\partial \tilde{\mathbf{N}}^{p}}{\partial \overline{\mathbf{T}}}\right|_{\mathbf{n}+\beta} \right\} \right]^{-1} \tag{A-8}$$

Note that, in order to calculate $\tilde{\mathbf{N}}^{p}_{n+\beta}$ and $\left.\partial \tilde{\mathbf{N}}^{p} \middle/ \partial \overline{\mathbf{T}}\right|_{\mathbf{n}+\beta}$ in the equation above, one must assume the stress $\overline{\mathbf{T}}_{\mathbf{n+1}}$, and so an iterative scheme is required.

$$\overline{\hat{\lambda}}^{ep} = \left[\ell^{e^{-1}} + \sqrt{\frac{3}{2}}\beta\Delta t \left\{ \sqrt{\frac{3}{2}}\lambda \tilde{\mathbf{N}}^{p}_{n+\beta} \otimes \tilde{\mathbf{N}}^{p}_{n+\beta} + \dot{\tilde{\varepsilon}}^{p}_{n+\beta} \left.\frac{\partial \tilde{\mathbf{N}}^{p}}{\partial \overline{\mathbf{T}}}\right|_{\mathbf{n}+\beta} \right\} \right]^{-1} \tag{A-9}$$

where

$$\begin{aligned} &\lambda = c_1 + \frac{\beta\Delta t c_2 d_1}{1 - \beta\Delta t d_2}; \\ &c_1 = \left.\frac{\partial f}{\partial \tilde{\sigma}}\right|_{n+\beta};\ c_2 = \left.\frac{\partial f}{\partial s}\right|_{n+\beta};\ d_1 = \left.\frac{\partial g}{\partial \tilde{\sigma}}\right|_{n+\beta};\ d_2 = \left.\frac{\partial g}{\partial s}\right|_{n+\beta} \end{aligned} \tag{A-10}$$

Now, using equation (4.15) we have

$$\left(\tilde{\mathbf{N}}^{p}\right)^{T} = \sqrt{\frac{3}{2}} \frac{1}{\tilde{\sigma}} \left\{ \overline{T}^{'}_{11}\ \overline{T}^{'}_{22}\ \overline{T}^{'}_{33}\ \overline{T}^{'}_{23}\ \overline{T}^{'}_{31}\ \overline{T}^{'}_{12} \right\}$$

Thus (A-11)

$$\tilde{\mathbf{N}}^{p} \otimes \tilde{\mathbf{N}}^{p} = \frac{3}{2\tilde{\sigma}^{2}} \mathbf{X}$$

where for plane and axially symmetric problems

$$\mathbf{X} = \begin{bmatrix} \left(\overline{\mathbf{T}}^{'}_{11}\right)^2 & \left(\overline{\mathbf{T}}^{'}_{11}\overline{\mathbf{T}}^{'}_{22}\right) & \left(\overline{\mathbf{T}}^{'}_{11}\overline{\mathbf{T}}^{'}_{12}\right) & \left(\overline{\mathbf{T}}^{'}_{11}\overline{\mathbf{T}}^{'}_{33}\right) \\ & \left(\overline{\mathbf{T}}^{'}_{22}\right)^2 & \left(\overline{\mathbf{T}}^{'}_{22}\overline{\mathbf{T}}^{'}_{12}\right) & \left(\overline{\mathbf{T}}^{'}_{22}\overline{\mathbf{T}}^{'}_{33}\right) \\ & & \left(\overline{\mathbf{T}}^{'}_{12}\right)^2 & \left(\overline{\mathbf{T}}^{'}_{12}\overline{\mathbf{T}}^{'}_{33}\right) \\ \textit{symm} & & & \left(\overline{\mathbf{T}}^{'}_{33}\right)^2 \end{bmatrix} \tag{A-12}$$

and

$$\frac{\partial \tilde{\mathbf{N}}^{p}}{\partial \overline{\mathbf{T}}} = \frac{\partial}{\partial \overline{\mathbf{T}}}\left(\sqrt{\frac{\mathbf{3}}{\mathbf{2}}}\frac{\partial \overline{\mathbf{T}}}{\partial \tilde{\sigma}}\right) = \sqrt{\frac{\mathbf{3}}{\mathbf{2}}}\frac{1}{\tilde{\sigma}}\left(\frac{\partial \overline{\mathbf{T}}'}{\partial \overline{\mathbf{T}}} - \tilde{\mathbf{N}}^{p} \otimes \tilde{\mathbf{N}}^{p}\right) \tag{A-13}$$

with

$$\mathbf{Y} = \frac{\partial \overline{\mathbf{T}}'}{\partial \overline{\mathbf{T}}} = \begin{bmatrix} \frac{2}{3} & -\frac{1}{3} & 0 & -\frac{1}{3} \\ & \frac{2}{3} & 0 & -\frac{1}{3} \\ & & 1 & 0 \\ symm & & & \frac{2}{3} \end{bmatrix} \tag{A-14}$$

For plane problems only the upper 3x3 portion is employed while for axially symmetric situations the complete matrices are utilized.

Finally,

$$\overline{\mathfrak{L}}^{ep} = \left[\ell^{e\,-1} + \frac{3}{2}\beta\Delta t\left\{\frac{3}{2\tilde{\sigma}^{2}_{n+\beta}}\left(\lambda - \frac{\dot{\tilde{\varepsilon}}^{p}_{n+\beta}}{\tilde{\sigma}_{n+\beta}}\right)\mathbf{X}_{\mathbf{n+\beta}} + \frac{\dot{\tilde{\varepsilon}}^{p}_{n+\beta}}{\tilde{\sigma}_{n+\beta}}\mathbf{Y}\right\}\right]^{-1} \tag{A-15}$$

The linearized modulus for the particular case of β=1 takes a simplified from which depends only on the trial stress $\overline{\mathbf{T}}^{trial}_{n+1}$. In summary, the material modulus for this case takes the following form:

$$\overline{\mathfrak{L}}^{ep} = \tilde{\ell}^{e} - 2\mathbf{G}(\eta_{n+1} - \mu)\tilde{\mathbf{N}}^{p} \otimes \tilde{\mathbf{N}}^{p} \tag{A-16}$$

where

$$\tilde{\ell}^{e} = -2\mathbf{G}\mathfrak{I} + \left(\mathbf{K} - \frac{2}{3}\tilde{\mathbf{G}}\right)\mathbf{I} \otimes \mathbf{I}$$
$$\tilde{\mathbf{G}} = \mathbf{G}\eta_{n+1} \tag{A-17}$$

with

$$\eta_{n+1} = \frac{\tilde{\sigma}_{n+1}}{\tilde{\sigma}^{trial}_{n+1}}$$
$$\mu = b_2 \Big/ (a_1 b_2 + b_1 a_2) \tag{A-18}$$

and

$$a_1 = 1 + 3\mathbf{G}\Delta t \left.\frac{\partial f}{\partial \tilde{\sigma}}\right|_{n+1} ; \qquad a_2 = 3\mathbf{G}\Delta t \left.\frac{\partial f}{\partial s}\right|_{n+1} ;$$
$$b_1 = \Delta t \left.\frac{\partial g}{\partial \tilde{\sigma}}\right|_{n+1} ; \qquad b_2 = 1 - \Delta t \left.\frac{\partial g}{\partial s}\right|_{n+1} \tag{A-19}$$

Appendix B: A solution to the simultaneous equations of equation (4.6b) by a modified Newton-Raphson scheme

In order to solve the nonlinear simultaneous system of algebraic equations arising out of the radial return method, the following method is employed [2].

We have to solve the following two equations:

$$\begin{aligned} s_{n+1} - s_n - \Delta t g\left(\tilde{\sigma}_{n+1}, s_{n+1}\right) &= 0 \\ \tilde{\sigma}_{n+1} - \tilde{\sigma}_* + 3\mu\Delta t f\left(\tilde{\sigma}_{n+1}, s_{n+1}\right) &= 0 \end{aligned} \tag{B-1}$$

These equations can be solved only by iterative means and because of their highly non-linear nature, the choice of the algorithm will heavily influence the number of iterations needed for convergence. To start with, an initial estimate of the solution is needed and starting from that point, linearization followed by solving the linear equations will provide the answer. The Newton-Raphson method is not applied on both equations simultaneously but for one equation at a time. A concise algorithm is given below.

- Level 1 iterations are performed to obtain subsequent values for s_{n+1}.
- level 2 iterations are performed to obtain subsequent values for $\tilde{\sigma}_{n+1}$.

1. First, the tolerances required for the convergence on $\tilde{\sigma}_{n+1}$ and s_{n+1} are fixed. A good choice is

$$\begin{aligned} \text{TOL}_S &= 1\text{X}10^{-5}\ s_n \\ \text{TOL}\,\sigma &= 1\text{X}10^{-5}\ \tilde{\sigma}_* \end{aligned} \tag{B-2}$$

where s_n is the value of the internal resistance variable at time t_n

and $\tilde{\sigma}_*$ is the vale of the equivalent deviatoric stress at time t_n

2. Make an initial estimate of $(\tilde{\sigma}_{n+1}, s_{n+1})$ by solving the equations obtained by forward gradient approximations of the governing equations. The functions f and g are approximated by Taylor series expansion about $(\tilde{\sigma}_n, s_n)$. This results in

$$\tilde{\sigma}_{n+1} \cong \tilde{\sigma}_n + \left\{ \frac{b_2\left(\tilde{\sigma}_* - \tilde{\sigma}_n - 3\mu\Delta t f\left(\tilde{\sigma}_n, s_n\right)\right) - a_2 \Delta t g\left(\tilde{\sigma}_n, s_n\right)}{b_2 a_1 + a_2 b_1} \right\} \tag{B-3}$$

and

$$s_{n+1} \cong s_n + \left\{ \frac{b_1\left(\tilde{\sigma}_* - \tilde{\sigma}_n - 3\mu\Delta t f\left(\tilde{\sigma}_n, s_n\right)\right) - a_1 \Delta t g\left(\tilde{\sigma}_n, s_n\right)}{b_2 a_1 + a_2 b_1} \right\} \tag{B-4}$$

where

$$\begin{aligned} a_1 &\equiv 1 + 3\mu\Delta t \frac{\partial f}{\partial \tilde{\sigma}_n} \\ a_2 &\equiv 3\mu\Delta t \frac{\partial f}{\partial s_n} \\ b_1 &\equiv \Delta t \frac{\partial g}{\partial \tilde{\sigma}_n} \\ b_2 &\equiv 1 - \Delta t \frac{\partial g}{\partial s_n} \end{aligned} \tag{B-5}$$

However, with certain models, (specifically, the sin hyperbolic model for Aluminum at 673 K) the value of $\tilde{\sigma}_{n+1}$ calculated by the above equation becomes so high that further substitution in the functions f and g blows up. Hence in such cases the value of $\tilde{\sigma}_{n+1}$ is taken to be equal to 0 or $\tilde{\sigma}_n$.

3. Now level 1 iterations are performed to obtain subsequent values for s_{n+1}. The iterations are performed till convergence is obtained on s_{n+1}. Consider a generic k^{th} step. Assume that the function f is invertible to give flow stress. i.e., assume that there exists a function f^{-1} such that

$$\dot{\tilde{\varepsilon}}^p = f\left(\tilde{\sigma}, s\right) \tag{B-6}$$

implies

$$\tilde{\sigma} = f^{-1}\left(\dot{\tilde{\varepsilon}}^{p}, s\right) \tag{B-7}$$

(a) Calculate an upper bound on $\tilde{\sigma}_{n+1}$, by evaluation the smaller of $f^{-1}\left(\frac{\tilde{\sigma}_{*}}{3\mu\Delta t}, s\right)$ and $\tilde{\sigma}_{*}$. Assign this value to $\tilde{\sigma}_{u}$.

(b) Fix the lower bound, assigning as $\tilde{\sigma}_{l}$, for $\tilde{\sigma}_{n+1}$ as 0.

(c) Do level 2 iterations to update $\tilde{\sigma}_{n+1}$ and to evaluate $\frac{d\tilde{\sigma}_{n+1}}{ds_{n+1}}$ (described below).

(d) Evaluate the error associated with s_{n+1}

$$E_{s}^{k} = s_{n+1}^{k} - s_{n} - \Delta t g_{n+1}^{k} \tag{B-8}$$

where

$$g_{n+1}^{k} = g\left(\tilde{\sigma}_{n+1}^{k}, s_{n+1}^{k}\right) \tag{B-9}$$

(e) Compare this error with the tolerance TOL_{s}. Iteration is assumed to be converged if

$$\left\| E_{s}^{k} \right\| \leq \mathrm{TOL}_{s} \tag{B-10}$$

Then $s_{n+1} = s_{n+1}^{k}$ and $\tilde{\sigma}_{n+1} = \tilde{\sigma}_{n+1}^{k}$. Otherwise the iteration is continued.

(f) If the iteration continues, the correction Δs^{k} is calculated.

$$\Delta s^{k} = \frac{-E_{s}^{k}}{dE_{s}^{k} / ds_{n+1}^{k}} \tag{B-11}$$

where

$$\frac{dE_{s}^{k}}{ds_{n+1}^{k}} = 1 - \Delta t \left\{ \frac{\partial g_{n+1}^{k}}{\partial s_{n+1}^{k}} + \frac{\partial g_{n+1}^{k}}{\partial \tilde{\sigma}_{n+1}^{k}} \frac{d\tilde{\sigma}_{n+1}^{k}}{ds_{n+1}^{k}} \right\} \tag{B-12}$$

were $d\tilde{\sigma}_{n+1}^{k} / ds_{n+1}^{k}$ calculated during the level 2 iterations.

(g) The estimate for the next level iteration is

$$s_{n+1}^{k+1} = s_{n+1}^{k} + \Delta s^{k} \tag{B-13}$$

(h) The initial estimate of $\tilde{\sigma}_{n+1}$ to start the next level 2 iterations is

$$\tilde{\sigma}_{n+1}^{k+1} = \tilde{\sigma}_{n+1}^{k} + \frac{d\tilde{\sigma}_{n+1}^{k}}{ds_{n+1}^{k}} \Delta s^{k} \tag{B-14}$$

4. Level 2 iterations are performed to obtain the updates on $\tilde{\sigma}_{n+1}^{k}$. Consider the generic step i within the k^{th} loop above.

(a) Evaluate the error associated with $\tilde{\sigma}_{n+1}$

$$E_{\tilde{\sigma}}^{k,i} = \tilde{\sigma}_{n+1}^{k} - \tilde{\sigma}_{*} + 3\mu f_{n+1}^{k,i} \tag{B-15}$$

where

$$f_{n+1}^{k,i} = f(\tilde{\sigma}_{n+1}^{k,i}, s_{n+1}^{k,i}) \tag{B-16}$$

(b) Compare this error with the tolerance. If

$$\left\| E_{\tilde{\sigma}}^{k,i} \right\| \leq \text{TOL}_{\tilde{\sigma}} \tag{B-17}$$

then the scheme has converged. Assign $\tilde{\sigma}_{n+1}^{k} = \tilde{\sigma}_{n+1}^{k,i}$. Evaluate $d\tilde{\sigma}_{n+1}^{k} \Big/ ds_{n+1}^{k}$,

$$\frac{d\tilde{\sigma}_{n+1}^{k}}{ds_{n+1}^{k}} = \frac{-3\mu\Delta t \left(\partial f_{N+1}^{k,i} \Big/ \partial s_{n+1}^{k} \right)}{1 + 3\mu\Delta t \left(\partial f_{N+1}^{k,i} \Big/ \partial \tilde{\sigma}_{n+1}^{k} \right)} \tag{B-18}$$

for using in level 1 iterations.

(c) If the scheme does not converge, calculate the Newton-Raphson correction factor $\Delta\tilde{\sigma}_{NR}^{k,i}$

$$\Delta\tilde{\sigma}_{NR}^{k,i} = \frac{E_{\tilde{\sigma}}^{k,i}}{dE_{n+1}^{k,i} \Big/ d\tilde{\sigma}_{n+1}^{k,i}} \tag{B-19}$$

where

$$\frac{dE_{n+1}^{k,i}}{d\tilde{\sigma}_{n+1}^{k,i}} = 1 + 3\mu\Delta t \frac{\partial f_{n+1}^{k,i}}{\partial \tilde{\sigma}_{n+1}^{k,i}} \tag{B-20}$$

(d) Depending upon the sign of $\Delta\tilde{\sigma}_{NR}^{k,i}$, update either the upper bound $\tilde{\sigma}_{u}$ or the

lower bound $\tilde{\sigma}_l$ for $\tilde{\sigma}_{n+1}^{k}$ and then calculate the maximum allowable correction.

If $\Delta\tilde{\sigma}_{NR}^{k,i} < 0,$

then

$$\tilde{\sigma}_u = \tilde{\sigma}_{n+1}^{k,i} \tag{B-21}$$

and $$\Delta\tilde{\sigma}_{\max}^{k,i} = \frac{1}{2}\left(\tilde{\sigma}_l - \tilde{\sigma}_{n+1}^{k,i}\right) \tag{B-22}$$

If $\Delta\tilde{\sigma}_{NR}^{k,i} > 0,$

then

$$\tilde{\sigma}_l = \tilde{\sigma}_{n+1}^{k,i} \tag{B-23}$$

and

$$\Delta\tilde{\sigma}_{\max}^{k,i} = \left(\tilde{\sigma}_u - \tilde{\sigma}_{n+1}^{k,i}\right) \tag{B-24}$$

(e) Determine the correction to be used.

If $\left|\Delta\tilde{\sigma}_{NR}^{k,i}\right| > \left|\Delta\tilde{\sigma}_{\max}^{k,i}\right|,$

then

$$\Delta\tilde{\sigma}^{k,i} = \Delta\tilde{\sigma}_{\max}^{k,i} \tag{B-25}$$

else

$$\Delta\tilde{\sigma}^{k,i} = \Delta\tilde{\sigma}_{NR}^{k,i} \tag{B-26}$$

(f) The estimate for the next iteration is

$$\tilde{\sigma}_{n+1}^{k,i+1} = \tilde{\sigma}_{n+1}^{k,i} + \Delta\tilde{\sigma}^{k,i} \tag{B-27}$$